



SCUOLA NORMALE SUPERIORE

**Electroweak Symmetry
Breaking
with a compact extra
dimension**

Michele Papucci

Advisor

Prof. Riccardo Barbieri

Ph.D. Thesis

Spring 2009

*To my parents
for their endless patience and support
And to Carla
without whom I could have never written it*

Contents

List of Tables	v
List of Figures	ix
Preface	xi
1 Introduction: Hierarchies, fine-tunings and all that	1
1.1 The present status: the Standard Model	1
1.2 Many reasons to go “beyond”	7
1.3 Solving to the Big Hierarchy Problem	10
1.3.1 Supersymmetry	11
1.3.2 Strong Dynamics	14
1.3.3 Large Extra Dimensions	15
1.4 The Little Hierarchy Problem	16
1.4.1 SUSY and the LEP Paradox	17
1.4.2 Models with strong dynamics	18
1.5 Compact Extra Dimensions as a tool for Model Building	20
2 Introducing the Constrained Standard Model	23
2.1 The Constrained Standard Model <i>ab initio</i>	24
2.1.1 The relation between the compactification scale and the cut-off	27
2.2 The complete model and the relevant parameter space	29
2.3 Residual symmetries after the orbifold projection	29
2.4 Gauge anomalies and hypermultiplet mass terms	32
2.5 The Fayet-Iliopoulos term	33
2.6 Hypermultiplet spectrum in presence of a mass term	35

3	The Constrained SM in presence of bulk masses.	39
3.1	Electroweak symmetry breaking in detail	39
3.1.1	The top mass and the top Yukawa coupling	39
3.1.2	One loop Higgs effective potential for arbitrary M_U, M_Q . .	40
3.1.3	Electroweak symmetry breaking in presence of a FI term . .	41
3.1.4	Electroweak symmetry breaking with sizable $M_U = M_Q$. .	42
3.2	Spectrum and phenomenological implications	44
3.2.1	Phenomenological implications	46
3.3	Extending the CSM	48
3.3.1	Models with $U(1)_R$ and P_5 symmetries	48
3.3.2	Models with $U(1)_R$ symmetry and broken P_5 symmetry . .	49
4	Electroweak Symmetry Breaking with a (quasi-)localized top.	53
4.1	The case of exact localization	54
4.2	(α_t, α_s) -corrections. General expressions	55
4.3	(α_t, α_s) -corrections. Results	57
4.4	The Case of a quasi-localized top	58
4.4.1	The Higgs potential	58
4.4.2	Determination of the Fermi scale	59
4.4.3	The Higgs mass as a function of $1/L$	61
4.5	Stability of the region: EWSB with $M_UL \neq M_QL$	62
4.6	Lower values of the compactification scale	63
5	Phenomenology in the QLT model.	67
5.1	The UV cutoff	67
5.2	Localized kinetic terms	69
5.3	Spectrum	71
5.4	Constraints from precision observables	73
5.4.1	Universal effects	73
5.4.2	Non universal flavor-diagonal effects	78
5.5	Flavor and CP violation	79
5.6	Phenomenology of Sparticle Production	82
5.6.1	General Features	82
5.6.2	Bounds from TeVatron searches	84
5.6.3	LHC searches scenarios in the QLT model	84
5.7	Neutrino Masses and Dark Matter	86

6	Conclusions	89
6.1	Models with negligibly small bulk masses	90
6.2	Models with sizable bulk masses for the top multiplets	92
6.3	Models with large bulk masses	94
6.4	Other directions	97
A	The spectrum	99
A.1	Matter hypermultiplets	100
A.2	Higgs hypermultiplet	101
A.3	Spectrum in presence of a VEV for the Higgs field	102
B	5D Propagators	105
C	Effects of localized terms	111
C.1	Boundary kinetic terms	111
C.1.1	Higgs hypermultiplets	111
D	Independence of EWSB from $M_{D_3}L$	113
E	The 2 loop contribution to the Higgs potential	115
F	1-loop Renormalization functions at order α_t, α_s	119

List of Tables

1.1	Lower bounds on Λ/TeV for the individual operators and different values of m_h	16
2.1	Continuous R charges for gauge, Higgs and matter components. Here, m represents q, u, d, l, e	31
3.1	The particle spectrum and $1/R$ in absence of any mass term (Column A, presently excluded) and in presence of a FI term (Column B). All entries are in GeV.	47
6.1	The particle spectrum and $1/R$ in absence of any mass term and in presence of a FI term, presented in Chapter 3.	91

List of Figures

1.1	The “famous” pull table of the Electroweak Precision Tests summarizing the discrepancies between the Standard Model predictions and the experiments.	2
1.2	Measured values of $\sin^2 \theta_W$ from leptonic and hadronic observables vs. the Higgs mass m_H in the Standard Model	3
1.3	Measured values of CP violation parameters in various decay modes of neutral B mesons.	5
1.4	χ^2 distribution of SM fit as a function of the Higgs mass. The shaded region corresponds to the LEP limit on m_H	7
2.1	Component diagram of a hypermultiplet in 5D.	24
2.2	Tree-level KK mass spectrum of a 5D multiplet with the indicated boundary conditions.	26
2.3	One-loop diagrams contributing to the mass squared of the Higgs boson.	27
2.4	Spectrum of a matter hypermultiplet, in units of $1/L$, as function of ML	35
2.5	As in Fig. 2.4 for the Higgs hypermultiplet.	36
2.6	Wave-functions of the lowest-lying modes for the fermionic $(+, +)$ and the bosonic $(+, -)$ matter fields for three different values of the hypermultiplet mass. The case of negative mass are symmetric with respect to $y = L/2$	36
3.1	Higgs mass as function of the dimensionless parameter a , Eq. (3.7).	42
3.2	Compactification scale and lightest stop masses as functions of a , Eq. (3.7).	43
3.3	Top-Higgs coupling (y_t) and $\hat{y}_t = \lambda_t/(4L)^{3/2}$ as functions of a , Eq. (3.7).	43

3.4	Higgs mass as function of ML	45
3.5	Stop mass and $1/R$ as functions of ML	45
3.6	Top-Higgs coupling y_t and $\hat{y}_t = \lambda_t/(4L)^{3/2}$ as functions of ML . . .	46
3.7	Higgs mass versus $1/R$ in presence of a Fayet-Iliopoulos term. The blue (red) shaded areas correspond to the LEP Higgs (CDF stop) exclusion limits.	47
4.1	The diagrams that contribute to the Higgs potential at order $\alpha_s\alpha_t$ and α_t^2 in superfield notation.	56
4.2	The mass of the left handed stop as a function of the localization parameter ML , compared with the same mass in the $ML \rightarrow \infty$ limit.	59
4.3	Slope of the full radiative Higgs potential, as discussed in the text, versus the top localization parameter ML , compared to the one loop approximation, for $m_t^{pole} = 173.1 \pm 1.25$ GeV.	60
4.4	Higgs mass as function of $1/L$ for $m_t^{pole} = 173.1 \pm 1.25$ GeV.	61
4.5	Higgs mass for $m_t^{pole} = 173.1$ GeV at different fixed values of the top localization parameter. The result with the full Higgs potential is compared with the one only including the standard top correction at one loop.	62
4.6	Region of allowed Electroweak Symmetry Breaking in the M_Q - M_U plane. The dashed lines represent the $1/L$ isocurves for $1/L = 1, 2, 3, 4, 5$ TeV.	64
4.7	The relation between the compactification scale and the Higgs mass for different values of the ratio M_U/M_Q	65
4.8	Expected range of Higgs masses with the inclusion of a hypermultiplet Higgs mass and a maximum fine tuning in the slope of the potential at 10% level. The gray (green) area is for $m_t^{pole} = 173.1$ (173.1 ± 1.25) GeV	66
5.1	Cutoff estimation from top and bottom Yukawa coupling perturbativity as a function of ML . The thick point represents the case of the CSM.	69

5.2	Physical masses for the squarks and sleptons from hypermultiplets with $M_Q = M_U = M_D = M_L = M_E = M$, and for the scalars of H_d with $M_{H_d} = 0$. As $1/L$ increases so does M , so that the squark and slepton masses become dominated by the radiative contributions of Eqs. (5.7a – 5.7e).	72
5.3	Bounds on the CSM and the QLT models from EWPT. The shaded region is excluded at 99 % of C.L.	77
6.1	Spectrum of a matter hypermultiplet, presented in Chapter 2.	90
6.2	Higgs mass versus $1/R$ in presence of a Fayet-Iliopoulos term, as shown in Chapter 3.	91
6.3	Higgs mass as function of ML . From Chapter 3.	93
6.4	Stop mass and $1/R$ as functions of ML . From Chapter 3.	93
6.5	Higgs mass as function of $1/L$ in the QLT model.	94
6.6	Physical masses for the squarks and sleptons from hypermultiplets with $M_Q = M_U = M_D = M_L = M_E = M$, and for the scalars of H_d with $M_{H_d} = 0$. Taken from Chapter 5.	95
6.7	Expected range of Higgs masses with the inclusion of a hypermultiplet Higgs mass and a maximum fine tuning in the slope of the potential at 10% level. Taken from Chapter 4.	96

Preface

During my Ph.D. course, under the supervision of Riccardo Barbieri, I started working on Theoretical High Energy Physics. In particular I focused on the problem of Electroweak Symmetry Breaking and in this context I investigated the benefits of introducing a compact extra dimension.

In a series of papers, together with Riccardo Barbieri, Guido Marandella, Lawrence Hall, Yasunori Nomura, Takemichi Okui and Steven Oliver I built supersymmetric models in 5D and studied their phenomenology in detail [1, 2, 3, 4]. In these models Supersymmetry is broken by boundary conditions in the fifth dimension and the ElectroWeak Symmetry Breaking is triggered by Supersymmetry breaking via the top/stop radiative corrections. The phenomenology of these models is significantly different than the one of the Minimal Supersymmetric Standard Model scenarios extensively studied in the literature.

These papers constitute the subject of this Thesis and their results will be presented in the following Chapters.

Besides these papers, during my Ph.D. course I also studied other issues in Particle Physics Beyond the Standard Model.

In [5], in collaboration with Thomas Hambye, Alessio Notari, Lin Yin, and Alessandro Strumia, I studied neutrino masses in models of thermal leptogenesis. Specifically, we addressed the question of what is the maximal lepton asymmetry that can be generated, given a particular spectrum for the right-handed Majorana neutrinos. We studied both the case of hierarchical and of quasi-degenerate spectra, correcting some statements present in the literature. We analyzed the mass bounds for left-handed neutrinos that comes out by the requirement that thermal leptogenesis accounts for the matter-antimatter asymmetry of the universe, and we compared these bounds to the one inferred from the precise measurements of the CMBR spectrum.

In [6] I studied the connections between unitarity bounds on W^+W^- gauge bosons scattering amplitudes and Naive Dimensional Analysis (NDA) estimates of the ultraviolet cutoff in Higgsless extra-dimensional models. In these models the

Electroweak Symmetry is broken directly by boundary conditions, providing an extra-dimensional realization of Technicolor. In particular, the energy growth of the gauge bosons scattering amplitude is changed from quadratic to logarithmic by the presence of the Kaluza-Klein “resonances” and unitarity is thus restored. In the paper I showed how the presence of many final states, that can be produced in W^+W^- scattering at high energy, transforms back this logarithmic energy growth into a linear one, compatible with 5D Naive Dimensional Analysis of the gauge interactions. Moreover, the determination of the slope of this energy growth provided a better estimation of the UV cutoff for these models.

Finally in [7], in collaboration with Roberto Foffa, Riccardo Sturani and Alice Gasparini, I studied the sensitivity of small atomic interferometers to the detection of gravitational waves. In particular, we showed that a small “table-size” atomic interferometer can be as sensitive as conventional optical interferometers like LIGO. At the same time we showed how these instruments can provide complementary information, reaching maximum sensitivity in a different frequency range than LIGO.

These latter papers will not be covered in the present Thesis.

Thanks

I really enjoyed working in Pisa in my Ph.D. years. Discussion with Riccardo Barbieri were illuminating and stimulating. I will never forget working in team with Guido Marandella.

I am also grateful to all the friends that shared with me the “Pisan experience” during those years and made my life a better life both on the workplace and outside. In particular I will always be in debt towards my housemates (Manuel Volpe, Alessio “J” Notari, Roberto “Zazui” Auzzi and Michele Trenti), to the “Combriccola del Blasco” of Studio 116 (Erik Tonni, Andrea Sportiello, Alessandro Romito, Stefano Bolognesi and Alessio Notari), to the Juventus F.C. supporters (Marco Polini, Leonardo Silvestri, Guido Marandella and Camelia Tiplea), and to Sant’Andrea Gambacci da Meleto.

A special thank also goes to Pasquale Calabrese, Giacomo Cacciapaglia, Marco Cirelli, Simone Gennai, Bahman Davoudi, Mehran Azghari, Valentina Cambi, Riccardo Catena, Lin Yin, Thomas Hambye, Asta Zelenkauskaitė, Alvisė Varagnolo, Giacomo Marmorini, Gabriele De Chiara, Bruno Garozzo and all the friends of Caffè Betsabea.

Chapter 1

Introduction: Hierarchies, fine-tunings and all that

1.1 The present status: the Standard Model

The Standard Model (SM) is presently the major achievement in theoretical Particle Physics. It unifies weak and electromagnetic forces under the spell of gauge invariance and the idea of symmetry breaking. It reproduces all the phenomenology observed in experiments, up to the highest energies explored so far. It has been tested to very high precision in the 90s, up to energies of the order of 200 GeV, and it is currently being probed at much higher energies at the Fermilab TeVatron.

With respect to the Physics described, the SM can be divided into three different sectors, *i.e.* the gauge, the Yukawa and the Higgs sectors, as indicated schematically by the following Lagrangian:

$$\begin{aligned}\mathcal{L}_{SM} &= \mathcal{L}_G + \mathcal{L}_Y + \mathcal{L}_H \\ &= -\frac{1}{4}F_{\mu\nu}F^{\mu\nu} + (i\bar{\psi}\not{D}\psi + \lambda\psi\psi\varphi) + (|D\varphi|^2 + V(\varphi)).\end{aligned}\quad (1.1)$$

As a first approximation one can say that the gauge sector describes the Physics involving the photon, the W and Z bosons and their interactions, the Yukawa sector is related to the masses of the quarks and the leptons and to the Flavor-Changing and CP-Violating processes, while the Higgs sector contains the description of the ElectroWeak Symmetry Breaking (EWSB).

Being directly involved in different physical processes, the experiments needed to test the various sectors of the SM are different too. In particular its gauge sector has been extensively tested both at e^+e^- colliders such as the CERN LEP and the SLAC Linear Collider (SLC), and at a hadronic $p\bar{p}$ collider, the Fermilab

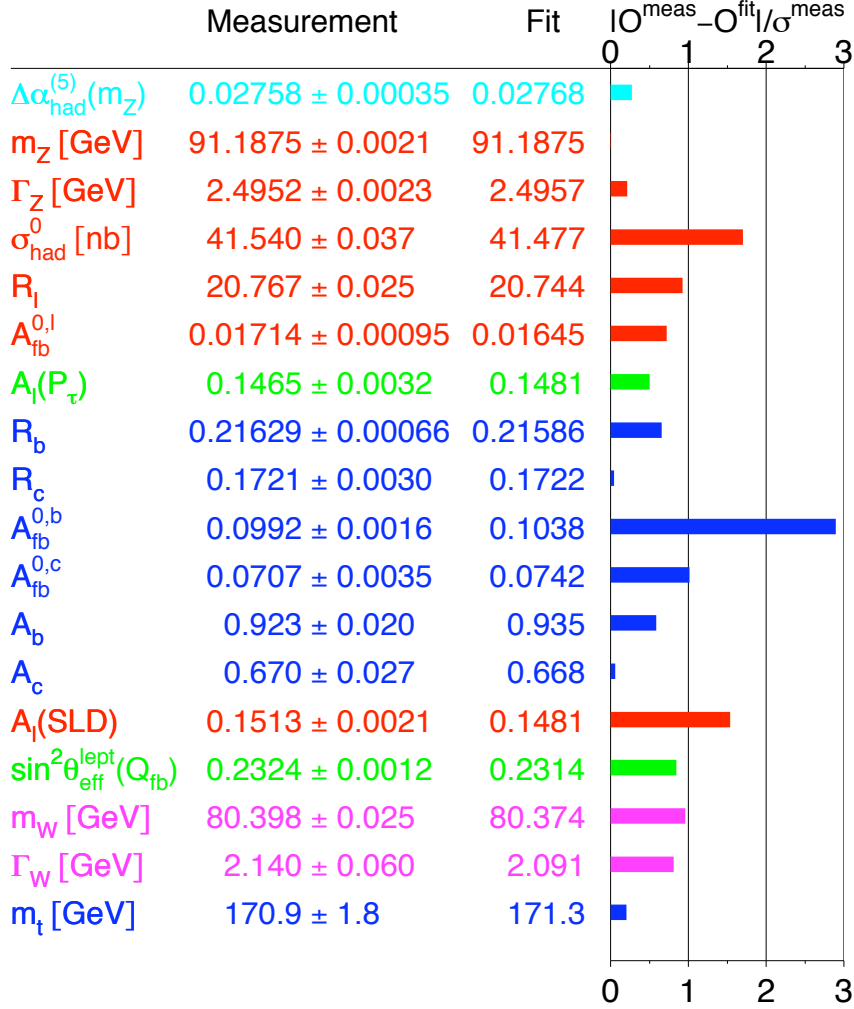


Figure 1.1: The “famous” pull table of the Electroweak Precision Tests summarizing the discrepancies between the Standard Model predictions and the experiments.

TeVatron. These series of tests, especially the ones performed at the “cleaner” leptonic machines, constitute the bulk of the so-called ElectroWeak Precision Tests (EWPT), summarized in Fig. 1.1.

They have probed the structure of $SU(2)_L \times U(1)_Y$ gauge interactions at the per-mille level, that is they have been able to probe the SM gauge sector together with its radiative corrections. The agreement of the theory with the data is rather

astonishing and no convincing signals of a departure from the Standard Model predictions has been found [8, 9]. Yet, there is some tension at the level of a few standard deviations in the hadronic measurements of the weak mixing angle, $\sin^2 \theta_W$, and in the forward-backward asymmetry of the Z boson decay to two b-quarks, A_{FB}^b . In the first case the theoretical uncertainties are probably been underestimated [10], while the significance of the second is still debated [11, 12]. Moreover, by considering purely leptonic data, in principle less prone to theoretical uncertainties, the fit favors a Higgs boson mass which is much lighter than the limit set by direct searches at LEP2, as shown in Fig. 1.2.

The difficulty to clearly identify a discrepancy as a signal of New Physics, due

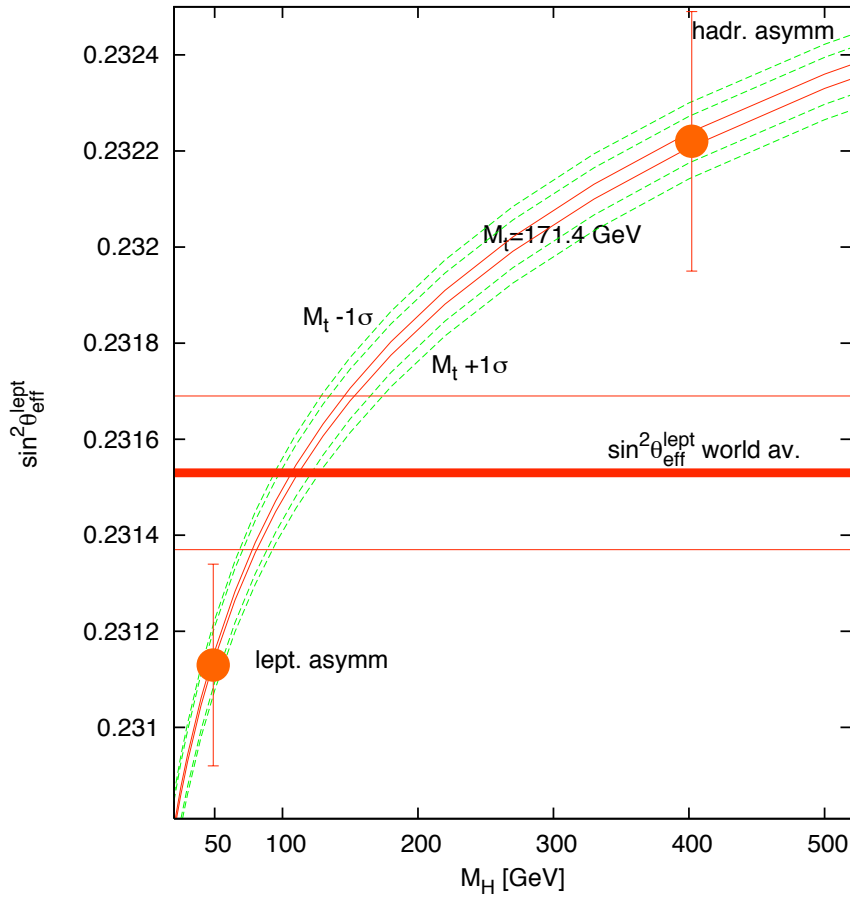


Figure 1.2: Measured values of $\sin^2 \theta_W$ from leptonic and hadronic observables vs. the Higgs mass m_H in the Standard Model (taken from [13, 14]).

to theoretical uncertainties, is also present in another (low-energy) “precision” observable, that is the muon anomalous magnetic moment $g_\mu - 2$. In this case some additional input to control the hadronic contributions has to be used. Depending on the source of the data, *i.e.* the cross section of $e^+e^- \rightarrow$ hadrons or the τ hadronic decays, the theoretical prediction presently differ from the experimental measurement by either 3.3σ or just 1σ [15], hinting again to theoretical uncertainties as the source of the discrepancy.

Whether we already probed a departure from the SM predictions in the gauge sector remains an open question that hopefully will be answered *a posteriori* in the next decade.

The experimental tests of the other two sectors do not share the same degree of precision. The Yukawa sector has recently entered in the Era of “precision” measurements, especially with the contributions of the B-factory experiments, BaBar and Belle, and with the collider experiments CDF and DØ, CLEO and CLEO-c. In particular, the SM description of the Flavor and CP-Violation, that is the Cabibbo-Kobayashi-Maskawa (CKM) mechanism, has only recently found its definitive confirmation into the experimental data as the main source of Flavor and CP-Violating phenomena. The current research in this sector is now focused in seeking for departures from the SM predictions. This is achieved by probing the Yukawa sector at the loop level accuracy [16, 17]. Various observables which are directly probing radiative corrections have been measured and, even though few “anomalies” are present, no significant deviation has been found so far, as shown in Fig. 1.3.

Indeed one could argue that the only experimental evidence for Physics Beyond the Standard Model does not come from phenomena at the electroweak scale. Two of them comes from much lower, sub-eV, scales: neutrinos are massive particles and there is evidence for the presence of an unknown *Dark Energy* in the Universe¹. The third one, the presence of unknown *Dark Matter* (DM) in the Universe, strictly speaking does not point to any specific energy scale unless some assumptions on its nature are made. For example, only if one assumes that the Dark Matter is composed by new particles thermally produced during the expansion of the Universe, then an upper bound on their mass can be cast around 30 TeV. In addition, if these particles are interacting only through forces with strength com-

¹Note that both scales are related to operators that are not probed by collider experiments: the first is an irrelevant dimension-5 operator breaking an accidental global symmetry of the SM. The other is the identity operator, that becomes physical only by considering gravitational interactions.

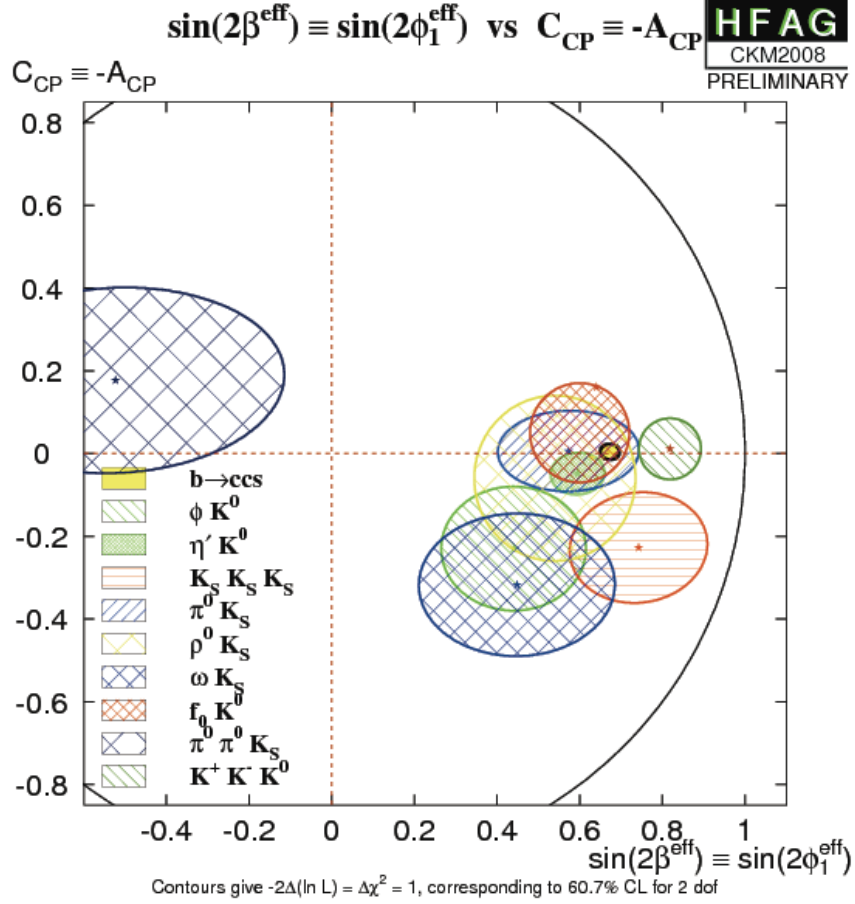


Figure 1.3: Measured values of CP violation parameters in various decay modes of neutral B mesons. Taken from [18].

parable to the weak force (Weakly Interactive Massive Particles or WIMPs), then one obtain an energy scale of the order of a TeV. This scale is not far from the Electroweak scale and renders the WIMP hypothesis quite appealing. However, both for the case of the Dark Matter and for the neutrino masses, the SM can be easily modified to account for them and these two modifications does not shed any light on the nature of the third sector of the SM, the Higgs sector.

In fact, while the gauge sector has already passed its tests and the Yukawa sector is still being analyzed, the Higgs sector has been the most elusive of the

three and no direct experimental evidence is available for it yet.

The SM certainly captures the essential features of how the $SU(2)_L \times U(1)_Y$ gauge symmetry is broken down to the $U(1)_{em}$ of the electromagnetism and how the masses for the W and Z bosons and for matter fields are generated. Despite its simplicity, the SM Higgs mechanism, accomplished with only a single scalar $SU(2)_L$ doublet, is effective in explaining the relations between the masses of the W and Z vector bosons, between their couplings, or in giving a rationale for the smallness of neutrino masses.

The problem is, in some sense, that the SM Higgs mechanism is “too simple”: it is just a parameterization of EWSB but it does not *explain* it. All the ElectroWeak Symmetry Breaking is described by the potential

$$V(\varphi) = -\mu^2|\varphi|^2 + \lambda|\varphi|^4, \quad (1.2)$$

with φ being the Higgs doublet. It depends only on two free parameters, the mass term μ and the quartic coupling λ of the Higgs field. Unfortunately, these are in a one-to-one correspondence with two observables, the vacuum expectation value, v (or the Fermi constant, G_F), and the physical Higgs boson mass, m_H . The first is already measured since a long time, the second is not. Within the SM there is no indication for a “preferred” range for the value of m_H , except an upper bound of ~ 1 TeV, coming from the fact that the Higgs boson is required to unitarize the scattering amplitude for the longitudinal modes of the weak gauge bosons at high energy [19, 20]. This lack of predictivity makes \mathcal{L}_H difficult to constrain and to test experimentally, until the Higgs boson will be found or the lower bound on its mass will be pushed up to ~ 1 TeV.

However, any specific model of EWSB leaves an indirect imprint in the EWPT through the radiative corrections. Even if this is not enough to pin down a specific model, it can constrain its parameter space.

How the SM Higgs mechanism confronts with the EWPT? The EW Precision Observables are logarithmically sensitive to m_H through loop effects and one can look at the significance of the SM global fit as a function of the Higgs mass. This is shown in Fig. 1.4, the famous “blue band” plot.

If the SM is the complete description up to energies of $\sim 5 \div 10$ TeV [21, 22, 23], the fit prefers a light Higgs boson, not too far from the Z , and lighter than the present experimental lower bound, set by LEP at 114.4 GeV. It suggests that the Higgs boson is not far from being discovered. However, as it will be explained in the following, there are various reasons to expect the presence of some New Physics (NP) in the same energy range and the above conclusion may also change.

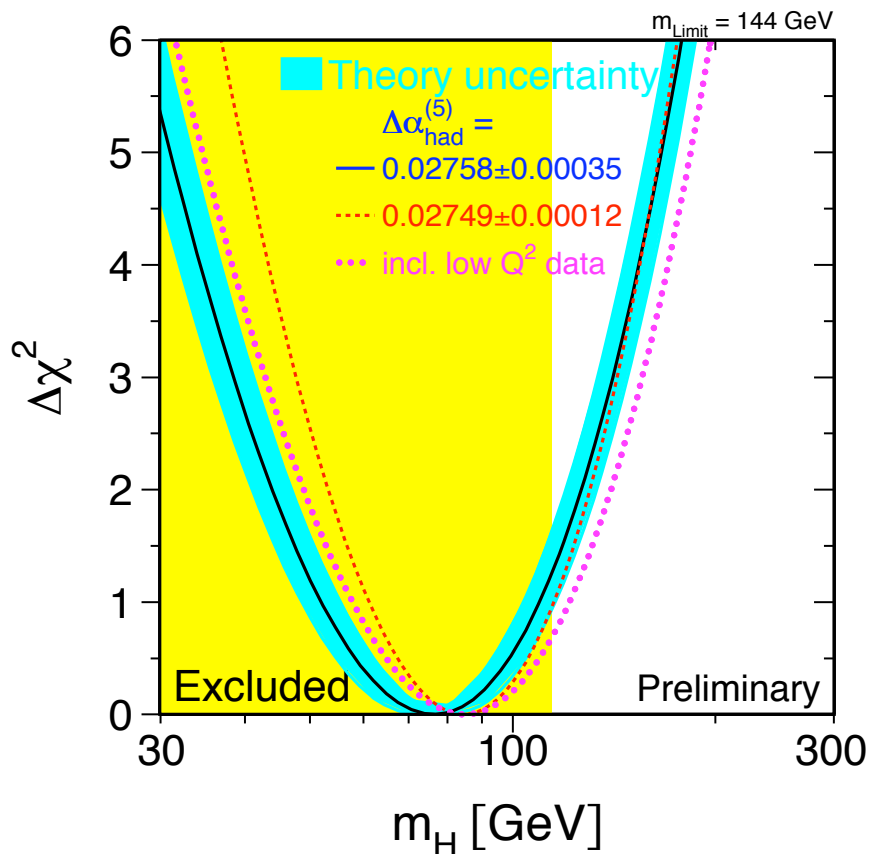


Figure 1.4: χ^2 distribution of SM fit as a function of the Higgs mass. The shaded region corresponds to the LEP limit on m_H .

1.2 Many reasons to go “beyond”

If the Standard Model fits the data quite well and the same data suggest that the Higgs boson is just behind the corner, why every theorist is uncomfortable with that and in the last 30 years there has been a lot of activity in formulating “Beyond the Standard Model” (BSM) theories? Indeed there are more profound reasons than just the need for the favorite candidate to have valid competitors in a challenge. These reasons directly involve the fact that the Higgs boson in the SM is an elementary scalar field, and elementary scalars are usually “bad”. One can see the problem, without leaving the SM, by looking at the radiative corrections to the Higgs mass parameter, μ , in Eq. (1.2). By computing, *e.g.* the

1-loop corrections due to the top quark one finds:

$$\delta\mu^2(top) = \frac{3}{\sqrt{2}\pi^2} G_F m_t^2 \Lambda^2 = (0.9 \text{ TeV})^2 \left(\frac{\Lambda}{3 \text{ TeV}} \right)^2. \quad (1.3)$$

It is quadratically divergent. From an effective field theory point of view, in which the SM is regarded as a theory valid below a cutoff energy Λ , it means that the Physics playing a major role in the determination of μ is the unknown one, near Λ , where the SM ceases to be valid. This reflects the fact that μ is a free parameter and that in the SM there is no rationale on what should be its “natural” size. Moreover if one looks at the value of μ at energies $\ll \Lambda$ one finds that

$$\delta\mu^2 \simeq \mu_0 + \delta\mu^2(top) + \delta\mu^2(gauge) + \delta\mu^2(Higgs). \quad (1.4)$$

It means that the value of μ is one loop factor below Λ , unless cancelations happen in the above formula [24], which are unexplained (unnatural) since the various terms come from different sectors of the theory (gauge, Yukawa and Higgs), unrelated by any symmetry with each other. Hence, values of $\mu \ll \Lambda/4\pi$ cry for an explanation and there is a *naturalness* problem. To understand how bad this problem is, one has to determine what is the size of Λ .

Before continuing, it is worth mentioning the possibility that this may not be the right question to ask. In fact there could be no “explanation” coming from the structure of the theory. Some have argued [25] that the naturalness problem could have an *environmental* solution, by postulating that the fundamental theory possesses many vacua and that μ assumes different values in different vacua. The probability of measuring a particular value for μ is then linked to the probability for an observer to live in a particular vacuum. In a continuously expanding Universe, bubble nucleation could create many different regions in which μ assumes many different values. The Physics (and the cosmological evolution) of bubbles with considerably different values of μ will be profoundly different from the one we observe. The naturalness problem could disappear (or it could be greatly ameliorated) once one convolves the (unknown) “a priori” distribution of vacua with the conditional probability of observing the particular realizations accessible to us. However, the fact that one has a single data point represented by our observed universe and that there is little theoretical understanding of the properties of this *landscape* of vacua, presently makes this argument difficult to translate into testable explanations, capable of making some predictions. Some progress in this direction has been recently made by seeking correlations among different observables in [26, 27, 28, 29].

For the rest of this work we will assume that the size of μ can be explained by the *microscopic* structure of the theory. The question is then what Λ_{SM} is and what we know about it.

There are various hints from known Physics that suggest the existence of physically relevant energy scales (much) above $G_F^{-1/2}$.

One reason is that the gauge structure of the SM and the hypercharge assignments for the various matter fields seem a little bit “artificial”². Another one is that the Yukawa sector has many free parameters (fermion masses and mixing angles) whose values are not explained by the SM.

Indeed a new mass scale appears upon noticing that the strengths of the different SM gauge interactions flow towards a common value at high energy. Pursuing this idea of strong-electroweak (Grand) Unification one finds an energy scale associated to the restoration of this enlarged symmetry, $M_{GUT} \sim 10^{16}$ GeV [30, 31]. This idea is also supported by the fact that, in some GUT theories, relations arise among certain entries of the Yukawa matrices and are in fair agreement with the data [32, 33].

Another argument leading to high energy scales is the recent measurements of the flavor oscillations among neutrinos, indicating that neutrinos are massive. The SM, with its minimal matter content and gauge structure, does not provide a mass term for the neutrinos at the renormalizable level. It has to be complemented either by adding a new interaction of non-renormalizable type, $(LH)^2/\Lambda$, or by extending the field content with additional gauge singlet fermions. In particular, in the first case³ $\Lambda \sim 10^{14}$ GeV, another mass scale not far from M_{GUT} .

If one considers the SM valid up to $\Lambda_{SM} = M_{GUT}$ then the naturalness problem of Eq. (1.4) assumes an embarrassing size, requiring a cancelation of 1 part in 10^{30} . Some kind of New Physics entering at an intermediate scale is required to take care of it. This constitutes the “old” Gauge (Big) Hierarchy Problem [34] and it alone already motivates the BSM research program (see Sect. 1.3).

Many of the proposed models predict the existence of NP at a much lower scale. The purpose of this NP is to shield the Higgs sector from the radiative corrections coming from much higher energy scales.

²Actually the $U(1)_Y$ quantum numbers can be justified by the requirements of consistency (*i.e.* absence of gauge anomalies) and parity invariance of the unbroken gauge sector (QCD and QED).

³In the second case one can write a Majorana mass M_N term for the right-handed neutrinos and there is no symmetry argument forcing this mass term to be small. In particular if $M_N \gg v$ then one can integrate out these states and at low energy, at leading order, one is left just with the $(LH)^2/M_N$ operator.

The paradigm that emerges by trying to solve the Big Hierarchy Problem is the presence of New Physics at a low scale, probably around a TeV, as suggested by Eq. (1.3). This unknown Physics is directly related to the mechanism generating the Fermi scale and it is likely to be responsible of triggering the EWSB. Discovering the presence (or absence) of NP at the TeV will be paramount in shedding some light on what really constitutes the “Higgs sector”, \mathcal{L}_H in Eq. (1.1), of the SM.

As already stated, in the last ten years other NP energy scales entered into this picture. The recent cosmological observations require the presence of unknown Dark Matter. If the DM is composed by stable particles, then the mass of these particles constitutes another interesting physical scale.

However, since we only observe the present abundance, the inferred mass depends on the DM interaction properties. The case in which the DM particles interact/annihilate into SM particles with weak strength is particularly interesting⁴. In this case one finds that $M_{DM} \sim \text{TeV}$, not far from the NP energy scale introduced in most of the models addressing the gauge hierarchy problem.

As we have seen from Eq. (1.4), experimental and theoretical hints point towards NP at energies of the order of a TeV (4π , a loop factor, above $G_F^{-1/2}$) and the next collider experiment, the LHC, will be devoted to carefully explore this energy range and help sorting out all these issues related to the EWSB.

1.3 Solving to the Big Hierarchy Problem

In principle there are two aspects of the Big Hierarchy Problem, the first and more important being the stabilization of the hierarchy against radiative corrections. Achieving this goal, renders the theory *technically natural*, since once a small parameter has been introduced to generate v/M_{GUT} , it remains radiatively stable. The second aspect of the Big Hierarchy Problem is to explain *why* $v \ll M_{GUT}$. A theory can be defined truly natural only if it also provides an explanation of the smallness of the EW scale.

Indeed the only known mechanism to generate naturally large hierarchies is based on non-perturbative effects in gauge theories where the gauge, interactions

⁴Having the DM particles charged under strong interactions usually creates problems in Astrophysics, *e.g.* by altering stellar evolution. The other possibility is to have these new particles interacting with a new kind of force (like axions, etc.): in this case the allowed mass range can be very different and it is only partially constrained from astrophysical processes like Supernova cooling, etc.

become strong at low energy. In this case the hierarchy exponentially depends on the size of the gauge coupling at the UV cutoff of the theory and large ratios may be easily generated.

On the other hand, the Standard Model can be rendered technically natural in various ways, even though it is not a completely easy task.

To show the generic issues involved when one is facing the problem perturbatively, let us consider a “toy” scalar $\lambda\phi^4$ theory. Working in the effective field theory language let us assume that it is valid below a cutoff energy scale Λ . In the theory, all the physical scales are controlled by the size of the mass parameter μ . One can ask what is the natural hierarchy achievable between $\langle\phi\rangle \sim \mu$ and Λ . By computing the loop corrections one finds that $\delta\mu^2 \sim \lambda\Lambda^2/16\pi^2$, which means that $\langle\phi\rangle/\Lambda \sim 1/4\pi$ and that the “natural” hierarchy achieved is of one order of magnitude⁵.

The way to overcome this result is to modify the theory and introduce a mechanism to effectively cancel those loop contributions to the mass parameter that are quadratically divergent. By canceling up to the k -th loop order, one can safely allow a smaller μ without prejudicing the naturalness. All the values of μ^2 larger than $\lambda^k\Lambda^2/(16\pi^2)^k$ are now “natural” and the hierarchy can increase up to $\sim 1/4\pi(\sqrt{\lambda}/4\pi)^{k-1}$, and ultimately it is limited only by the scale at which the quartic coupling hits its Landau pole, which is controlled by the logarithmic running of the couplings and can be exponentially large. However ensuring this kind of cancelations is not easy, and it is usually achieved by relying on some sort of symmetry. The only known symmetry allowing this cancelation to all orders in perturbation theory (necessary to create the GUT/Fermi hierarchy) is the “chiral symmetry” for scalar fields, *i.e.* Supersymmetry.

1.3.1 Supersymmetry

Supersymmetry (SUSY) [35, 36, 37] is a spacetime symmetry that relates particles of different spin. An irreducible representation of SUSY includes both bosons and fermions, whose masses and coupling constants are constrained by it. In particular the masses have to be the same and only a certain set of their interactions are allowed. This enhanced symmetry reduces the UV freedom of the theory, rendering it better behaved. For example a famous result states that in a supersymmetric theory the matter (scalar/Yukawa) potential is not renormalized to all orders in perturbation theory [38, 39]. In practice this less divergent behavior is due to a

⁵In the case of multiple scalar fields like in an $O(N)$ theory it is even smaller: $\sqrt{N}/4\pi$.

cancelation between bosonic and fermionic loops containing particles belonging to the same SUSY multiplet. This clearly is a step forward to ameliorate/solve the hierarchy problem, since the quadratic divergence in the Higgs mass term can be completely canceled in a SUSY theory. The problems arise when one tries to use SUSY to build realistic models. This “doubling” of the spectrum is not observed in Nature and SUSY should be broken at some energy scale. The size of the mass splitting between the SM particles and their superpartners, m_{SUSY} , will be proportional to the size of the breaking. The UV divergences of the non-supersymmetric theory will be cutoff by this scale. This means that m_{SUSY} can not be very far from the electroweak scale if Supersymmetry has to cure the Hierarchy Problem. Moreover the breaking cannot be spontaneous if SM particles are directly involved: in fact spontaneous SUSY breaking leaves SUSY still imprinted in the spectrum as a set of relations among the masses of the particles belonging to the same multiplet [40, 41]. A spontaneous SUSY breaking scenario in the SM is ruled out experimentally by combining the SM spectrum with the lower bounds on supersymmetric particles coming from direct searches at colliders. The general framework is then to assume SUSY breaking (either spontaneous or dynamical) happening in an *hidden* sector, which is then *mediated* by some mechanism to the *visible* sector consisting in the SUSY version of the SM.

Such supersymmetrization of the SM, on top of the doubling of the spectrum prescribed by SUSY, requires the addition of another Higgs doublet (and its SUSY partner) with opposite hypercharge. This is needed for two reasons: the first is the cancelation of the Higgsino contribution to the $U(1)_Y$ -anomaly and the second is the requirement to write the masses for both the up and down quarks in a SUSY-invariant way. This fact extends the SM Higgs sector to the one of a Two Higgs Doublet Model (2HDM) and one expects to find additional scalar states after EWSB: two other neutral ones (one CP-even and one CP-odd), and a charged one.

A phenomenological approach to encode SUSY breaking in the supersymmetric SM is to add all possible non-supersymmetric terms coming from the mediation of SUSY breaking. A specific model of SUSY breaking generates relations among these different terms, but keeping them free allows to cover all the possibilities. These additional terms includes masses for scalar superpartners of SM fermions (sfermions), for the fermionic superpartners of the gauge bosons (gauginos), for the Higgs bosons and some trilinear Higgs-sfermion-sfermion interactions (A-terms). They are all “soft” breaking-terms, meaning that are dimensionful parameters whose effects in radiative corrections vanish in the limit in which they vanish. This

implies that no quadratic divergences are reintroduced and that it is technically natural for them to be small, of the order of m_{SUSY} . The addition of these soft terms to the supersymmetric version of the SM constitutes what is called the Minimal Supersymmetric Standard Model (MSSM) [31].

The virtue of this approach is that in principle it is possible the study of phenomenology without having to specify the details of SUSY breaking. One then finds that generically the EWSB is triggered by the top-stop loop, driving the Higgs mass term towards negative values at energies below the scale of superparticle masses, that a stable particle exists⁶, in most of the cases neutral and weakly-interacting, providing a candidate particle for the Dark Matter, that the gauge couplings unify at a high scale, that the Higgs quartic coupling is of the order of the weak coupling constant at tree level and it is raised mostly by the top/stop loop contributions, generically implying a light Higgs boson.

In practice the number of additional parameters in the *phenomenological* MSSM is enormous and to work out a quantitative analysis one has to assume some relations among the soft parameters, motivated by the known mediation mechanisms. Two of the most popular mediation mechanisms are Gravity Mediation [42], *i.e.* by higher dimensional operators suppressed by the Planck scale, and Gauge Mediation [43, 44], *i.e.* through gauge radiative corrections. In general each mechanism has its virtues and drawbacks (for example the Flavor Problem in Gravity Mediation or the $\mu/B\mu$ Problem in Gauge Mediation) and a lot of model building activity of the last two decades was devoted to devising possible solutions to these problems.

Even if one has achieved very interesting results by supersymmetrizing the SM (gauge coupling unification, DM candidate, stabilization of radiative corrections, explanation of the EWSB as triggered by the top radiative corrections, etc.) still problems remain. They are all related to the unknown SUSY breaking mechanism. In fact, to fully understand the Gauge Hierarchy Problem, one has to find a mechanism to generate a mass scale of $\mathcal{O}(\text{TeV})$ (which is now a technically natural scale), needs a mechanism that naturally gives the suppression to the Flavor and CP-Violating contributions coming from superparticle loops [45, 46, 47] and has to be consistent with the EWPT and with direct searches of SUSY particles.

⁶If R-parity is intact, which is required by proton stability in Grand Unified Theories.

1.3.2 Strong Dynamics

The other known methods to create large hierarchies does not rely on (explicitly) enforcing a symmetry to cancel radiative corrections in perturbation theory, but on something else. One way is to directly exploit the rich dynamics in strongly coupled gauge theories. It is well known from the example of QCD, that asymptotically free gauge theories become strong in the IR at an energy scale Λ_{IR} , exponentially suppressed with respect to the theory cutoff Λ_{UV} , since $\Lambda_{IR}/\Lambda_{UV}$ is essentially determined by the (logarithmic) running of the coupling constant. It is also known that in these theories the dynamics at (and below) Λ_{IR} can be very interesting: the low energy degrees of freedom are bound states of the fundamental ones and composite operators can get non-zero expectation values, dynamically breaking the symmetries of the theory⁷.

For this mechanism to be usable for the EWSB, one has to assume that uncalculable effects in the strong dynamics select a vacuum in which some operators have non-zero vevs. This breaks some of the global symmetries of the theory, containing or coinciding with the EW $SU(2)_L \times U(1)_Y$ group. In particular, the effective theory below Λ_{IR} may contain scalar degrees of freedom without introducing a naturalness problem: at the scale Λ_{IR} their composite nature becomes manifest and quantum loops are naturally cut off at this scale. In practice the main difficulty of these theories is their (un-)calculability, due to the intrinsic necessity of having a strong coupling regime, where standard perturbation theory is not applicable.

Nevertheless, during the years, various techniques have been developed to cope with this issue and an exploration of these ideas in certain limits has been feasible. Some of the results found have been tested by lattice simulations, especially with the recent improvements of computational techniques [48, 49, 50].

Besides the naive energy rescaling of the (known) dynamics of QCD (that has almost immediately found phenomenological difficulties [51]), the most commonly used method is based on the expansion in the large number of colors N_c [52]. Many results in the 80s and early 90s have been derived in this limit.

Moreover at the end of the 90s, a weak/strong duality, the AdS/CFT, has been found between a (SUSY) conformal gauge theory and a string theory in a curved background [53]. This duality is such that the large- N_c , strong 't-Hooft coupling limit of the conformal gauge theory is dual to the low energy, weak

⁷This is the case of chiral symmetry breaking in QCD or of SUSY breaking in SQCD with a suitable matter content.

gravity limit of a string theory on a $AdS_5 \times S_5$ space. While this duality involves a specific SUSY theory, it has motivated the study of five dimensional field theories on warped Anti-de-Sitter (AdS) space as “templates” for strongly coupled 4D theories, *i.e.* the Randall-Sundrum models [54, 55, 56]. “Dictionaries” between the 4D and 5D languages has been derived [57, 58, 59]. For example global symmetries in the 4D picture correspond to gauge symmetries in the bulk of the AdS space; fields whose 5D wave-functions are localized close to the AdS boundary correspond to 4D elementary degrees of freedom; fields whose support is localized deeply in the AdS bulk describe 4D composite objects.

The geometrical structure and the improved calculability of the AdS theories boosted a lot of investigation of large- N_c strongly coupled theories in the past years. However, while providing a very natural solution of the Big Hierarchy Problem, these theories generically face serious problems when confronted with Precision Tests, as it will be explained in the following Section. While it is clear that many of these problems are actually connected with the necessity of taking the large N_c limit, it remains an open question whether a consistent small- N_c theory of EWSB may exist [60, 61].

1.3.3 Large Extra Dimensions

Recently a third, conceptually different, way to create a large hierarchy between the Planck scale and the Fermi scale has been introduced. It relies on the existence of additional spatial dimensions [62, 63]. The key mechanism is “volume suppression”: if there are additional dimensions and some interactions (gravity) can propagate in all of them, while others (SM forces) are confined to propagate only in the standard 3+1 ones, then the former will appear “diluted”, hence weak, to the eyes of a 4-dimensional observer. Thus the fundamental Planck scale M_* can easily be at a few TeV while the gravitational interactions can still appear much weaker, by a factor of $(M_*R)^n$, with R the typical size of the extra dimensions and n their number. The Fermi scale is now natural because the fundamental cutoff of the theory (where a more fundamental theory like string theory will show up) can be at the TeV scale. This power law dependence of the volume suppression factor with the number of extra dimensions is the key to create a large hierarchy between the strengths of the various forces. Given the fact that the $1/r^2$ behavior of gravity has been probed down to 10^{-2} mm, one can allow “large”, μm -sized, extra dimensions and easily achieve the required suppression. Large extra dimensions provide another technical solution of the Big Hierarchy Problem, while for a

Dimensions six operators	$m_h = 115 \text{ GeV}$	
	$c_i = -1$	$c_i = +1$
$\mathcal{O}_{WB} = (H^\dagger \tau^a H) W_{\mu\nu}^a B_{\mu\nu}$	9.7	10
$\mathcal{O}_H = H^\dagger D_\mu H ^2$	4.6	5.6
$\mathcal{O}_{LL} = \frac{1}{2} (\bar{L} \gamma_\mu \tau^a L)^2$	7.9	6.1
$\mathcal{O}'_{HL} = i(H^\dagger D_\mu \tau^a H) (\bar{L} \gamma_\mu \tau^a L)$	8.4	8.8
$\mathcal{O}'_{HQ} = i(H^\dagger D_\mu \tau^a H) (\bar{Q} \gamma_\mu \tau^a Q)$	6.6	6.8
$\mathcal{O}_{HL} = i(H^\dagger D_\mu H) (\bar{L} \gamma_\mu L)$	7.3	9.2
$\mathcal{O}_{HQ} = i(H^\dagger D_\mu H) (\bar{Q} \gamma_\mu Q)$	5.8	3.4
$\mathcal{O}_{HE} = i(H^\dagger D_\mu H) (\bar{E} \gamma_\mu E)$	8.2	7.7
$\mathcal{O}_{HU} = i(H^\dagger D_\mu H) (\bar{U} \gamma_\mu U)$	2.4	3.3
$\mathcal{O}_{HD} = i(H^\dagger D_\mu H) (\bar{D} \gamma_\mu D)$	2.1	2.5

Table 1.1: 95% lower bounds on Λ/TeV for the individual operators and different values of m_h . χ_{\min}^2 is the one in the SM for $m_h > 114.4 \text{ GeV}$. Taken from [64].

truly natural solution one further needs to describe the stabilization of the radii of these μm -sized new dimensions.

1.4 The Little Hierarchy Problem

In the previous Section we argued that there are many indications pointing out to the presence of unknown NP at energies around a TeV.

However TeV-scale New Physics is sufficiently low in energy to possibly leave its imprints on the EWPT. One can search for such signatures. A way to summarize the results of such searches is to use the language of Effective Field Theories. It is possible to parameterize the possible contributions of New Physics that can affect electroweak observables by adding to the SM Lagrangian a set of operators of dimension greater than 4, organized as a power series in Λ^{-1} , the cutoff scale of the SM. Assuming $\mathcal{O}(1)$ coefficients, one can put lower bounds on Λ from the data collected at LEP and SLC [21].

The results of this analysis are summarized in Table 1.4 with the most stringent ones suggesting $\Lambda_{SM} > 5 \div 10 \text{ TeV}$ (mostly coming from the S-parameter). By looking at the SM only, one finds that the requirement of $\Lambda_{SM} = 10 \text{ TeV}$ implies a cancelation in Eq. (1.4) of 1 part in (600,100,60) for the top, gauge and Higgs sectors respectively: not as dramatic as in the Gauge Hierarchy Problem, but still

somewhat troublesome. A more quantitative estimate is usually given in terms of the so-called finetuning parameters [65]: if a is a fundamental parameter of the theory and it plays a role in EWSB, then

$$D_a = \frac{\partial \log v^2}{\partial \log a} \quad (1.5)$$

measures the sensitivity of the Fermi scale to small variations of a .

The data collected in the EWPT render the EWSB *Hierarchy problem* a completely low energy problem. This has been called *Little Hierarchy Problem* stressing its low energy aspects, or *LEP Paradox* stressing its origin in the EWPT data [64].

One can think of this tension as a hint towards the correct description of EWSB from the presently available experimental data. It is therefore interesting to pursue the study of models that solve the Little Hierarchy Problem, that achieve EWSB naturally (*i.e.* without too much finetuning) and are consistent with the EWPT.

From an experimental point of view, it strengthens the expectation that the answers to questions like “which is the correct theory of EWSB?” or “is the theory of EWSB natural?” may lie just behind the corner of the current energy frontier. This expectation motivates the present activity of the Fermilab TeVatron and the construction of the forthcoming CERN LHC, an hadronic (pp) machine able to explore energies up to a few TeV.

Given that the *Little Hierarchy Problem*, defined as above, is such in the sole SM, where there are no new states between the Fermi scale and the multi-TeV UV cutoff, one can ask himself which is the status of the other models presently available that have addressed the question of explaining EWSB and solving the *Big Hierarchy Problem*, after the information contained in the EWPT is used. Does any of these models already solve the *LEP Paradox* or do they have *Little Naturalness* issues as well?

1.4.1 SUSY and the LEP Paradox

In the case of the MSSM, EWSB is triggered radiatively by the top-stop loop. In this way the Fermi scale is naturally related to the SUSY breaking scale.

Within the MSSM, the top corrections to the Higgs mass include the contribution from the supersymmetric partner of the top quark, which is of the opposite sign. Eq. (1.3) becomes

$$\delta m_H^2(\text{top} - \text{stop}) = \frac{3}{\sqrt{2}\pi^2} G_F m_t^2 m_{\tilde{t}}^2 \log \frac{\Lambda^2}{m_{\tilde{t}}^2} = 0.1 m_{\tilde{t}}^2 \log \frac{\Lambda^2}{m_{\tilde{t}}^2}. \quad (1.6)$$

Now the finetuning in the determination of the Fermi scale is controlled by $m_{\tilde{t}}$ and by the logarithm of $\Lambda/m_{\tilde{t}}$, with Λ the scale at which SUSY breaking is mediated to the MSSM. A natural theory would have $m_{\tilde{t}} \sim \mu \sim v$ and a small argument of the logarithm. However in many SUSY breaking scenarios, in order not to spoil unification or create other phenomenological problems, SUSY breaking is mediated at a quite high scale, thus leading to a large logarithm⁸. The problem is even worse since in the MSSM the Higgs boson mass at tree level is bounded from above by the Z mass, and the loop corrections from the top sector are given by⁹

$$\delta m_h^2 = \frac{6}{\sqrt{2}\pi^2} G_F m_t^4 \log \left(\frac{m_{\tilde{t}}^2}{m_t^2} \right). \quad (1.7)$$

In order to evade the LEP bound on the Higgs mass one has to have $m_{\tilde{t}} \gg m_t$. At the end one finds that the MSSM still requires a cancellation at a few % level to have a successful EWSB and a Higgs boson mass larger than the current experimental bound. This partly recreates the *LEP paradox*.

In view of a solution of the ‘‘Little Hierarchy Problem’’ which does not involve sizable amount of unnatural finetunings, the current MSSM is not enough. This motivates further research and analysis on EWSB.

Given that part of the problem is due to the absence of a large tree level quartic for the Higgs, one can still remain in the framework of SUSY but extend the MSSM. The simplest extension, *i.e.* the NMSSM, obtained by adding a singlet superfield to the MSSM, already seems to be beneficial. It allows in fact a heavier Higgs [68], and/or opens up some decay channel for the Higgs boson that can circumvent the LEP direct searches, allowing a lighter, less tuned, supersymmetric Higgs boson [69].

1.4.2 Models with strong dynamics

Technicolor/Higgsless models in which strong dynamics breaks directly the Electroweak symmetry, usually have problems with EWPT. In particular the contribution to the S-parameter, which is not protected by any symmetry¹⁰, generically turns out to be fairly large [73, 74] unless some finetuning is introduced [75]. These estimates are based on a large N_c limit or on some ‘‘dual’’ 5D warped model. In

⁸Ways to reduce the size of the log have been pointed out *e.g.* in [66, 67].

⁹In absence of A-terms. In principle an additional positive contribution proportional to $G_F m_t^4 X_t^2$ with $X_t = A_t/m_{\tilde{t}}$ is possible.

¹⁰On the other hand, large corrections to the T-parameter and to the $Zb\bar{b}$ coupling can be successfully eliminated by the usage of a *custodial* symmetry [70, 71, 72].

general the models can be made consistent with the EWPT at the price of fine-tuning two independent contributions to the S-parameter, one arising from the excited resonances of the electroweak gauge bosons, the other coming from the matter sector [76]. Stronger constraints come from the Flavor and CP-Violating observables (especially $K - \bar{K}$ mixing), once the problem of generating masses for the quarks is addressed [77]. While there is no proof that a non-finetuned low- N_c higgsless model does not exist, in order to solve the Little Hierarchy Problem one is led to explore models in which the strong dynamics breaks a larger symmetry group and there a Higgs boson appears as a composite state (like a pion) at lower energies. Given the fact that the separation of scales required to solve the LHP is a factor of $\mathcal{O}(100)$, a two-loop factor, it means that the requirements imposed by the EWPT constrain up to the leading radiative corrections. Thus it is worth studying the perturbative low-energy “chiral” effective Lagrangian of these composite Higgs models, in order to explore different avenues in solving the LEP Paradox.

One interesting way to proceed is to make the Higgs a Pseudo-Goldstone boson (PGB) [78]. Suppose that the Higgs sector enjoys an extended global symmetry with group G , broken spontaneously to a smaller symmetry group H . Then one expects the presence of a certain set of massless Goldstone bosons, associated to the quotient G/H . However, if this symmetry is a property of the Higgs sector alone and the SM electroweak and Yukawa interactions do not respect it, there will be a small source of explicit breaking. Radiative corrections then generate a potential for the Goldstone modes, lifting their masses.

However, declaring the Higgs to be a PGB can not be the end of the story: in this way one has just forbidden the tree level mass term, but the size of the radiative corrections needs to be controlled to create the required mass hierarchy. In fact the generic potential generated for the PGB is

$$V(\varphi) = f^4 \cos\left(\frac{\varphi}{f}\right), \quad (1.8)$$

where f is the $G \rightarrow H$ symmetry breaking scale (naively $4\pi/\sqrt{N}$ below the cutoff Λ , where N is a generic multiplicity factor). This shows that without doing anything else $v \sim f$ and nothing is gained. There are two ways out of this problem, as suggested from the minimization of the formula Eq. (1.2), $v = \mu/\sqrt{\lambda}$: either by suppressing the quadratic term or by enhancing the quartic. The second possibility is in general more attractive since it easily allows for a heavier physical Higgs boson, above the direct search bound. However it is also more difficult because one has to avoid that the new large quartic coupling reintroduces large radiative

corrections in the quadratic term, lifting it and keeping the ratio $\mu/\sqrt{\lambda}$ practically constant. There has been a few directions pursued here, like using the idea of collective breaking [79] in the “Little Higgs” models, or by using discrete symmetries [80] like in the “Twin Higgs” or by parametrically enhance the separation between f and v by large symmetry group factors [56].

For example in the case of Little Higgs theories, the idea behind collective breaking is to render the Higgs mass term an explicit breaking term of (at least) two different global symmetry groups. In this case a mass term can only be generated by the interplay of at least two different sectors with their own interactions. The radiative corrections to the Higgs mass term are thus pushed to two-loops, gaining an additional $\sqrt{\lambda}/4\pi$ in the v/f formula.

In practice the enhanced symmetry is enforced by the presence of partners of the SM fields (with the same spin, differently from SUSY) that cancel the 1-loop quadratic divergence to the Higgs mass. These partners need to be at the intermediate scale f in order to solve the Little Hierarchy Problem. However, being just a loop factor above the weak scale, they too contribute to the EWPT and if their contribution comes at the tree level the effect is disastrous. In fact the simplest versions of the Little Higgs have problems with EWPT coming from these states at the TeV. In general additional model building is required¹¹, besides the collective breaking idea, that considerably complicates the models.

1.5 Compact Extra Dimensions as a tool for Model Building

The existence of Extra Dimensions is a fundamental ingredient of more complete theories like string theory. In general these new spatial dimensions should be compact and their size should be determined by some dynamical mechanism. Once the radii of the extra dimensions are fixed, they constitute new mass scales in the theory. It is therefore interesting to explore the possibilities that one (or more) extra dimension(s) have size of the order of the electroweak scale $\sim \text{TeV}^{-1}$. Moreover, they also provide new possibilities to address the issues of symmetry breaking and the creation of hierarchies while improving calculability.

The crucial fact is that a compact extra dimension can have “preferred points”.

¹¹For example adding an additional discrete symmetry, T-parity, that prevents these states to contribute dangerously to the precision observables, but still guarantees the cancelation of the divergences in the Higgs potential [81].

These are determined either by the presence of extended objects called branes, similar to topological defects (like domain-walls or kinks), or by the nontrivial topology of the extra dimensional space itself as in the case of an orbifold (a singular space where couples of points are identified under the action of a parity symmetry, like $y \leftrightarrow -y$).

These special points provide special places where some of the fields can be localized or where symmetries of the extra-dimensional (bulk) theories can be broken. While the consistency requirements are different for the case of an orbifold, of a segment or of a non-singular space containing branes, from the low energy point of view they all can be regarded as points in which one can specify a different field content and different symmetries with respect to the bulk theory.

This opens up a number of possibilities to translate common model building issues to geometrical problems, easier to visualize and address. For example by localizing different fields in different locations in the extra-dimensional space one can explain small numbers in their couplings by the smallness of the superposition integral of the corresponding wave-functions. By assigning different boundary conditions to different fields belonging to the same multiplet, one can break symmetries, etc.

In the last fifteen years it has been suggested that the existence of compact extra dimensions possibly can play a role in the EWSB [82, 83, 84, 85]. In particular, in extra dimensional models, one has additional ways to break symmetries, essentially non-local in the extra dimension. The idea behind it is to break symmetries by boundary conditions along the compact extra dimensions. The non-local nature ensures a less UV-sensitive symmetry breaking pattern, reducing the number of parameters and/or milder the impact of the unknown UV contributions on low energy observables, by suppressing them with the volume of the extra dimension. This mechanism, first explored by Scherk and Schwarz [86, 87] in the late seventies as a way to break Supersymmetry, recently came into specific models of EWSB. The most promising ones make use of both the ideas of Supersymmetry and extra dimensions [84, 85, 88, 2]. They use Supersymmetry to reduce the sensitivity of EWSB to the unknown UV Physics and the extra dimension(s) to break Supersymmetry with a reduced number of parameters.

In the following we analyze two specific models of EWSB in extra dimensions [88, 1, 2, 3, 4]. They are five dimensional supersymmetric theories in which the fifth dimension is compact and Supersymmetry is broken by boundary conditions (à la Scherk Schwarz). The size of the Fermi scale and the Higgs boson mass are related to the size of the extra dimension through a small number of

parameters¹² rendering a highly constrained and predictive picture, testable at the Tevatron and the LHC. Furthermore the size of the extra dimension, being the scale of SUSY breaking, determines the spectrum of superparticles. These theories, even though effective low energy theories, remain perturbative up to the multi-TeV region, providing a possible solution of the “LEP Paradox”. Finally the residual symmetries present in the models improve the calculability rendering finite the radiative contributions to non-supersymmetric observables and reducing the sensitivity to the UV Physics.

¹²Zero in the first model, one in the second, plus other few additional parameters that contribute only giving some small corrections.

Chapter 2

Introducing the Constrained Standard Model

In the Introduction we have shown how experimental data favor a perturbative extension of the Standard Model. We have also presented Supersymmetry as one of the most attractive ways to solve the Hierarchy Problem while ensuring perturbativity of the Physics Beyond the Standard Model. We also pointed out why the minimal implementation of this idea, the Minimal Supersymmetric Standard Model, is not completely satisfactory. Naturalness issues arise when the model is confronted with precision electroweak data and direct searches of the Higgs boson and of supersymmetric particles. The model fails to generate the Electroweak Symmetry Breaking scale in a natural way and the reasons reside in the way the Higgs sector and the supersymmetry breaking are described.

One can pursue the idea of using Supersymmetry to ensure perturbativity at least to energies of the order of $5 \div 10$ TeV, those probed by the Electroweak Precision Tests, while adopting another description of supersymmetry breaking.

The use of a compact extra dimension to break supersymmetry has been used in many different models (*e.g.* [89, 90, 85]). Here we will review one of these models, the Constrained Standard Model, introduced in [88]. It constitutes the basis of all the work presented in the subsequent Chapters.

We will take a bottom-up approach in presenting the model, as followed in [1], stressing the choices that are relevant in its definition.

For all the issues concerning supersymmetric field theories with compact extra dimensions and Scherk-Schwarz symmetry breaking, the reader is directed to the literature, in particular to [91, 92, 93, 94].

2.1 The Constrained Standard Model *ab initio*

In the previous Chapter it has been shown that the reason of the hierarchy problem are the large radiative corrections to the Higgs mass and that the largest ones come from the top sector. Since one wants to use supersymmetry to mild divergences and an extra dimension to break it, one can minimally start by introducing only the top quark as a field living in 5 dimensions and by requiring that the theory will be supersymmetric.

Then the $SU(2)$ doublet $Q_3 = (t, b)_L$, containing the left handed top, and the right handed top t_R will depend on 5D coordinates (x_μ, y) and they will fall into two 5D hypermultiplets, \hat{Q}_3 and \hat{U}_3 respectively.

At this point 5D Poincaré and $N = 1$ 5D supersymmetry fix the field content and the quantum numbers of the top sector.

For every matter Weyl spinor f this amounts to introducing a hypermultiplet of (x_μ, y) -dependent fields: for each fermionic state there are another fermionic and 2 complex scalar partners. This is graphically presented in Fig. 2.1, where f^c denotes a spinor with the same chirality of f but opposite quantum numbers. This theory (after dimensional reduction) has 4D $N = 2$ supersymmetry and it is vector-like with respect to $SU(2)_L \times U(1)_Y$. In order to get at low energy the chiral non-supersymmetric top sector of the SM, one must break $N = 2$ SUSY completely and the 5D Lorentz group down to 4D Lorentz.

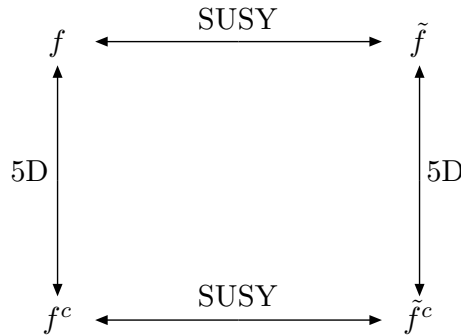


Figure 2.1: Component diagram of a hypermultiplet in 5D.

Since we have decided to use Scherk-Schwarz mechanism [86, 87] to achieve symmetry breaking, we have to say something on the nature of the extra dimension. We take it to be compact, a segment $[0, L]$ or, equivalently, an $S^1/Z_2 \times Z'_2$

orbifold, with a circle of radius R , such that¹ $L \equiv \pi R/2$. All the fields are periodic over the circle of radius R . In this way our extra dimension has two inequivalent endpoints, $y = 0, L$, and we have the freedom to specify two independent sets of boundary conditions, one for each of them. We can specify them on the generators of the 5D SuperPoincaré group. We choose²

- at $y = 0$

$$P^\mu(+)P^5(-) \tag{2.1}$$

$$Q_\alpha^1(+)Q_\alpha^2(-) \tag{2.2}$$

- at $y = L$

$$P^\mu(+)P^5(-) \tag{2.3}$$

$$Q_\alpha^1(-)Q_\alpha^2(+) \tag{2.4}$$

where the upper index of the Q 's is the $SU(2)_R$ index of the 4D $N = 2$ language. As explained in Sect. 2.3. The net effect of this choice is to completely break global supersymmetry while maintaining a residual local supersymmetry unbroken. This residual local supersymmetry will have a fundamental role in determining the UV properties of the theory.

At this point the boundary conditions for all the component fields of a generic 5D supersymmetric multiplet are specified. The resulting spectrum is shown in Fig. 2.2, where the (\pm, \pm) notation refers to the parities (*i.e.* Dirichlet or Neumann boundary conditions) at $y = 0$ and $y = L$ respectively.

In the case of the hypermultiplet however there is still a discrete residual choice, *i.e.* the choice of the $(+, +)$ mode to be a spinor or a scalar. Since this is the only boundary condition that allows for a massless mode and we want to retrieve the SM spectrum at the massless level, we are forced to choose a $(+, +)$ spinor for the Q_3 and U_3 hypermultiplets.

Consistently with supersymmetry, the top Yukawa coupling can be introduced only as a superpotential term localized at one of the boundaries. The reason is due to the $N = 2$ nature of the theory: the hypermultiplets transform as doublets under the $SU(2)_R$ symmetry group and one cannot build a singlet out of 3 doublets. Hence Yukawa couplings can exist only where $N = 2$ SUSY is broken down to

¹Throughout this thesis we will use both L and R , depending on conveniency.

²For a more general analysis see for example [91].

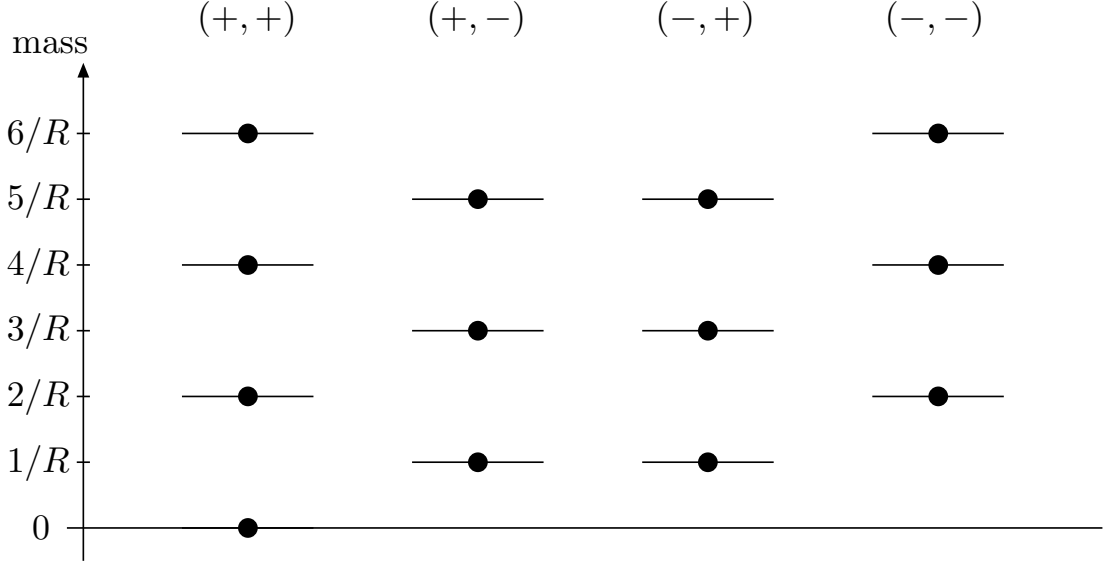


Figure 2.2: Tree-level KK mass spectrum of a 5D multiplet with the indicated boundary conditions.

$N = 1$, *i.e.* at the two fixed points. For concreteness we will introduce the top Yukawa coupling at $y = 0$:

$$\mathcal{L}_Y = \int dy \delta(y) \int d^2\theta \lambda_t \hat{h} \hat{Q} \hat{U} + \text{h. c.}, \quad (2.5)$$

where \hat{h} , \hat{Q} , \hat{U} are $N = 1$ chiral multiplets. In particular \hat{Q} and \hat{U} each contain the fields f and \tilde{f} of Fig. 2.1 with the corresponding quantum numbers. It is irrelevant at this stage whether \hat{h} does or does not have a y -dependence. We assume that the scalar \hat{h} contains a y -independent component $h^0(x)$ which plays the role of the standard Higgs field.

At this point one can repeat in this new setup the computation of the 1-loop top contribution to the Higgs mass performed in Chapter 1 for the SM and the MSSM.

This is most readily done by means of the propagators in mixed momentum-coordinate space $G_i(p; y, y')$ for the different components of the superfield, $i =$

f, \tilde{f}, F [95]. By computing the diagrams of Fig. 2.3 one obtains:

$$\delta m_H^2 = 3 \frac{\lambda_t^2}{4L} \int \frac{d^4 p}{(2\pi)^4} [-\text{Tr}(G_t(p) G_u(p)) + G_{F_u}(p) G_{\tilde{t}}(p) + G_{F_t}(p) G_{\tilde{u}}(p)], \quad (2.6)$$

where $G_i(p) = G_i(p; 0, 0)$. Using Eq. (B.9) of Appendix B one has [88]

$$\begin{aligned} \delta m_H^2 &= -\frac{3\hat{y}_t^2}{4\pi^2 L^2} \int_0^\infty dx x^3 [\coth^2(x) - \tanh^2(x)] \\ &= -\frac{63 \zeta(3)}{32 \pi^2} \frac{\hat{y}_t^2}{L^2}, \end{aligned} \quad (2.7)$$

where $\zeta(3) = 1.20$ and $\hat{y}_t = \lambda_t/(4L)^{3/2}$ is the top Yukawa coupling in 4D (anticipating a Higgs field living in the bulk of the extra dimension as well). The finiteness of Eq. (2.7) is a consequence of local supersymmetry conservation in 5D, as discussed in Sect. 2.3.

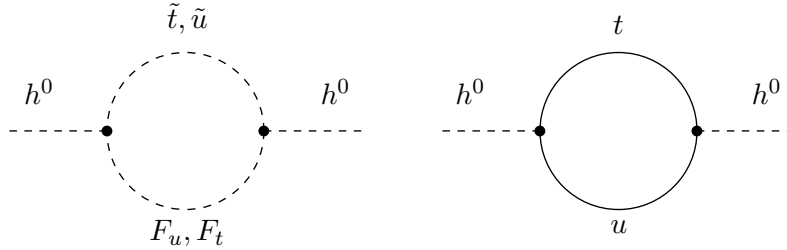


Figure 2.3: One-loop diagrams contributing to the mass squared of the Higgs boson.

2.1.1 The relation between the compactification scale and the cut-off

The finiteness of Eq. (2.7) and the spectrum in Fig. 2.2, with all extra particles in the top hypermultiplet living at or above the compactification scale $1/R$, look as a right step in the direction of solving the LEP paradox. The price to be paid, however, is the non-renormalizability of the coupling, Eq. (2.5), in 5D. Any model that incorporates the physics of Section 1.4 must be thought of as an effective field theory valid up to some cut-off scale Λ . This is not necessarily a problem, however, as long as Λ is sufficiently larger than the compactification scale $1/L$ so

that Eq. (2.7), or similar ones, remain quantitatively meaningful in the usual sense of effective field theories.

Ideally for a solution of the Little Hierarchy Problem one wants at least $\Lambda > 5$ TeV, in order not to assume anything about the effects of the UV completion on the EWPT.

The relation between $1/L$ and Λ can be fixed by requiring that the top Yukawa coupling in Eq. (2.5) becomes non perturbative at Λ , taking into account the increasing number of states whose thresholds are crossed at every unit of $1/R$. With this assumption, the value of \hat{y}_t at Λ can either be estimated by means of usual dimensional arguments, properly adapted to 5D [96],

$$\hat{y}_t(\Lambda) \simeq \frac{1}{16\pi^2} \left(\frac{24\pi^3}{4\Lambda L} \right)^{3/2} \simeq 16.1 (\Lambda L)^{-3/2}, \quad (2.8)$$

or by noticing that the expansion parameter in a 4D calculation involving the top Yukawa coupling is³

$$\frac{2\hat{y}_t^2}{16\pi^2} (N_{KK})^3,$$

where $N_{KK} \simeq \Lambda R = 2\Lambda L/\pi$ is the number of modes below Λ , hence

$$\hat{y}_t(\Lambda) \simeq \pi^{5/2} \left(\frac{1}{\Lambda L} \right)^{3/2} \simeq 17.5 (\Lambda L)^{-3/2}. \quad (2.9)$$

Matching this value with the measured top Yukawa coupling at the weak scale gives $\Lambda L \simeq 8$ [88]. Note that \hat{y}_t at Λ has not increased from 1 by more than 20% or so. The one-loop evolved \hat{y}_t starts growing rapidly at $\Lambda \simeq 10/L$. From the 4D viewpoint, it is the multiplicity of states, rather than the increase of \hat{y}_t itself, that causes the loss of perturbativity.

Is $\Lambda L \simeq 8$ enough to defend the predictivity of an equation like Eq. (2.7)? We claim that it is, as it can be checked by writing the most general Lagrangian, involving the top and the Higgs fields, consistent with the various symmetries and containing operators of arbitrarily high dimensions, all assumed to saturate perturbation theory at Λ . The corrections that these extra couplings induce are not large. The value of Λ itself, or of $1/L$, will be set in the following. We also anticipate that the gauge couplings, growing more slowly than \hat{y}_t , remain perturbative below or at Λ .

³A factor of 2 is included to account for the coupling of the non-zero KK modes, $\sqrt{2}$ times stronger than for the zero mode.

2.2 The complete model and the relevant parameter space

The most straightforward way to include the gauge and Higgs multiplets is to take every field in 5D. In fact the other option of taking the Higgs localized at $y = 0$ requires the introduction of an additional Higgs doublet to write down the down quarks and lepton Yukawa couplings as in the usual MSSM (see below). Moreover with matter and gauge fields in 5D, (discrete) momentum conservation holds in the 5th direction. Higher KK modes need to appear in pairs, thus weakening the lower bounds on $1/L$.

The parity assignments of the fields in the gauge multiplet, a 4D vector A_μ , a 4D complex scalar $\varphi = \frac{1}{\sqrt{2}}(\Sigma + iA_5)$ and two Weyl spinors $\tilde{\lambda}, \tilde{\lambda}^c$ for every generator of the gauge group $SU(3)_C \times SU(2)_L \times U(1)_Y$, are fixed to be $(+, +)$, $(-, -)$, $(+, -)$ and $(-, +)$ respectively by Lorentz, gauge and supersymmetry invariance in 5D. Hence, as shown in Fig. 2.2, the only massless particles are the vector zero modes.

The parity assignments of all the matter fields follow the ones of $\widehat{Q}_3, \widehat{U}_3$ in order to reproduce the SM matter spectrum at low energy. As for the Higgs hypermultiplet two choices are in principle possible for the parity assignments: the $(+, +)$ given to a fermionic component (as for the matter hypermultiplets) or to a scalar component, with the parities of all other fields fixed automatically. Only the second choice leads to a non anomalous theory and leaves the zero mode of the Higgs field massless. In this case the two Higgsinos, $(+, -)$ and $(-, +)$, are all paired into Dirac fermions with masses $(2n + 1)/R$, $n = 0, 1, \dots$ (see Fig. 2.2).

2.3 Residual symmetries after the orbifold projection

The 5D supersymmetric gauge Lagrangian is completely fixed at this stage. The symmetries that survive the orbifold projection other than gauge and flavor symmetries are:

1. 5D supersymmetry with an y -dependent transformation parameter $\Xi = (\xi_1, \xi_2)$. $N = 1$ supersymmetric theories possess a $SU(2)_R$ symmetry that rotates two 4D Weyl-spinors transformation parameters, ξ_1 and ξ_2 , the generators of the 2 supersymmetries in the $N = 2$ theory in 4D language. In general this R-symmetry can be broken by boundary conditions. This can be accomplished à la Scherk-Schwarz imposing a twisted periodicity on the

supersymmetry generators:

$$\begin{pmatrix} \xi_1 \\ \xi_2 \end{pmatrix} (y + 4L) = e^{i/2\pi\alpha\sigma_2 y/L} \begin{pmatrix} \xi_1 \\ \xi_2 \end{pmatrix} (y). \quad (2.10)$$

In the supergravity picture this $SU(2)_R$ is gauged by an auxiliary vector field V in the supergravity multiplet [97]. Scherk-Schwarz breaking corresponds to turn on a Wilson line of V along the compact direction [98, 99].

In the case of the CSM described here, global $SU(2)_R$ is broken completely by the parity assignments on the gaugino fields⁴ and correspond to the choice of $\alpha = 1/2$ in Eq. (2.10). This signals that also global supersymmetry is completely broken by boundary conditions, as can be easily seen from the mass spectrum of Fig. 2.2. Nevertheless it is still present a residual local supersymmetry whose transformations are generated by ξ_1 and ξ_2 subject to the boundary conditions $(+, -)$ and $(-, +)$ respectively [91]. This residual SUSY leaves a local $N = 1$ SUSY unbroken. In particular at the fixed points there are 2 residual 4D global $N = 1$ theories, generated by ξ_1 and ξ_2 respectively, that constrain the structure of the boundary-localized terms in the Lagrangian. This implicitly assumes the promotion of supersymmetry to a local symmetry, hence to supergravity. However, we note here that the scale of the supergravity couplings need not to be connected with the cut-off Λ of Section 1.4.

2. A $U(1)_R$ -like global symmetry with R-charges given in Table 2.1, intact even after EWSB. This is specific of the $S^1/(Z_2 \times Z'_2)$ compactification. In some sense, this particular compactification represents a point of enhanced symmetry among all the 5D compactifications that break global supersymmetry completely⁵. The absence of any A-terms or Majorana gaugino masses can be traced back to this $U(1)_R$ symmetry.
3. A local y -parity P_5 under which any field transforms as

$$\varphi(y) \rightarrow \eta \varphi(L - y), \quad (2.11)$$

where η is the parity assignment at any one of the two boundaries. Note that this cannot be extended to a global 5D parity symmetry which includes the

⁴Gauginos form an $SU(2)_R$ doublet.

⁵This is due to the “geometric” orthogonality between the two orbifold projections in $S^1/(Z_2 \times Z'_2)$, obtained for $\alpha = 1/2$ in the language of Scherk-Schwarz $SU(2)_R$ twisting.

R	gauge V	Higgs H	matter M
+2		h^c	
+1	$\tilde{\lambda}$	\tilde{h}^c	\tilde{m}, \tilde{m}^c
0	A^μ, A^c	h	m, m^c
-1	$\tilde{\lambda}^c$	\tilde{h}	

Table 2.1: Continuous R charges for gauge, Higgs and matter components. Here, m represents q, u, d, l, e .

two boundaries since $Z_2 \times Z'_2$ is the most general discrete symmetry group on S^1 [91]. However this symmetry is enough to forbid any Chern-Simons term or local mass terms for the hypermultiplets.

These symmetries strongly constrain the form of the 5D tree-level (bulk) Lagrangian, \mathcal{L}_5 , but leave open the possibility of suitable Lagrangian terms at the two boundaries, so that, for the total Lagrangian

$$\mathcal{L} = \mathcal{L}_5 + \delta(y) \mathcal{L}_4 + \delta(y - L) \mathcal{L}'_4. \quad (2.12)$$

Some of the terms in \mathcal{L}_4 and \mathcal{L}'_4 will in fact be anyhow generated, subject only to the usual non-renormalization properties of supersymmetry. As stated above, one important fact about \mathcal{L}_4 and \mathcal{L}'_4 is that they respect different $N = 1$ supersymmetries, associated to the parameters ξ_1 and ξ_2 , which vanish respectively at $y = L$ and $y = 0$. In practice, to write down the most general \mathcal{L}_4 and \mathcal{L}'_4 one employs the usual rules of 4D $N = 1$ supersymmetry after identification of the proper supermultiplets [94, 100]. In particular the 5D $N = 1$ vector multiplet, constituted by a gauge field A_M , a real scalar B , two gauginos λ^a that transform as a doublet under $SU(2)_R$ and a triplet X^b of auxiliary fields, decomposes into a vector+chiral multiplet in 4D. The hypermultiplet, with a Dirac fermion, 2 complex scalars and 2 auxiliary fields transforming as a $SU(2)_R$ doublets decompose in two chiral multiplets.

If one looks at the Higgs hypermultiplet it is immediate to see, anyhow, that the supermultiplets whose components have the same orbifold parities and do not vanish at the boundaries are $(h(+, +), \tilde{h}(+, -))$ and $(h^\dagger(+, +), \tilde{h}^c(-, +))$ respectively at $y = 0$ and $y = L$. This is what makes possible to write down Yukawa couplings both for up and for down quarks or for the leptons to a single Higgs field $h(+, +)$ and still be consistent with (local) supersymmetry. The Yukawa cou-

plings for the up quarks are located at $y = 0$, while the Yukawa couplings for the down quarks and the leptons at $y = L$ [88].

Finally we note that \mathcal{L}_4 and \mathcal{L}'_4 can contain a Fayet-Iliopoulos term associated with the hypercharge $U(1)$. We shall come back to this possible term in Section 2.5.

2.4 Gauge anomalies and hypermultiplet mass terms

The boundary conditions, or the orbifolding, turn the vector-like 5D Lagrangian into a chiral theory. This is obviously the case in the pure gauge–matter sector since the orbifold projections select chiral fermionic zero modes. It is also true however in the gauge–Higgs sector in spite of parity conservation and of the Dirac nature of all Higgsino masses. Some of the Kaluza Klein vector bosons couple to vector currents and some others to axial currents. Similarly some of the KK states of the gauge multiplet φ are scalars and some pseudoscalars. One wonders then if gauge anomalies may appear localized on the boundaries [101, 102].

The naive answer to this question turns out to be correct. To ensure gauge invariance and the conservation of the corresponding 5D gauge current, it is enough that the fermionic zero modes, after the orbifold projection, satisfy the usual 4D anomaly cancellation condition [101]. In this case one can implicitly cancel any anomaly by the addition of a 5D Chern-Simons term with a y -dependent piecewise constant coefficient $\eta(y)$, such that the term $\eta(y)F \wedge F \wedge A$ respects the two parities at $y = 0$ and $y = L$. Since the matter fermions are anomaly free and there are no massless Higgsinos, the orbifold construction described above is anomaly free. A qualification of this statement is necessary however. Because of the Higgs sector, gauge invariance can be maintained at the quantum level, but not, at the same time, the local parity symmetry defined in Sect. 2.3. In particular there is no regularization that preserves both symmetries [103, 104].

The breaking of the local y -parity makes it possible that there be mass terms for the hypermultiplets. For the hypermultiplet of components $(\psi, \psi^c, \varphi, \varphi^c)$, the 5D mass term consistent with the residual supersymmetry after the orbifold projection is [104]

$$\begin{aligned} \mathcal{L}_m = & +(\psi m(y)\psi^c + \text{h. c.}) - M^2 \left(|\varphi|^2 + |\varphi^c|^2 \right) \\ & + 2M (\delta(y) + \delta(y - L)) \left(|\varphi|^2 - |\varphi^c|^2 \right), \end{aligned} \quad (2.13)$$

irrespective of the specific boundary conditions for the different components. Note the appearance of the boundary term. In the formulation of the theory on a circle

S^1 , the mass term $m(y)$ has to satisfy $(-, -)$ boundary conditions to be also $Z_2 \times Z'_2$ invariant. Furthermore, bulk supersymmetry implies that $m(y)$ be piecewise constant in the four different patches of the circle, hence

$$m(y) = M\eta(y), \quad \eta(y) = \begin{cases} +1, & y \in (0, L) \cup (2L, 3L) \\ -1, & y \in (L, 2L) \cup (3L, 4L) \end{cases} \quad (2.14)$$

The effect of a mass term like Eq. (2.13) on the spectrum is discussed in Section 2.6. We point out, however, that if these mass terms are vanishing at tree level, the non-renormalization theorems guarantee that they can only be renormalized by finite, negligibly small, non-local corrections associated to the orbifold breaking of global supersymmetry.

2.5 The Fayet-Iliopoulos term

It was pointed out in [105, 106] that a Fayet-Iliopoulos (FI) term on the boundaries is induced in the model under examination by one loop corrections involving the gauge coupling to the hypercharge Y . At first this is not surprising since a FI term in 4D is both gauge invariant and globally supersymmetric. It is however also somewhat worrisome, still in view of the 4D properties of a FI term. In 4D the FI term breaks supersymmetry and/or the gauge symmetry in the vacuum, something we would not like to happen in view of the previous discussion. Furthermore, it is not gauge invariant in supergravity if the $U(1)$ -charge of the gravitino vanishes [41, 107], which is the case for Y . Finally the one loop FI term arises only in presence of mixed $U(1)$ -gravitational anomalies.

None of these unpleasant features necessarily survive in 5D [104]. In particular they are not shared by the FI term in the model under consideration, which takes the form

$$\mathcal{L}_\xi = \xi (\delta(y) (X_3 - \partial_y \Sigma) + \delta(y - L) (X_3 + \partial_y \Sigma)), \quad (2.15)$$

where Σ is the real scalar in the vector hypermultiplet and X_a is the $SU(2)_R$ triplet of auxiliary fields of the 5D vector multiplet [108]. X_3 and Σ intervene in the quadratic Lagrangian without a mixed term

$$\mathcal{L}^{(2)} = \frac{1}{2} X_3^2 + \frac{1}{2} (\partial_M \Sigma) (\partial^M \Sigma). \quad (2.16)$$

For the purposes of this paper, it is important to observe that, in the vacuum,

from Eqs. (2.15,2.16)

$$X_3 = -\xi (\delta(y) + \delta(y - L)), \quad (2.17a)$$

$$\partial_y \Sigma = -\xi (\delta(y) - \delta(y - L)), \quad (2.17b)$$

showing explicitly that the D-flatness conditions at both boundaries $D = X_3 - \partial_y \Sigma = 0$, $D' = X_3 + \partial_y \Sigma = 0$ are satisfied. Note that, on the S^1 circle, the vacuum form of Σ is $\langle \Sigma \rangle = -\frac{\xi}{2} \eta(y)$ with $\eta(y)$ as in Eq. (2.14). This amounts to a spontaneous breaking of the local y -parity. In turn, after replacement of Eq. (2.17) in the interaction terms of the X_3 and Σ fields with a generic hypermultiplet of hypercharge Y ,

$$\begin{aligned} \mathcal{L}_{\text{int}} = & g_Y Y (X_3 - \partial_y \Sigma) \left(|\varphi|^2 - |\varphi^c|^2 \right) \\ & - |(\partial_y - g_Y Y \Sigma) \varphi|^2 - |(\partial_y + g_Y Y \Sigma) \varphi^c|^2 \\ & + \psi^c (\partial_y - g_Y Y \Sigma) \psi + \text{h.c.}, \end{aligned} \quad (2.18)$$

one obtains a supersymmetric mass term as in Eq. (2.13), with $M = g_Y Y \xi / 2$, where g_Y is 5D hypercharge coupling.

Once more we are led to consider a mass term for the hypermultiplets. With a momentum cut-off Λ , the radiatively generated FI term is

$$\xi = \frac{g_Y}{16\pi^2} \frac{\Lambda^2}{2}, \quad (2.19)$$

which, in turn, translates itself into a mass term for a hypermultiplet of hypercharge Y

$$M_\xi(Y) = Y \frac{g_Y^2}{16\pi^2} \frac{\Lambda^2}{4} = Y \frac{g'^2 L}{16\pi^2} \Lambda^2, \quad (2.20)$$

where g' is the usual $U(1)$ coupling in 4D.

For $\Lambda L \simeq 8$ this is a small mass, compared for example with the one loop mass induced for the Higgs by the top loop Eq. (2.7). One can nevertheless consider an arbitrary value of ξ , as done in Sect. 3.1.3. Finally it should be pointed out that this induced FI term has a geometric interpretation in 5D supergravity, suggesting that its renormalization vanishes beyond one loop and that, with a proper regularization, the case $\xi = 0$ is not unconceivable as coming from a suitable more fundamental theory [104].

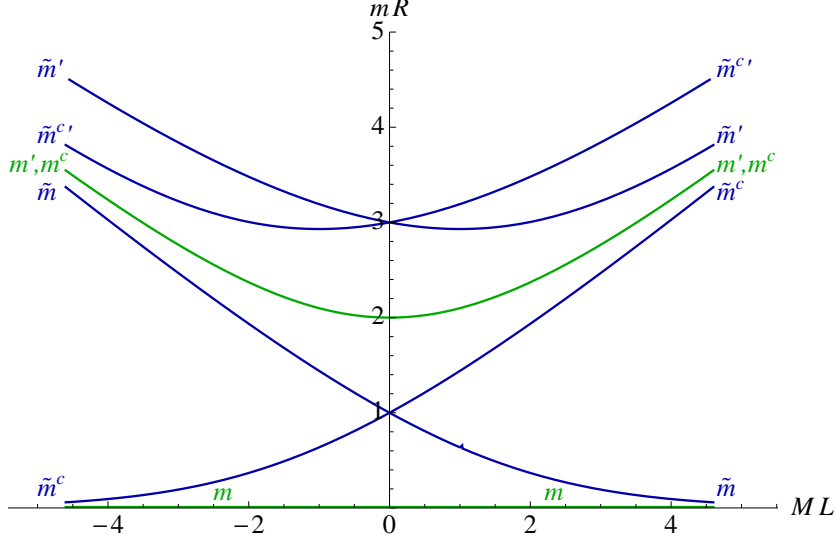


Figure 2.4: Spectrum of a matter hypermultiplet, in units of $1/L$, as function of ML .

2.6 Hypermultiplet spectrum in presence of a mass term

It is useful to summarize how the hypermultiplet spectrum of Fig. 2.2 is modified in presence of a mass term M as in Eq. (2.13). This spectrum is worked out in Appendix A both in the case of matter-like and Higgs-like boundary conditions. The spectra in the two cases are shown in Figs. 2.4,2.5 respectively. We also show the wave-functions for the lowest-lying modes in the matter hypermultiplet in Fig. 2.6 for three different values of the mass term. A few things are useful to note. In the large $|ML|$ limit a supersymmetric spectrum is restored, with bound states localized at the boundaries.

In particular in the case of the matter multiplet, the states tend to organize themselves in one $N = 1$ massless chiral multiplet and in $N = 2$ massive hypermultiplets whose masses go like $m^2 = M^2 + 4n^2/R^2$ with n integer, decoupling from the spectrum in the large $|ML|$ limit. Furthermore the lightest states are bound states whose wave-functions are progressively localized toward one of the two boundaries of the 5th dimension.

In the case of the Higgs hypermultiplet, the states are always grouped in $N = 2$ hypermultiplets in the large $|ML|$ limit. The masslessness of the lightest multiplet

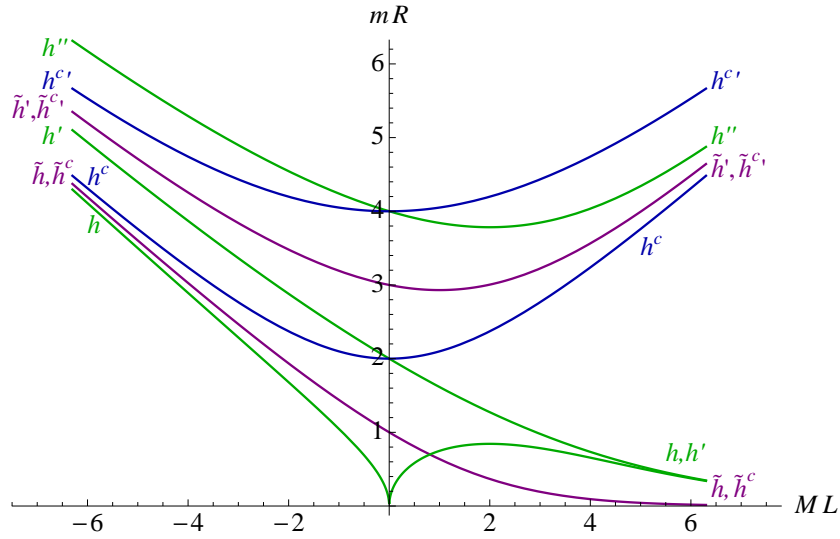


Figure 2.5: As in Fig. 2.4 for the Higgs hypermultiplet.

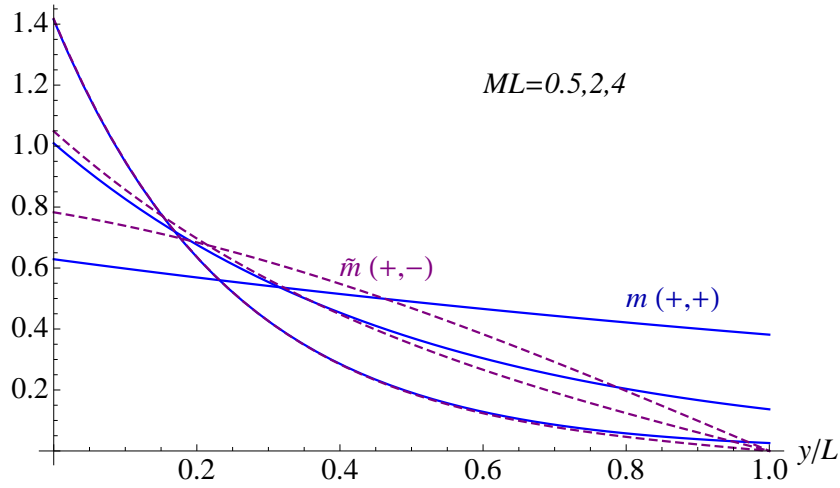


Figure 2.6: Wave-functions of the lowest-lying modes for the fermionic (+, +) and the bosonic (+, -) matter fields for three different values of the hypermultiplet mass. The case of negative mass are symmetric with respect to $y = L/2$.

when $|ML| \rightarrow \infty$ depends on the sign of M and there is no localization for the wave-functions of the lightest states. Furthermore as one can see in Fig. 2.5, the lightest state which passes through zero at vanishing ML is the Higgs, with the cusp at $ML = 0$ reflecting the change of sign of the squared mass, being $(m_h L)^2 \simeq -2ML$ at $|ML| \ll 1$.

Chapter 3

The Constrained SM in presence of bulk masses.

3.1 Electroweak symmetry breaking in detail

The purpose of this Chapter is to study in detail the possible effects of hypermultiplet masses on EWSB. In this Chapter we consider the cases where these masses do not exceed $1/L$, leaving the exploration of the alternative possibility to the following Chapter. As seen in Sect. 2.2, moderate values of ML are consistent with radiative corrections. Other than the modification of the spectrum, hypermultiplet masses have 3 types of effects on the EWSB:

1. a mass term for the top Q or U hypermultiplets changes the relation between the top mass and the top-Higgs coupling, crucial in EWSB;
2. a mass term for the top Q or U hypermultiplets influences the one loop Higgs mass or the complete one loop effective potential;
3. a mass term for the Higgs hypermultiplet gives a tree level mass to the zero mode Higgs field (see Fig. 2.5), which feeds directly in the effective potential.

3.1.1 The top mass and the top Yukawa coupling

The relation between the top mass and the top-Higgs coupling y_t is obtained by solving the equation of motion for the lowest mode of the fermions in the top hypermultiplets Q and U , coupled by Eq. (2.5) at the $y = 0$ boundary. The interaction Eq. (2.5) is itself a localized mass term when the Higgs scalar is replaced

by the vacuum expectation value v . This is done in Appendix A. The result can be expressed as

$$y_t = \widehat{y}_t \eta_0^U \eta_0^Q \eta_0^h, \quad (3.1)$$

where

$$\widehat{y}_t = \frac{\lambda_t}{(4L)^{3/2}} = \frac{m_t}{v} \frac{1}{\sqrt{\omega_+^U \omega_+^Q}}, \quad (3.2)$$

$$\omega_{\pm}^i = k_i L \coth(k_i L) \pm M_i L, \quad i = U, Q \quad (3.3)$$

$$k_i = (M_i^2 - m_t^2)^{1/2} \quad (3.4)$$

and $\eta_0^{U,Q,h}$ are the wave functions for the lightest U, Q, h modes at $y = 0$, normalized to $\int_0^{4L} dy |\eta^i(y)|^2 = 4L$ and given in Appendix A. At $M_U = M_Q = M_h = 0$, Eq. (3.1) reduces to

$$y_t = \frac{m_t}{v} \frac{2 \sin(2m_t L)}{2m_t L + \sin(2m_t L)}. \quad (3.5)$$

Note that in the limit $M_h = 0$, $|M_{U,Q}| \gg 1/L \gg m_t$, y_t reduces to the standard value, m_t/v , no matter what the sign of M is. For negative M , when the top wave function and the Yukawa coupling are localized at opposite boundaries, this is due to a compensating increase of \widehat{y}_t , which is directly related to the fundamental coupling in the Lagrangian. When y_t and \widehat{y}_t differ significantly, it is \widehat{y}_t that enters into Eqs. (2.8–2.9) to determine the point of saturation of perturbation theory.

3.1.2 One loop Higgs effective potential for arbitrary M_U, M_Q

The one loop Higgs mass Eq. (2.7) from the diagrams of Fig. 2.3 gets corrected by the presence of M_U and M_Q . This is in fact also true for the entire one loop effective potential which has to be computed anyhow because of the large correction to the quartic coupling and because of the higher order terms in $(vL)^2$ which may be important insofar as L is not determined.

The calculation described in Sect. 2.1 immediately generalizes to the massive case in terms of the propagators in presence of masses. Considering, as in Eq. (2.6), the mixed propagators at $y = y' = 0$ the effective potential due to top–stop

exchanges is

$$V_t(h; M_U, M_Q) = N_c \sum_{N=1}^{\infty} \int \frac{d^4 p}{(2\pi)^4} \frac{(-1)^{N+1}}{N} \left(\frac{\lambda_t h \eta_0^h}{\sqrt{4L}} \right)^{2N} \times \left\{ \left[G_\varphi^U(p, 0) G_F^Q(p, 0) \right]^N + \left[G_\varphi^Q(p, 0) G_F^U(p, 0) \right]^N - 2 \left[G_\psi^U(p, 0) G_\psi^Q(p, 0) \right]^N \right\}, \quad (3.6)$$

where $G_i^{U,Q}(p, y) = G_i(p, y; M_{U,Q})$ with $i = \phi, F, \psi$. The propagators $G_i(p, y; M)$ are given in Appendix B, while the wave function of the Higgs zero mode η_0^h is given in Appendix A. The integral is performed over the Euclidean 4-momentum.

3.1.3 Electroweak symmetry breaking in presence of a FI term

As shown in Sect. 2.5, a FI term is equivalent for any hypermultiplet of hypercharge Y to a mass term, which we parameterize in terms of a dimensionless variable a as

$$M(Y) = \frac{a}{L} Y, \quad (3.7)$$

to be inserted in Eqs. (2.13,2.14).

In presence of these masses the potential we consider to determine the VEV of the Higgs field is

$$V(h; L, a) = m^2(M(1/2)) h^2 + \frac{21\xi(3)}{64\pi^2} \frac{g^2}{L^2} h^2 + \frac{g^2 + g'^2}{8} h^4 + V_t(h; M(-2/3), M(1/6)). \quad (3.8)$$

Other than the standard tree-level quartic coupling and the one loop contribution from the top-stop exchanges, Eq. (3.6), the potential includes the tree level mass $m(M)$ computed in Sect. 2.6 and Appendix A (first term on the r.h.s. of Eq. (3.8)) and a one loop mass term from the KK tower of the $SU(2)_L$ gauge multiplets (second term on the r.h.s. of Eq. (3.8)) [89]. The latter is easily computed by the y, y' propagators presented in Appendix B.

Imposing the occurrence of the minimum at $h = v = 174.1$ GeV, determines the Higgs mass m_h and $1/R$, together with the entire spectrum, as functions of a . The Higgs mass is shown in Fig. 3.1. The lightest stops, which are non degenerate when $a \neq 0$ because $M_U \neq M_Q$, occurs in two chiralities. Their mass difference depends on the parameter a and is about 70 GeV at $a = -0.15$. The stop masses together with $1/L$ are shown in Fig. 3.2. These figures refine those of [106].

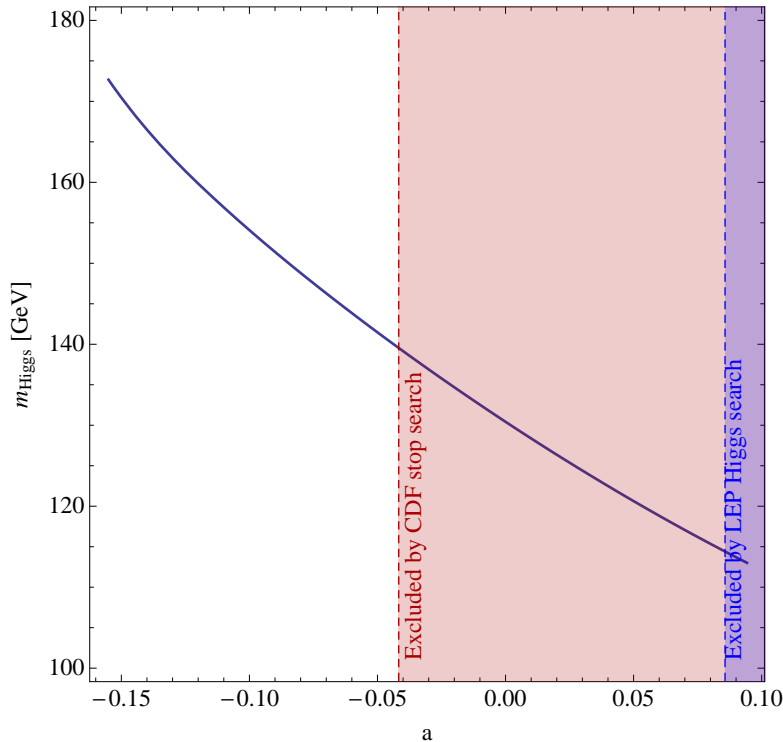


Figure 3.1: Higgs mass as function of the dimensionless parameter a , Eq. (3.7).

The sharp increase of $1/R$ with $-a$ is due to an increasingly precise accidental cancellation (at about 10% level for $a = -0.15$) between the positive tree level squared mass in Eq. (3.8) and the negative contribution from the top-stop loop. Note that the estimate of the radiatively induced FI term in Eq. (2.20) corresponds to a small $a \sim 0.05$ [106].

Through L , M_U and M_Q , also the Higgs-top coupling acquires a dependence on a , determined in Eq. (3.1) and shown in Fig. 3.3. Note that the top Yukawa coupling y_t is reduced from the Standard Model value by about 10% due to the localization of the interaction at the boundary.

3.1.4 Electroweak symmetry breaking with sizable $M_U = M_Q$

As we have seen, the mass terms from the FI term have to be small. Their effect can however be significant due to a possible cancellation occurring in the Higgs potential between the tree level Higgs squared mass and the radiatively induced effect. Here we consider the possible effects of direct masses for the U, Q hyper-

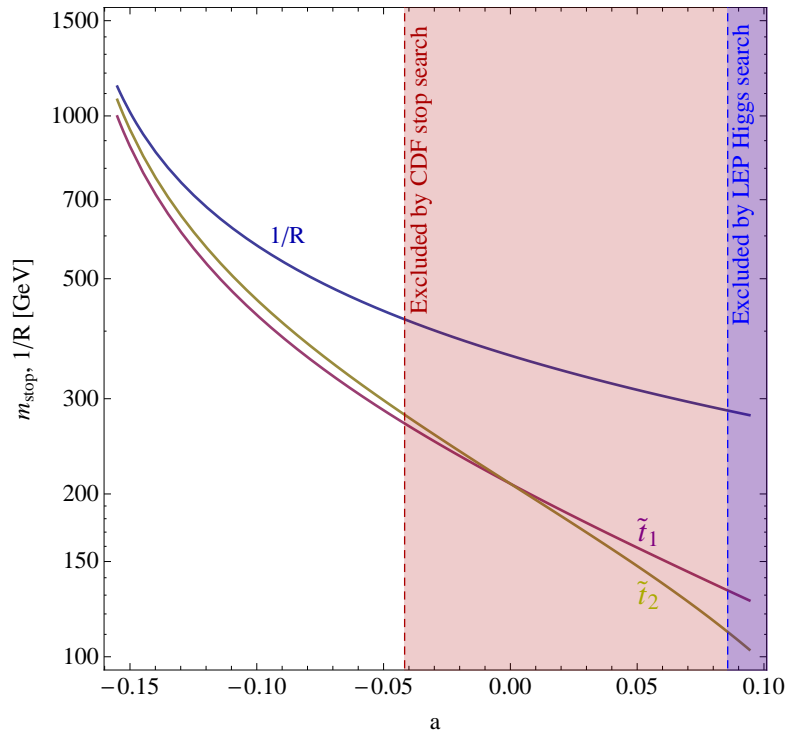


Figure 3.2: Compactification scale and lightest stop masses as functions of a , Eq. (3.7).

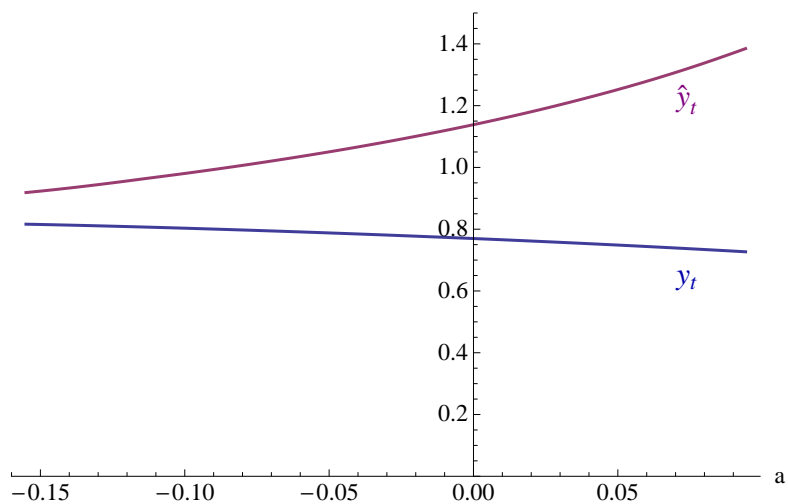


Figure 3.3: Top-Higgs coupling (y_t) and $\hat{y}_t = \lambda_t/(4L)^{3/2}$ as functions of a , Eq. (3.7).

multiplets, taking $M_U = M_Q = M$ for simplicity, and limiting ourselves to the case of $|ML| \lesssim 1$. At the same time, again for simplicity, we set the FI term, or the a parameter, to zero.

Proceeding as in the previous section, the Higgs potential we consider is

$$V(h; L, M) = \frac{21\xi(3)}{64\pi^2} \frac{g^2}{L^2} h^2 + \frac{g^2 + g'^2}{8} h^4 + V_t(h; M, M) \quad (3.9)$$

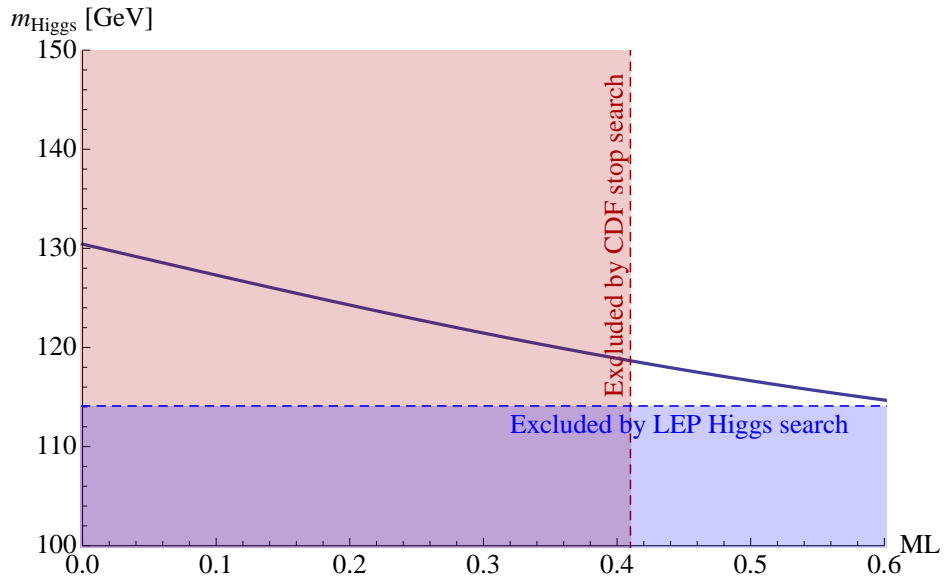
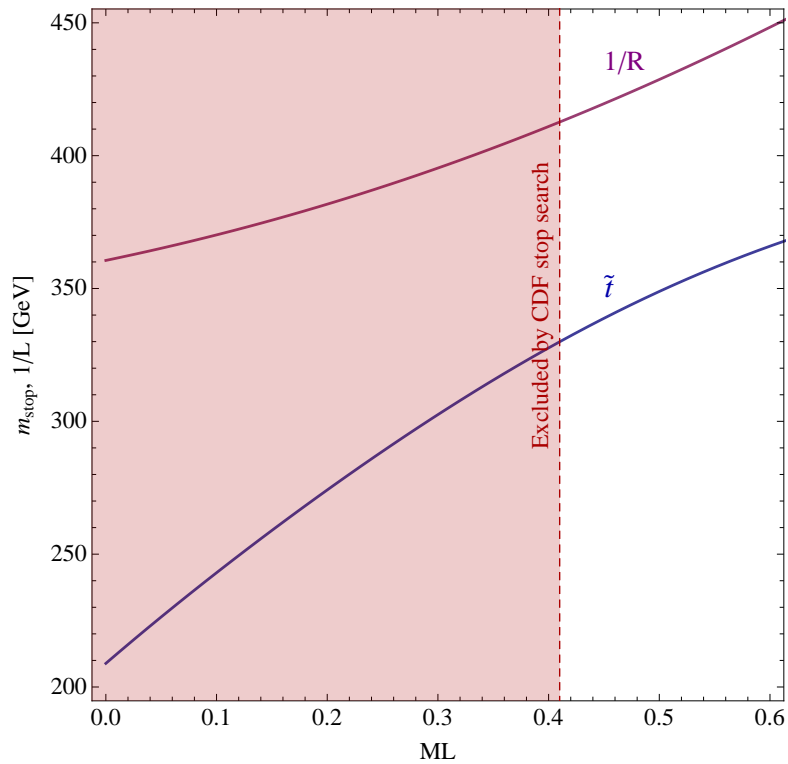
whose minimization determines m_h and L as functions of M . The Higgs mass is shown in Fig. 3.4 for $0 \leq ML \leq 0.6$. The reason for not considering negative values of ML due to the lightness of the stops¹, that falls below the experimental lower bound of about 270 GeV [109] around $ML \sim 0.2$, as can be seen in Fig. 3.5. For ML above 0.6, instead, it is the Higgs boson which becomes too light. This result, however, may not persist for $ML > 1$, where higher-loop gauge corrections become important [110]. This case will be analyzed in Chapter 4. In the interval $0 \leq ML \leq 0.6$, both $1/L$ and $m_{\tilde{t}}$ have a non negligible dependence on M , as shown in Fig. 3.5. The degeneracy between the two lightest stop masses would be resolved by taking $M_U \neq M_Q$. The Top-Higgs couplings y_t and \hat{y}_t in this case are shown in Fig. 3.6.

3.2 Spectrum and phenomenological implications

In absence of hypermultiplet mass terms, the value of the compactification scale and the spectrum of the lightest particles is given in Table 3.1 with an error that estimates the uncertainties due to the presence of the extra couplings and the operators mentioned in Sect. 2.1.1 [88]. By letting the mass terms vary in a moderate range, well consistent with radiative corrections, the main deviation from the massless case is due to a possible mass term for the Higgs hypermultiplet which can partially counteract the top-stop radiative corrections that trigger EWSB. This can in turn drive up the compactification scale and, consequently, the entire spectrum.

In Sect. 3.1.3 we have explicitly discussed the effects of a FI term, which is a particular example of this case. The entire spectrum becomes therefore effectively determined by $1/R$ in the range of Fig. 3.2, $420 \text{ GeV} \lesssim R^{-1} \lesssim 1 \text{ TeV}$. The dependence of m_h on $1/R$ is shown in Fig. 3.7 obtained from Figs. 3.1–3.2, whereas the masses of the other particles is again given in Table 3.1. Note that the lightest stop \tilde{t}_1 is the Lightest Supersymmetric Particle (LSP), except possibly for large

¹The lightest stops now come in two degenerate chiralities.

Figure 3.4: Higgs mass as function of ML .Figure 3.5: Stop mass and $1/R$ as functions of ML .

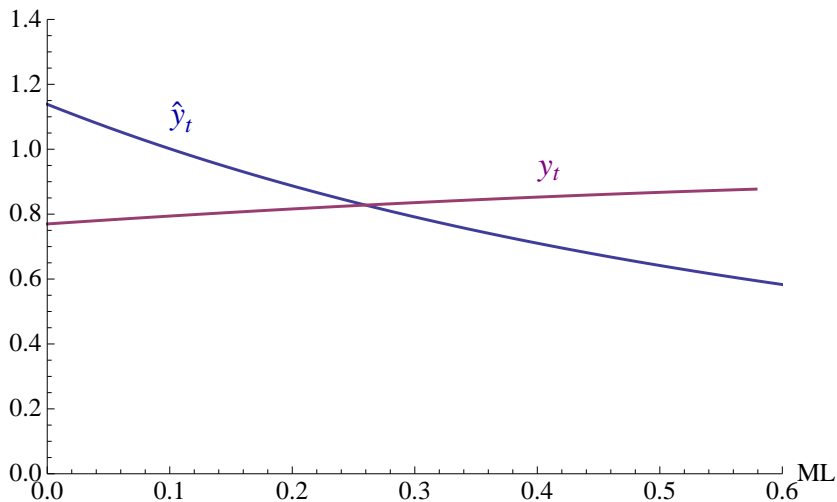


Figure 3.6: Top-Higgs coupling y_t and $\hat{y}_t = \lambda_t/(4L)^{3/2}$ as functions of ML .

values of $1/R$ where the corrections due to kinetic terms localized on the boundaries, giving rise to the main uncertainty indicated in Table 3.1, could reverse the order with any of the other superpartners at $1/R$. Unless an explicit violation of the $U(1)_R$ -symmetry were introduced at the boundaries, the LSP would be stable. A moderate effect could also arise from an explicit mass term for the top hypermultiplets, as shown in Fig. 3.5.

3.2.1 Phenomenological implications

Except for the large, somewhat fine tuned values of $1/R$, the Higgs boson is below the WW threshold, with a preferred mass in the 120 GeV range. It has SM-like couplings to $b\bar{b}$ and $\tau\bar{\tau}$ and WWh , ZZh gauge couplings, but has suppressed coupling to two photons [111]. It could therefore be looked at in associated production of Zh , followed by $b\bar{b}$ and $\tau\bar{\tau}$ decays [112, 113, 114]. We have already mentioned the deviation of the top Yukawa coupling from the SM value (see Figs. 3.3, 3.6 and the discussion in Chapter 5). More important for the possible discovery in a hadron collider like the LHC is the suppression of the Higgs–gluon–gluon squared coupling, ranging from 10% to 60% relative to the SM value as $1/R$ increases from 190 to about 450 GeV, where the WW threshold is crossed [111].

A main feature of the model is that the two degenerate light stops are the LSP and are stable if $U(1)_R$ is exact. Their mass is approximately $(\pi/(2L) - m_t)$ with

	A	B
$1/R$	360 ± 70	$420 \div 1000$
h	133 ± 10	Fig. 3.7
\tilde{t}_1, \tilde{u}_1	210 ± 20	$1/R(1 \pm 8\%) - m_t$
$\chi^\pm, \chi^0,$ $\tilde{g}, \tilde{q}, \tilde{l}$	360 ± 70	$1/R(1 \pm 20\%)$
\tilde{t}_2, \tilde{u}_2	540 ± 30	$1/R(1 \pm 8\%) + m_t$
A_1, q_1, l_1, h_1	720 ± 140	$2/R(1 \pm 20\%)$

Table 3.1: The particle spectrum and $1/R$ in absence of any mass term (Column A, presently excluded) and in presence of a FI term (Column B). All entries are in GeV.

a lowest preferred value in the 200 GeV range. As it will explained in Sect. 5.6 these stable stops will hadronize in superhadrons by picking up one or two light quarks. In the case of charged superhadrons they will give rise to muon-like tracks, distinguishable from a muon via dE/dx and time-of-flight. Their mass is presently constrained by TeVatron searches, as shown in the plots.

Finally one should discuss the present constraints from EWPT and Flavor

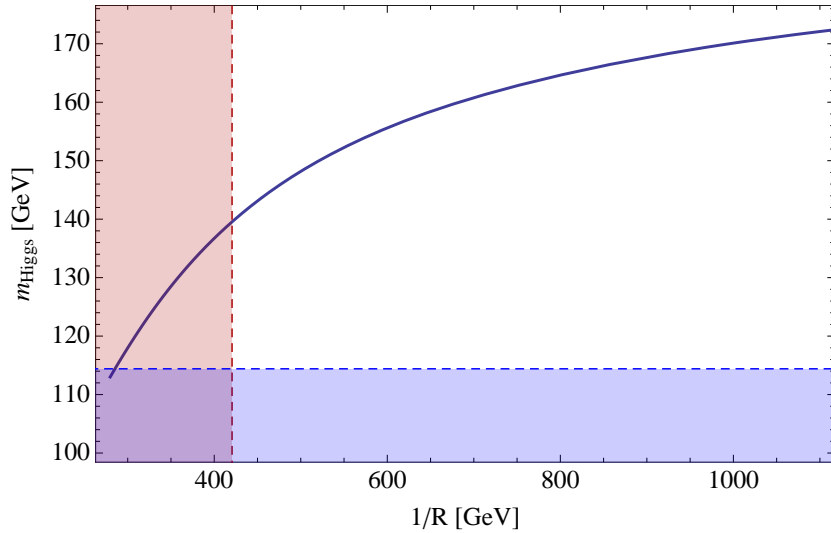


Figure 3.7: Higgs mass versus $1/R$ in presence of a Fayet-Iliopoulos term. The blue (red) shaded areas correspond to the LEP Higgs (CDF stop) exclusion limits.

Physics. This will be done in Chapter 5, together with the model presented in the next Chapter.

The heavier supersymmetric particles in Table 2 could be looked at through their chain decay into the LSP. Similarly the discovery of the first states at $2/R$ of the KK tower of SM particles (heavy quarks, leptons with their mirror partners, heavy gauge and Higgs bosons) would be strong evidence for the picture of EWSB described in this Chapter. Note that (discrete) momentum conservation in the 5th dimension forbids unsuppressed gauge couplings of the heavy gauge bosons to the standard fermions.

3.3 Extending the CSM

In Chapter 2 we have seen that the parameter space of the minimal version of the CSM has been enlarged because of the presence of bulk masses for the hypermultiplets as a consequence of the breaking of the P_5 parity. From the analysis performed in this Chapter, it comes out that points near the CSM in this enlarged parameter space represents slightly distorted versions of the original theory but without any novel feature. One then can asks himself whether there are other 5D models in flat space that describe EWSB successfully and that differ from the CSM. In this search one can move to different directions: either modifying the theory to keep both P_5 and $U(1)_R$ intact or to keep one of the two only. In particular if one keeps $U(1)_R$ only, as in the CSM, it is interesting to inspect different regions of the parameter space, far from it.

3.3.1 Models with $U(1)_R$ and P_5 symmetries

A predictive theory of EWSB should have only a few parameters, and therefore as much symmetry as possible. One can try at first to modify the theory and keep both P_5 and $U(1)_R$ in addition to local 5D Supersymmetry and all the symmetries of the SM.

Hence, we must cancel the FI term introducing a second Higgs hypermultiplet with boundary conditions that give rise to a second massless scalar with opposite hypercharge to the first. Let's call them for simplicity H_u and H_d with hypercharges $1/2$ and $-1/2$ respectively².

²Here H_u and H_d do not necessarily correspond to the fields giving up-type and down-type quark masses, respectively: for instance, down-type quark masses can arise from the VEV of H_u , as seen in Eq. (3.10).

Is it possible to construct a completely realistic theory with these symmetries? Other than gauge interactions, the symmetries allow brane-localized Yukawa interactions. For the case of bulk matter these are:

$$\begin{aligned} \mathcal{L}_{\text{Yukawa}} = & \delta(y)[\lambda_u Q U H_u + \lambda_d Q D H_d]_{\theta^2} \\ & + \delta(y - L)[\lambda'_u Q' U' H_d'^c + \lambda'_d Q' D' H_u'^c]_{\theta^2}, \end{aligned} \quad (3.10)$$

where Q, U, D and $H_{u,d}$ are chiral multiplets containing quark and Higgs-boson zero modes of the $N = 1$ Supersymmetry acting at $y = 0$, while Q', U', D' and $H_{u,d}'^c$, which also contain quark and Higgs-boson zero modes, are the chiral multiplets of the $N = 1$ Supersymmetry acting at $y = L$. Even though one-loop radiative corrections lead to contributions to the soft mass terms $m_u^2 H_u^\dagger H_u + m_d^2 H_d^\dagger H_d + m_3^2 (H_u H_d + \text{h.c.})$ in the Higgs potential, successful EWSB does not occur. The Yukawa contributions dominate $m_{u,d}^2$ and are large and negative, so that $m_u^2 + m_d^2 < 0$, giving an unbounded potential along the D -flat direction. It is interesting that the addition of an extra Higgs doublet hypermultiplet to the CSM destroys the theory. If the quark fields reside on a boundary, only one pair of the Yukawa couplings survive [115]. In this case the squark masses arise only at one loop, and we find (see Chapter 4) that the corresponding two-loop top Yukawa contribution to m_u^2 is not sufficiently negative to overcome the positive contribution from the one-loop gauge radiative correction: $m_{u,d}^2$ are both positive, and $m_3^2 = 0$, so that there is no EWSB.

We conclude that we must give up either the bulk parity P_5 or the continuous $U(1)_R$ symmetry to construct realistic theories. Theories with P_5 but no $U(1)_R$ were constructed in [95]. They are theories with two Higgs doublet VEVs resulting from a scalar potential having terms induced by $U(1)_R$ breaking boundary operators.

3.3.2 Models with $U(1)_R$ symmetry and broken P_5 symmetry

In the following we will focus on the possibility of a $U(1)_R$ -symmetric theory with P_5 broken. This is exactly the possibility, mentioned above, of analyzing the existence of other regions of successful EWSB in the CSM enlarged parameter space. Furthermore, being now free to move to arbitrary values of the hypermultiplet masses, one can stick on the theory with two Higgses: it is easy to realize that the theory with only one Higgs can be viewed as a theory with two Higgses in which only one of them gets a VEV while the other has a big negative bulk mass and decouples. This can be directly seen from the spectrum of Fig. 2.4. Another

evidence supporting this viewpoint comes from the structure of the FI term:

$$\xi_{div}(y) = \frac{g_Y^2}{16\pi^2} \sum_i \{ (Y_i \Lambda^2 - 2M_i Y_i \Lambda) [\delta(y) + \delta(y - L)] + \text{higher deriv.} \} \quad (3.11)$$

When M_{H_d} becomes big and negative, of the order of Λ , its contribution in the linear divergent part recreates the quadratic divergence of the one-Higgs theory.

While the one Higgs theories have a quadratically divergent FI term, the two Higgs theories are less sensitive to unknown physics at the cutoff. The quadratic divergence of the FI term is canceled by the presence of the second Higgs hypermultiplet — indeed this may be a motivation for considering two Higgs theories. In the presence of hypermultiplet masses, however, a further condition arises if one requires ultraviolet insensitivity of the FI term, since there is a residual linear divergence proportional to $\text{Tr}[YM]$, where Y and M are hypercharge and bulk-mass matrices for the hypermultiplets as shown in Eq. (3.11). This may motivate interesting relations among the hypermultiplet masses, *e.g.* the case in which they are all equal, or $M_Q = M_U = M_D$, $M_{H_u} = M_{H_d}$ or $M_Q = M_U = -M_{H_d}$ and all other masses equal to zero. These relations make the radiative FI term identically vanishing. In fact, $M_{H_u} = 0$ then becomes a perfectly stable condition.

Ensuring one of these condition is necessary if we want to examine the case of a quasi-localized top quark, $M_{Q,U} \gtrsim 1/L$: in this limit the top 1-loop contribution is substantially reduced in size and, if the FI term is non vanishing, the induced value for M_{H_u} gives a mass squared to the lightest mode of H_u of comparable size to the other radiative contributions, rendering the theory too sensitive to UV physics. Further conditions on the hypermultiplets masses can arise from phenomenology as it will be discussed in Chapter 5. In particular the condition $M_{U_i} = M_{Q_i}$, $M_{D_i} = M_{L_i} = M_{E_i} = 0$, $M_{H_d} = M_{H_u}$ may keep at a minimum level unwanted effects in low energy physics, like FCNC or violation of universality, as discussed in detail in Chapter 5.

Let's now turn to EWSB: the bulk mass terms of most importance are those of the third generation and the Higgs multiplets. For most of the following Chapters we assume that the bulk mass for the H_u hypermultiplet vanishes $M_{H_u} = 0$, and we concentrate on the bulk masses for the third generation quarks: $M_{Q,U,D}$. Having already analyzed the case in which the masses are $\ll 1/L$, we consider values of $M_{Q,U}$ comparable to or larger than $1/L$, so that the corresponding zero-mode wave-functions are peaked at the boundaries of the fifth dimension. In particular we choose M_Q positive so that the left-handed top and bottom quarks are located near $y = 0$ where the top Yukawa coupling to h_u reside. The equality of the hyper-

multiplet masses for U , Q , D automatically avoid large wave-function suppression factors in the top quark mass. Furthermore, if the b quark must get its mass from a Yukawa coupling at $y = L$, the m_b/m_t mass ratio receives an exponential suppression of $\exp(-2M_Q L)$ due to the small value of the q and d wave-functions at $y = L$ [110]. It is significant that localization necessarily destroys the symmetry between up and down sectors, leading to a small value for m_b/m_t without the need for a hierarchy of 5D Yukawa couplings.

However having two Higgs hypermultiplets at disposal this picture can be altered by the possibility of four Yukawa couplings, as shown in Eq. (3.10), and two Higgs VEVs. Nevertheless, one can try to analyze if the minimal possibility in which only the H_u acquires a vev leads to successful EWSB³. This can be ensured for example introducing a global symmetry $U(1)_{H_d}$ which rotates the phase of only H_d . This symmetry therefore sets the Yukawa couplings $\lambda'_u = \lambda_d = 0$ as well as $m_3^2 = 0$. Only H_u acquires a VEV, so that the physics of both EWSB and quark mass generation is identical to the case of the one Higgs theory.

The analysis performed above defines a new model: a two Higgs theory with definite relation between hypermultiplet masses, equal large masses for the third generation quarks multiplets, and with EWSB performed by only one Higgs, the other being inert. In the following Chapter we will refer to this model as the Quasi Localized Top (QLT) model.

Before starting the study whether the QLT leads to successful EWSB, it is interesting to better identify which is the relevant parameter space. The Higgs potential, and therefore EWSB, depends only on the unknown parameters $1/L$, M_Q , M_U and $M_H \equiv M_{H_u}$. The absence of any dependence on other bulk mass parameters, in particular M_D , is discussed in Appendix D. The top Yukawa coupling $\lambda_{u_3} \equiv \lambda_t$ enters, but it is determined by the top mass, m_t . In the next Chapter we will first study the region of parameter space with $M_Q = M_U$ and $M_H = 0$. In this case we find a restrictive and therefore predictive region in which EWSB is successful. In particular having assumed $M_U = M_Q$ and $M_H = 0$ one can establish a relation between $1/L$ and the Higgs boson mass. In Section 4.4.1 we will perform a detailed calculation to determine this relation at a few percent level of accuracy. In Section 4.5 we will then relax the condition $M_U = M_Q$ to check the stability of the EWSB region⁴, and we study the dependence of the solution on M_U/M_Q .

³In the MSSM this is impossible because H_u does not couple to the down quarks and to the leptons and a vev also for H_d is required to generate their masses.

⁴The motivation of this analysis is due to the fact that in principle higher order brane-localized kinetic operators for the top U and Q multiplets can renormalize differently M_U and M_Q , thus

Finally in Section 4.6 we will let M_H assume values different from 0 while keeping $M_U = M_Q$. This allows us to lower the values of $M_{U,Q}$ and make contact between the Quasi-Localized Top (QLT) model and the CSM.

Chapter 4

Electroweak Symmetry Breaking with a (quasi-)localized top.

We are now ready to analyze the details of the EWSB in the QLT model. As we have seen in the previous Chapter, as the localization becomes more effective, the top quark and squark tree level masses become degenerate and the radiative corrections are the main source of their splitting. Moreover, the compactification length L is not fixed anymore as it was in the original CSM, but it is now allowed to vary together with the Higgs boson mass. Since L determines also (part) of the spectrum of the theory, it is of primary importance, for determining the predictions of the model, to control the relation $m_H(L)$ at a few percent of accuracy. This is the goal of the analysis performed here. We will identify the contributions to the Higgs potential which are relevant for EWSB and for a precise determination of the relation between the Higgs mass and the compactification scale $1/L$. The aimed precision will require us to consider 2-loop contributions to the Higgs potential. To simplify the discussion and the computation, we will first perform the analysis in the case in which the top multiplet is exactly localized on the boundary at $y = 0$. This is, for some contributions, a good approximation for the case of quasi-localization. Later we will deal with the general case, showing how to modify the results obtained for an exact localization.

4.1 The case of exact localization

We can express the reference Lagrangian as

$$\mathcal{L} = \mathcal{L}_{5D}^{N=1} (\text{gauge} \oplus \text{Higgs}) + \mathcal{L}_{4D}^{N=1} (Q \oplus U) \delta(y), \quad (4.1)$$

where the $4D$, $N = 1$ supersymmetric Lagrangian for the Q, U chiral supermultiplets includes the top Yukawa coupling

$$\mathcal{L}_{4D}^{N=1} (Q \oplus U) = \int d^4\theta Q^\dagger e^V Q + \int d^4\theta U^\dagger e^V U + \left[\int d^2\theta \lambda_t H Q U + \text{h.c.} \right]. \quad (4.2)$$

We have not included here any additional kinetic terms for the gauge and Higgs multiplets localized at the boundaries. They are compatible with all the symmetries and indeed, if not present, are generated by radiative corrections. The effects of such terms on EWSB will be discussed in Sect. 5.2. See also Appendix C.

With the boundary conditions in Figure 2.2, after the integration over y , the tree level potential for the real part of the zero mode of the Higgs field is

$$V^{\text{tree}}(h^2) = \frac{g^2 + g'^2}{32} h^4. \quad (4.3)$$

We are interested in the effective potential $V(h^2)$ which, expanded around $h = v$, gives

$$V(h^2) \simeq 2v V'(v^2) h + [V'(v^2) + 2v^2 V''(v^2)] h^2. \quad (4.4)$$

Hence

$$V'(v^2) = 0 \quad (4.5)$$

is the equation which determines v , or the Fermi scale $G_F^{-1/2}$, and

$$m_h^2 = 4v^2 V''(v^2) \quad (4.6)$$

is the physical Higgs boson squared mass. We aim to an accuracy of a few percent in the determination of V' and V'' .

The 1 loop electroweak contribution to V' has been computed first in [89]

$$\delta V'_{\text{ew}}(v^2) \simeq \delta V'_{\text{ew}}(0) = \frac{7\zeta(3)(3g^2 + g'^2)}{128\pi^2 L^2} = 0.93 \frac{10^{-2}}{L^2}, \quad (4.7)$$

up to corrections of relative order $(gvL)^2$.

The one loop $(g^2 + g'^2)\alpha_t$ correction to V'' , in localized approximation for the top, coincides, at logarithmic level, with the same correction in the MSSM for appropriate values of the stop masses m_Q^2, m_U^2 (see below). Its contribution to the Higgs squared mass is [116]

$$\delta m_h^2 ((g^2 + g'^2)\alpha_t) = \frac{-3}{4\sqrt{2}\pi^2} G_F m_t^2 M_Z^2 \log \frac{m_Q^2 m_U^2}{m_t^4}. \quad (4.8)$$

Our task is to compute to the relevant order of approximation the (α_t, α_s) -dependent contributions to Eqs. (4.5,4.6).

4.2 (α_t, α_s) -corrections. General expressions

The corrections of interest contain log's of the fine structure constants, α_s and α_t , which arise from the infrared behavior of the integrals. This is due to the masslessness of the squarks \tilde{Q} and \tilde{U} at tree level, which become massive only at one loop. To deal properly with this situation we introduce, as infrared regulators, the squark masses $m_{0,Q}^2$ and $m_{0,U}^2$ for the two multiplets, also localized at $y = 0^1$. These masses will be sent to zero at the end of the calculation. With these masses the potential of interest, $\delta V_{\text{top}}(v^2)$, has a one loop contribution

$$\delta V_{\text{top}}^{1 \text{ loop}} = 3 \int \frac{d^4 p}{(2\pi)^4} [\log(p^2 + m_{0,Q}^2 + m_{0,t}^2) + \log(p^2 + m_{0,U}^2 + m_{0,t}^2) - 2 \log(p^2 + m_{0,t}^2)], \quad (4.9)$$

where $m_{0,t} = y_t v / \sqrt{2}$ is the unrenormalized top quark mass, and a two loop contribution $\delta V_{\text{top}}^{2 \text{ loop}}$ which arises from the diagrams in Fig. 4.1, in superfield notation, and is explicitly given in Appendix E.

The propagators for all the components of the Q, U supermultiplets are in the background of the field h . Since Q and U propagate in ordinary Minkowsky space, at $y = 0$, the only components of the Higgs and gauge supermultiplets, H and V , that contribute in Fig. 4.1 are those with (+) boundary conditions at $y = 0$. Up to trivial kinematic factors, after the Wick rotation, their propagators are proportional to

$$\begin{aligned} S^{+,+}(k) &\propto \coth \sqrt{k^2} L, \\ S^{+,-}(k) &\propto \tanh \sqrt{k^2} L. \end{aligned} \quad (4.10)$$

¹This also helps in keeping right track of the order in the loop expansion.

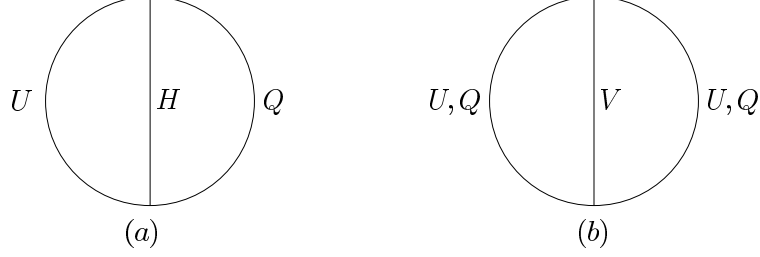


Figure 4.1: The diagrams that contribute to the Higgs potential at order $\alpha_s\alpha_t$ and α_t^2 in superfield notation.

From

$$\delta V_{\text{top}} = \delta V_{\text{top}}^{1 \text{ loop}} + \delta V_{\text{top}}^{2 \text{ loop}}, \quad (4.11)$$

the contributions to $v^2\delta V'(v^2)$ and $v^4\delta V''(v^2)$ are finite after replacement in Eq. (4.9) of $m_{0,t}, m_{0,Q}^2, m_{0,U}^2$ with the physical masses²

$$m_t^2 = m_{0,t}^2 \left(1 + B_\psi^U + B_\psi^Q + 2Z_{y_t} \right), \quad (4.12a)$$

$$m_Q^2 = m_{0,Q}^2(1 + B_\varphi^Q) + m_{0,t}^2(1 + B_\varphi^Q + B_F^U) + \delta m_Q^2, \quad (4.12b)$$

$$m_U^2 = m_{0,U}^2(1 + B_\varphi^U) + m_{0,t}^2(1 + B_\varphi^U + B_F^Q) + \delta m_U^2 \quad (4.12c)$$

and after making an expansion in the one loop quantities: $\delta m_{U,Q}^2$, the one loop corrections to the squared masses, Z_{y_t} , the Higgs-top-top vertex correction, and the various B -factors, the corrections to the wave functions of the various fields. To the precision of interest all these quantities are computed at zero external momenta, except for those involved in Eq. (4.12a) where we use for m_t the running mass at $p^2 = -m_t^2$. The explicit expressions for all these factors are given in Appendix F.

Finally, as anticipated, the fictitious bare masses $m_{0,Q}^2, m_{0,U}^2$ are set to zero. Note that they only appear in m_Q^2, m_U^2 in Eqs. (4.12a,4.12b,4.12c). To leading order in α_t and α_s one has [82]

$$m_U^2 = m_t^2 + \frac{7\zeta(3)}{24\pi} \frac{8\alpha_s + 6\alpha_t}{L^2} + \mathcal{O}(\alpha_t^2, \alpha_t\alpha_s), \quad (4.13a)$$

$$m_Q^2 = m_t^2 + \frac{7\zeta(3)}{24\pi} \frac{8\alpha_s + 3\alpha_t}{L^2} + \mathcal{O}(\alpha_t^2, \alpha_t\alpha_s). \quad (4.13b)$$

² m_Q is the mass of the stop-left. For the mass of the sbottom-left, which only enters in the two loop diagrams, we use $m_B^2 = m_Q^2 - m_t^2$.

4.3 (α_t, α_s) -corrections. Results

To calculate explicitly the corrections of interest we make a systematic expansion of $v^2\delta V'_{\text{top}}(v^2)$ and $v^4\delta V''_{\text{top}}(v^2)$ in α_t, α_s and m_Q^2, m_U^2, m_t^2 , all formally treated as quantities of the same order. In so doing, care must be taken in avoiding spurious infrared divergences. In $v^2\delta V'_{\text{top}}(v^2)$ we keep terms quadratic in these quantities, whereas in $v^4\delta V''_{\text{top}}(v^2)$, which starts quadratic in m_t^2 , we keep those cubic terms which also include at least a factor of $\log m_Q^2 L^2, \log m_U^2 L^2$ or $\log m_t^2 L^2$. In $v^2\delta V'_{\text{top}}(v^2)$ the $5D$ propagators in Eqs. (4.10) are crucial in giving a finite result, whereas in $v^4\delta V''_{\text{top}}(v^2)$, which is more convergent in the ultraviolet (but less convergent in the infrared), the $5D$ propagators can be approximated with their low momentum expansion. We find

$$v^2\delta V'_{\text{top}}(v^2; m_Q, m_U) = \frac{3m_t^2}{16\pi^2} \{ m_Q^2 [2\log(m_Q L) - c] + m_U^2 [2\log(m_U L) - c] - 2m_t^2 [2\log(m_t L) - c] \}, \quad (4.14)$$

$$\begin{aligned} v^4\delta V''_{\text{top}}(v^2; m_Q, m_U) &= \frac{3m_t^4}{8\pi^2} \log\left(\frac{m_Q m_U}{m_t^2}\right) + \\ &\frac{3m_t^4}{16\pi^3} \left\{ \frac{m_t^2 G_F}{\pi\sqrt{2}} \left[2\log^2\left(\frac{m_Q}{m_t}\right) + \log(m_t L) \log\left(\frac{m_Q}{m_U}\right) + \log^2(m_U m_Q L^2) + \log^2\left(\frac{m_U}{m_t}\right) \right] \right. \\ &\quad - \frac{8\alpha_s}{3} \left[\log^2\left(\frac{m_Q}{m_t}\right) - 4\log^2(m_t L) - 4\log(m_t L) \log\left(\frac{m_Q m_U}{m_t^2}\right) + \log^2\left(\frac{m_U}{m_t}\right) \right] \\ &\quad + \frac{m_t^2 G_F}{4\pi\sqrt{2}} [10\log(m_Q L) + 6\log(m_t L) + 12\log(m_U L)] \\ &\quad \left. - \frac{16\alpha_s}{3} \left[(1 - 6\log 2) \log\left(\frac{m_Q m_U}{m_t^2}\right) - 3\log(m_t L) \right] \right\}, \quad (4.15) \end{aligned}$$

where $c = 4 - 2\gamma - (12\log 2)/7 + 2\zeta'(3)/\zeta(3) \simeq 1.33$.

Numerically in view of Eqs. (4.13), the result for $v^2\delta V'_{\text{top}}(v^2)$, for $m_t^{\text{pole}} = 173.1 \pm 1.25$ GeV, is

$$\delta V'_{\text{top}}(v^2) = -(0.71 \pm 0.01) \frac{10^{-2}}{L^2}, \quad (4.16)$$

with the coefficient computed at $1/L = 3$ TeV, with a negligible residual dependence on $1/L$ in the range $1/L = 2 \div 4$ TeV due to $(m_t L)^2$ terms. Note the near cancellation in $\delta V'(v^2)$, at the 20% relative level, between the electroweak term, Eq. (4.7), and the two loop (α_t, α_s) -contribution, Eq. (4.16), with a predominance of the first positive term. To the extent that this calculation is reliable (see below),

the Higgs potential has a positive curvature at $h = 0$, so that EWSB does not take place with exactly localized Q, U multiplets.

In the case of $\delta V'(v^2)$ no simple connection can be established between this theory and a suitably defined MSSM, because of the difference in the way Higgsinos get a mass: by a μ -term in the MSSM, by pairing with conjugate states here. Since $\delta V'(v^2)$ is ultraviolet sensitive in the MSSM, this makes an essential difference. On the contrary, the stronger ultraviolet convergence of the momentum integrals in $\delta V''(v^2)$, relative to $\delta V'(v^2)$, renders this quantity closer to its analogue in a suitably defined MSSM. Indeed the leading m_t^4 -term coincides. The same is also true for the next order terms $m_t^4 G_F m_t^2$ and $m_t^4 \alpha_s$, in the leading \log^2 approximation, if one compares Eq. (4.15) at $1/L = m_Q = m_U \equiv M_S$ with the MSSM result for $\tan \beta = \infty, A_t = 0$ and all superpartners at M_S [117].

4.4 The Case of a quasi-localized top

4.4.1 The Higgs potential

As anticipated in Section 2.2, with the Q, U hypermultiplets not exactly localized, all their components acquire a KK tower of states with M -dependent masses. Most importantly, for finite ML , this tree level spectrum is not supersymmetric. As a consequence, already at one loop, the Higgs potential receives a non vanishing contribution from Q, U exchanges, $\delta V_{\text{top}}^{\text{1loop}}(v^2; ML)$, calculated in [1]. For $ML \leq 2.5$ the slope of this potential, of negative sign, dominates over the electroweak contribution in Eq. (4.7) and triggers EWSB. For $ML \geq 1.5$, however, $\delta V_{\text{top}}^{\text{1loop}}$ is not a sufficiently accurate description of the top-stop contribution to the Higgs potential, as we shall see explicitly: in localized approximation, $ML = \infty$, $\delta V_{\text{top}}^{\text{1loop}}$ vanishes, whereas the top-stop contribution at two loop does not, as seen in the previous Section.

The most important effect of a finite ML , compared to $ML = \infty$, is on the tree level mass of the lightest squarks in the corresponding KK tower. Although this mass converges exponentially to m_t for the stops, or to zero for the sbottom left, its effect is still significant at $ML \simeq 2 \div 3$. In Fig. 4.2 we compare $m_Q(ML)$ with the corresponding quantity, $m_Q(\infty) = m_Q$, Eq. (4.13b), in localized approximation. The radiative one loop contribution is only weakly sensitive to ML and dominates over the tree level mass. Nevertheless the deviation of $m_Q(ML)$ from m_Q in the region of interest is sizable. A similar situation holds for $m_U(ML)$. To account for this effect in the potential, we consider the first and second derivatives of δV_{top} in

Eqs. (4.14,4.15) with m_Q and m_U replaced by $m_Q(ML)$ and $m_U(ML)$ respectively, so that

$$\delta V_{\text{top}}(v^2, ML) \equiv \delta V_{\text{top}}(v^2; m_Q(ML), m_U(ML)). \quad (4.17)$$

A better approximation of δV_{top} (of its derivatives) is in fact the following

$$\delta V_{\text{top}}(v^2, ML) \equiv \delta V_{\text{top}}^{\text{1loop}}(v^2, ML) + \delta V_{\text{top}}^{\text{2loop}}(v^2, ML), \quad (4.18)$$

where

$$\delta V_{\text{top}}^{\text{2loop}}(v^2, ML) = \delta V_{\text{top}}(v^2; m_Q(ML), m_U(ML)) - \delta V_{\text{top}}(v^2; m_Q^{\text{tree}}(ML), m_U^{\text{tree}}(ML)), \quad (4.19)$$

properly subtracted to avoid double counting with the one loop term. For $ML \geq 2$, however, the difference between Eqs. (4.17) and (4.18) is negligible.

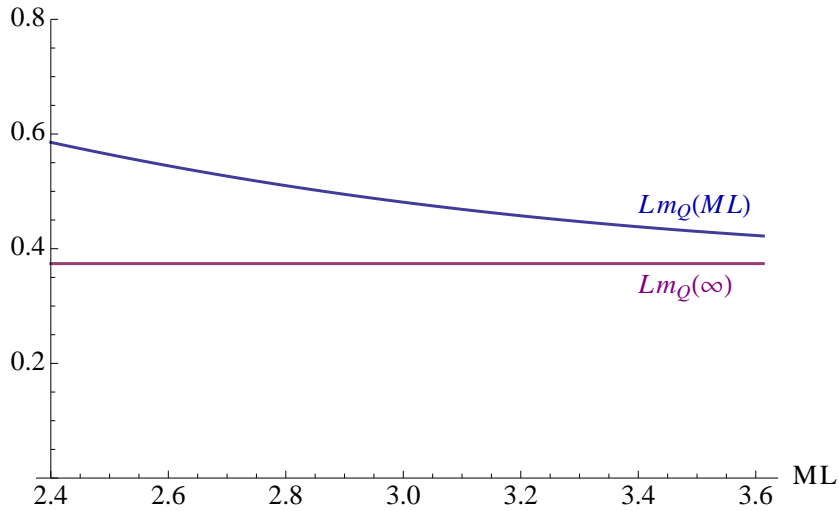


Figure 4.2: The mass of the left handed stop as a function of the localization parameter ML , compared with the same mass in the $ML \rightarrow \infty$ limit.

4.4.2 Determination of the Fermi scale

With the inclusion of the tree level contribution from Eq. (4.3), the minimum equation (4.5) reads

$$\frac{M_Z^2}{4} = -\delta V'(v^2), \quad (4.20)$$

which must be viewed as a relation between the compactification scale $1/L$ and the localization parameter ML . Fig. 4.3 shows

$$-L^2\delta V'(v^2) = -L^2\delta V'_{\text{ew}}(v^2) - L^2\delta V'_{\text{top}}(v^2; ML), \quad (4.21)$$

with the electroweak contribution given in Eq. (4.7) and the top contribution from Eq. (4.17) or (4.18). After rescaling by $1/L^2$, $\delta V'(v^2)$ has no significant residual

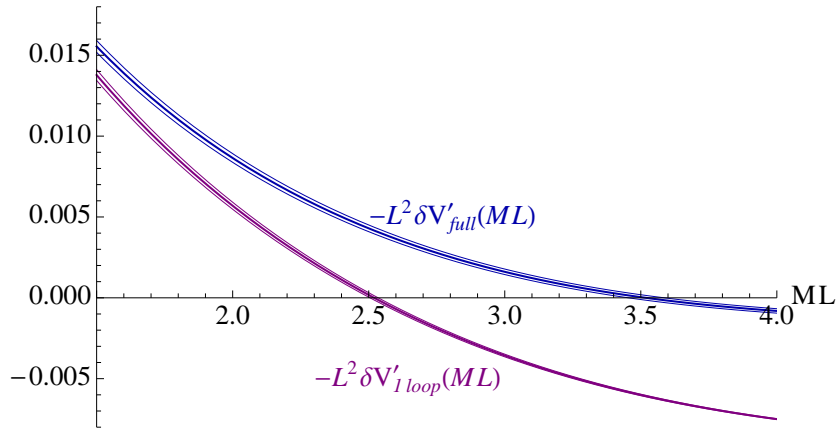


Figure 4.3: Slope of the full radiative Higgs potential, as discussed in the text, versus the top localization parameter ML , compared to the one loop approximation, for $m_t^{\text{pole}} = 173.1 \pm 1.25$ GeV.

dependence on $1/L$ in the region of interest, $1/L \geq 2$ TeV. For these values of $1/L$, it is $(M_Z L)^2 \simeq 10^{-3}$, so that the one loop approximation to $\delta V'_{\text{top}}$ is clearly inadequate. The flattening of $\delta V'(v^2)$ at $ML \simeq 3$, due to the partial cancellation between $\delta V'_{\text{top}}$ and $\delta V'_{\text{ew}}$, is important in reducing the tuning between ML and $1/L$. Also in view of the uncertainties to be discussed below, this same flattening of $\delta V'(v^2)$ makes the precise relation between ML and $1/L$ uncertain. This has little influence, however, on the relation between the Higgs mass and $1/L$, as we discuss shortly.

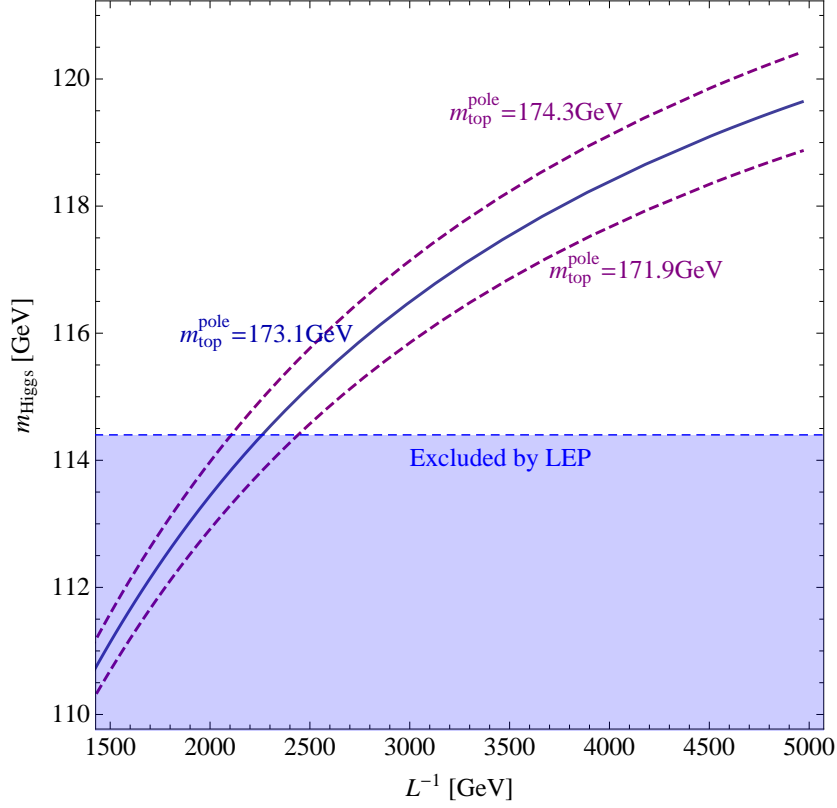


Figure 4.4: Higgs mass as function of $1/L$ for $m_t^{pole} = 173.1 \pm 1.25$ GeV.

4.4.3 The Higgs mass as a function of $1/L$

With the inclusion of the correction in Eq. (4.8) and of the top contribution from Eq. (4.17), Eq. (4.6) reads

$$m_h^2 = M_Z^2 \left[1 - \frac{3}{4\sqrt{2}\pi^2} G_F m_t^2 \log \left(\frac{m_Q^2(ML)m_U^2(ML)}{m_t^4} \right) \right] + 4\sqrt{2}G_F v^4 \delta V_{top}''(v^2; ML). \quad (4.22)$$

By means of the relation between ML and $1/L$ as determined from the minimum equation, m_h is plotted in Fig. 4.4 as function of $1/L$ only, for three different values of the pole top mass, $m_t^{pole} = 173.1 \pm 1.25$ GeV. In Figure 4.5 we show the band of values that would be obtained if ML were not related to $1/L$ by the minimum equation (4.20), but kept fixed at values between 2 and 4. This shows that the precise relation between ML and $1/L$ is almost irrelevant in order to determine

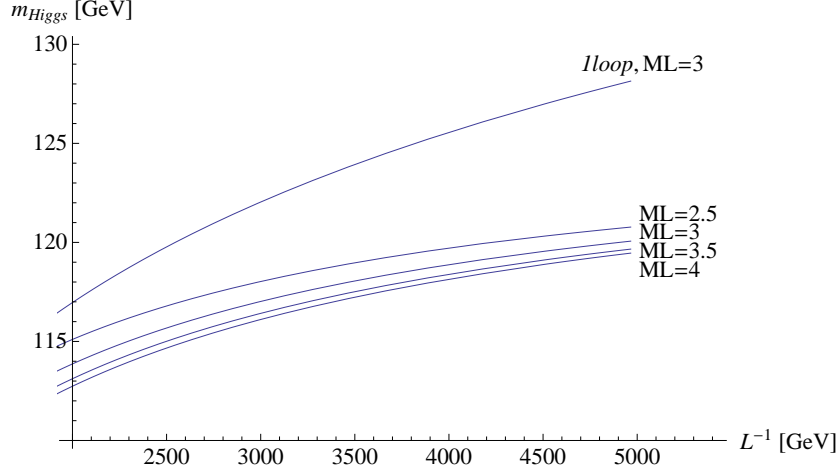


Figure 4.5: Higgs mass for $m_t^{pole} = 173.1$ GeV at different fixed values of the top localization parameter. The result with the full Higgs potential is compared with the one only including the standard top correction at one loop.

the connection between m_h and the compactification scale. In the same Fig. 4.5 we also compare the Higgs mass, calculated on the basis of Eq. (4.22), with the one that would be obtained from a minimally improved lowest order formula

$$m_h^2(\text{naive}) = M_Z^2 + \frac{3\sqrt{2}}{4\pi} G_F m_t^4 \log \left(\frac{m_Q^2(ML)m_U^2(ML)}{m_t^4} \right) \quad (4.23)$$

and $ML = 2 \div 4$. This comparison makes clear that the improved two loop potential is essential for a better determination of m_h .

4.5 Stability of the region: EWSB with $M_UL \neq M_QL$.

We now consider the full parameter space of our model, namely (M_Q, M_U, M_H) . Let us begin by removing the previous restriction $M_Q = M_U$. This modifies the Higgs effective potential in a straightforward way. The squark masses in δV_{top} now contain different tree level bulk masses for U and Q :

$$\delta V_{top}(v^2, M_QL, M_UL) \equiv \delta V_{top}(v^2; m_Q(M_QL), m_U(M_UL)). \quad (4.24)$$

Analogous replacements also apply to the better approximation of Eq. (4.18), where in δV_{top}^{1loop} one must use the mixed momentum-position propagators with

different bulk masses for fields in the Q and U hypermultiplets. The rest of the calculation is straightforward and brings to the results illustrated in Fig. 4.6.

Despite the uncertainties in the determination of the specific values of the ML 's as anticipated in Sect. 4.4.1, this plot shows that the region of successful EWSB is sufficiently wide to allow significant departures from the phenomenologically preferred condition $M_U = M_Q$. Moreover the figure shows that there is no upper bound on $M_Q L$, $M_U L$. Of course this is not the case. In fact consistency of the effective field theory requires that their values are bounded from the cutoff ΛL that will be computed in Sect. 5.1.

Analyzing the isocurves of constant $1/L$ and m_H one could note that both quantities increase as one of the two M s become bigger. Then one can ask what happens to the relation between $1/L$ and m_H . As explained before in the case $M_U = M_Q$, this relation depends little from the specific value of ML . This turns out to be true also in the case $M_U \neq M_Q$. Fig. 4.7 shows the relation for different values of the ratio M_U/M_Q indicating that changing the ratio between the masses by a sizable factor accounts only in a shift in m_H comparable to the spread due to the experimental error on m_{top} .

The analysis with $M_U \neq M_Q$ allows us to make a comment also on [110]. Localization of the top quark by hypermultiplet masses has also been discussed there. They considered the limit of exact localization of U , $M_U L \rightarrow \infty$, and took a very high degree of localization of Q , $M_Q L = 4$, so that the m_t/m_b ratio is entirely understood by the profile of Q . In this case they argue that EWSB is triggered by the two-loop top contribution, since the one-loop top term is negligible. However, our explicit two-loop calculation shows that their estimate of the two-loop contribution significantly exaggerates its effect, and that EWSB does not occur in this region.

4.6 Lower values of the compactification scale

An interesting question is what happens for $1/L$ lower than 2 TeV. Below this value the Higgs mass gets nominally lower than the experimental bound. Had we drawn the same figure as Fig. 4.4 for lower $1/L$, m_h would have reached values as low as 105 GeV at $1/L \simeq 600$ GeV to grow again up to $\simeq 130$ GeV at $1/L \simeq 300$ GeV. At the same time, ML progressively decreases from about 2 at $1/L \simeq 2$ TeV, to zero at the lowest value of $1/L \simeq 300$ GeV, where one makes contact with the ‘‘Constrained Standard Model’’ of [88]. We do not show this plot because in the intermediate region of $1/L \approx 1$ TeV or $ML \simeq 1$, our calculation is not

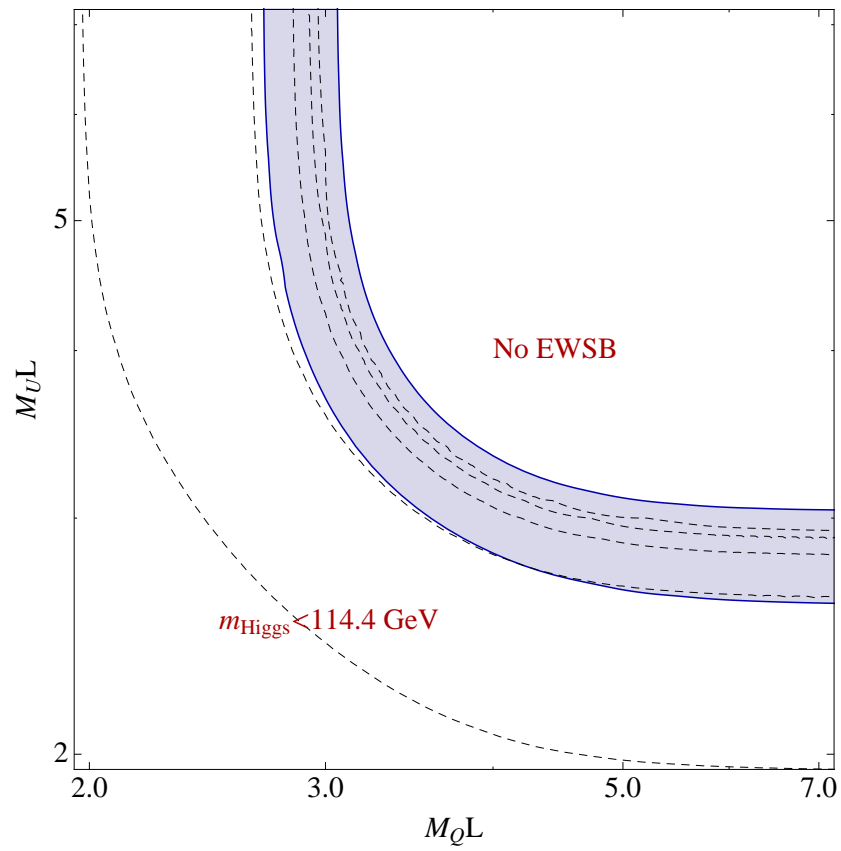


Figure 4.6: Region of allowed Electroweak Symmetry Breaking in the M_Q - M_U plane. The dashed lines represent the $1/L$ isocurves for $1/L = 1, 2, 3, 4, 5$ TeV.

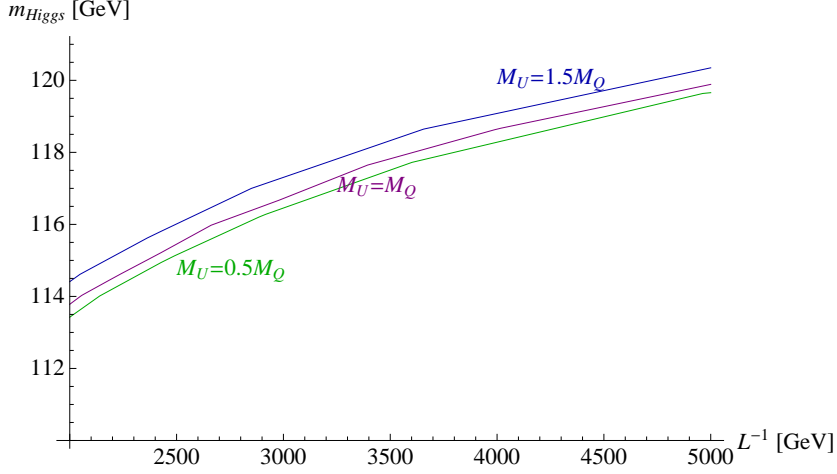


Figure 4.7: The relation between the compactification scale and the Higgs mass for different values of the ratio M_U/M_Q .

fully reliable: $\delta V_{\text{top}}^{1loop}$ does not clearly dominate over the 2 loop contribution we computed, which is only to be trusted for sufficiently large ML because of the approximations made.

To make sense of the model at these lower values of $1/L$, one has also to make sure that the potential with two Higgs doublets, h and h^c , does not get destabilized, given the absence of a bilinear term hh^c . This is possible, without introducing a FI term, by adding a small common mass, $|M_H L| \lesssim 0.1$ for the Higgs hypermultiplets.

A non zero M_H does not affect the physical Higgs mass, through V'' , but only the determination of the Fermi scale, via V' . With an extra term $M_H L$, present in the right hand side of Eq. (4.21), $1/L$ is not tied anymore to ML , which can in turn vary in a range consistent with a moderate amount of fine tuning. The result of this is shown in Fig. 4.8. Different values of ML are used, but always in such a way that no fine tuning occurs stronger than 10% in the determination of $G_F^{-1/2}$. The rise in m_h is due to the stronger influence, for low ML , of $\delta V_{\text{top}}^{1loop}$, a fact which has no correspondence in the MSSM [1, 88].

Taking into account the uncertainties mentioned above, a value of m_h marginally consistent with the experimental lower bound of 114.4 GeV cannot be excluded in the entire region of $1/L$. The existence of independent lower bounds on $1/L$ becomes then of relevance. This in turn crucially depends on the masses

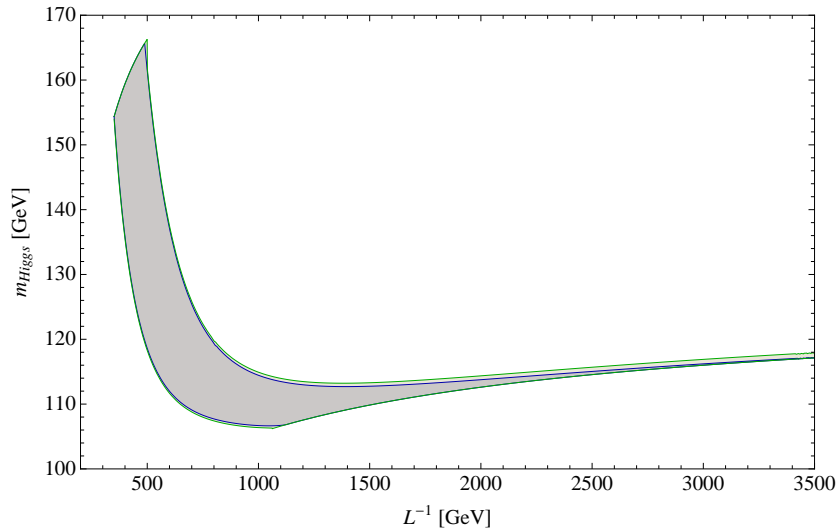


Figure 4.8: Expected range of Higgs masses with the inclusion of a hypermultiplet Higgs mass and a maximum fine tuning in the slope of the potential at 10% level. The gray (green) area is for $m_t^{\text{pole}} = 173.1$ (173.1 ± 1.25) GeV

M_{Q_i} , M_{L_i} for the quark and lepton hypermultiplets of the different generations, $i = 1, 2, 3$ [2]. In the next Chapter we will analyze in detail the bounds on $1/L$ coming from these various effects.

Chapter 5

Phenomenology in the QLT model.

This Chapter will be devoted to the various phenomenological aspects of the QLT model. In Sect. 5.2 the uncertainties on the analysis presented in the previous Chapter will be further discussed. In Sect. 5.3 the spectrum of the model is described. Sect. 5.4 and 5.5 are devoted to the constraints coming from EWPT and flavor physics respectively, while Sect. 5.6 contains a discussion of the possible collider signals of this model. In that section also the present experimental constraints on the CSM and on the models with intermediate-size bulk masses introduced in Chapter 3 will be discussed. Finally Sect. 5.7 will briefly discuss the issues of Dark Matter and of neutrino masses for the QLT model.

5.1 The UV cutoff

Both the CSM and the QLT are formulated in 5D and are non-renormalizable. Indeed they have to be regarded as effective field theories, valid up to an energy scale Λ where they will be completed by some kind of a more fundamental theory.

Since perturbative calculations in an effective field theory are organized as an expansion series in (E/Λ) , the range of their validity is controlled by the size of the cutoff Λ . It is then necessary to estimate its value.

A lower bound on the cutoff can be given by estimating the lowest scale at which one of the interactions of the model ceases to be perturbative. Then the theory (or at least one of its sectors) should be completed by unknown physics at energies of the order of Λ . If the UV completion enters at an energy scale $\Lambda_{UV} \simeq \Lambda$,

it will be strongly coupled at energies $E \gtrsim \Lambda$. For a perturbative UV completion Λ_{UV} should be less than Λ .

As already shown in [88, 2] and in Sect. 2.1.1 the first interactions that become strong are the Yukawa couplings of the third generation.

This is due to the fact that Yukawa couplings are localized at the boundaries and break discrete 5th-momentum conservation. The number of open channels in a process mediated by a Yukawa interaction grows more than linearly with the energy, leading the 5D Yukawa couplings to become strong before any gauge coupling of the same 4D strength.

Here, we recall the estimation of Λ from top and bottom Yukawa interactions. We consider also bottom Yukawa interactions because in presence of hypermultiplet masses the hierarchy m_b/m_t can be generated from localization effects alone and the size of λ_t and λ_b in 5D can be comparable.

Let us focus first on the CSM case. Here only λ_t matters since all the hypermultiplets masses are zero. $\lambda_t(\Lambda)$ can be estimated either by Naive Dimensional Analysis (NDA) [118] properly adapted to 5D [96] or by 4D NDA, taking into account the number N_{KK} of KK modes below the cutoff. In the first case we get

$$\widehat{\lambda}_t(\Lambda) \simeq \frac{1}{16\pi^2} \left(\frac{24\pi^3}{4\Lambda L} \right)^{3/2} \simeq 16 (\Lambda L)^{-3/2}, \quad (5.1)$$

while in the second

$$\widehat{\lambda}_t(\Lambda) \simeq 4\pi \left(\frac{\pi}{2\Lambda L} \right)^{3/2} \simeq 25 (\Lambda L)^{-3/2}, \quad (5.2)$$

where $\widehat{\lambda}_t = \lambda_t/(4L)^{3/2} \simeq m_t/v$, so that $\Lambda L \sim 8$. This means that $N_{KK} \simeq 5$.

In the QLT model since the third generation is localized towards $y = 0$, the Yukawa coupling of both the top and the bottom are relevant for perturbativity and are indeed equal at $ML \simeq 2$. The relation between $\widehat{\lambda}_{t,b}$ and Λ now depends on the localization parameter ML . This dependence comes from two sources: the most important one is the relation between the 5D and the 4D couplings, the other one is the fact that the KK towers are shifted in presence of non-zero masses. Both sources are important for large masses and the second one is particularly relevant for low cutoffs. The impact of these two effects on the perturbativity range can be easily estimated by means of 4D NDA, remembering that the masses of the excited states go like $m^2 = (2n/R)^2 + M^2$ for large ML and that the relation between the 5D and 4D couplings reads

$$\widehat{\lambda}_{t,b}(\Lambda_{t,b}) \simeq \frac{m_{t,b}}{v} \frac{1}{ML(\coth(ML) \pm 1)}, \quad (5.3)$$

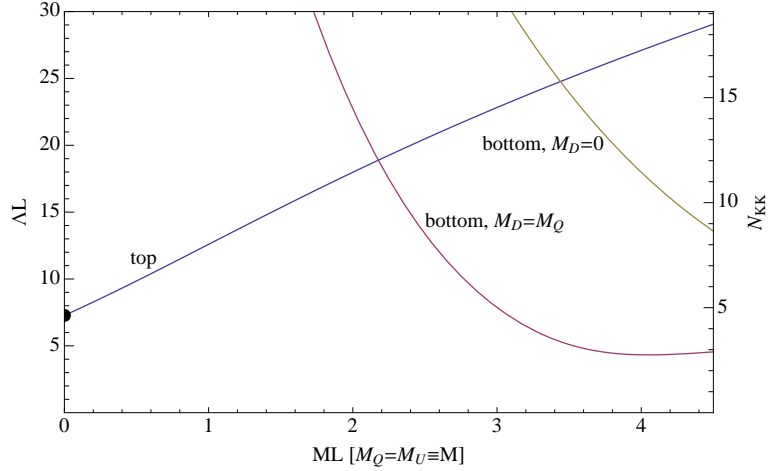


Figure 5.1: Cutoff estimation from top and bottom Yukawa coupling perturbativity as a function of ML . The thick point represents the case of the CSM.

with the sign $+$ for the top and $-$ for the bottom.

The estimated cutoff is shown in Fig. 5.1. For values of $ML \lesssim 2$ the cutoff is determined by the top Yukawa coupling and increases with ML , while for larger values ΛL is controlled by the bottom Yukawa and decreases exponentially with the localization parameter. In particular for the QLT one has successful EWSB for $ML \lesssim 3.6$; at that maximum value of ML one has $\Lambda L \simeq 5$ for $M_D = M_Q$ and $\Lambda L \simeq 25$ for $M_D = 0$.

If the model is not UV completed before Λ , a strong interacting sector appears at one of the boundaries. For $\Lambda L \gg 1$ we can think of the theory in this regime as composed by a bulk sector with perturbative gauge couplings coupled to a strong interacting sector localized at one of the boundary, involving the Higgs and either the top or the bottom multiplets. This motivates the possibility, when considering the effects of higher order SUSY operators on EWPT, to focus on those localized at the boundaries.

5.2 Localized kinetic terms

In this section we will analyze how the results of the previous Chapter are affected by the presence of localized dimension-6 operators. In Sect. 4.4.1 we have found a relation between L^{-1} and m_h and we have claimed that it is determined at a few percent of accuracy. This has a phenomenological impact since L^{-1} determines

the scale of the KK particles, which distinguish the model from other 4D SUSY theories. The deviation from the localized approximation is properly accounted for by Eqs. (4.17)-(4.18). Furthermore we have seen in Sect. 4.5 that altering the condition $M_U = M_Q$ does not sensibly affect the result of Fig. 4.4. The real question, then, is the validity of Eqs. (4.14)-(4.15) with an exactly localized top. The presence of operators other than those in Eq. (4.2) can modify these equations. Among those operators, the potentially most important ones are the kinetic terms of the Higgs and the gauge multiplets localized on the boundaries. In the notation of Eq. (4.1), the constants z_H , z_a in

$$\delta\mathcal{L} = \delta(y) \left[z_H \int d^4\theta H^\dagger e^V H + \sum_a \left(z_a \int d^2\theta W_\alpha^{(a)} W_\alpha^{(a)} + \text{h.c.} \right) \right], \quad (5.4)$$

with $a = SU(3)_C, SU(2)_L, U(1)_Y$ and similar terms localized at $y = L$, have to be treated as additional parameters. For them we need an estimate or a natural assumption for their size. Since H and $W_\alpha^{(a)}$ are 5D fields, their z -factors in Eq. (5.4) have dimension of an inverse mass. Pure dimensional analysis leads to an estimate $z \sim 1/\Lambda$, where Λ could either be the scale Λ_{np} at which some of the couplings become non perturbative or a cutoff scale $\Lambda_{cutoff} \lesssim \Lambda_{np}$ below which our 5D theory represents the low energy effective description of some more fundamental theory. It is then necessary to estimate the value of $\Lambda_{np}L$.

Assuming a strongly coupled UV completion (at least in the 3rd generation Yukawa sector) one can use the estimates of Sect 5.1. With those we are now in the position to estimate the size of the the dimensionless Z -factors, defined as the coefficients after the zero mode rescaling *i.e.* $Z = z/(4L)$, assuming the natural hypothesis that they saturate perturbation theory at energies not lower than Λ :

$$z \lesssim \frac{24\pi^3}{16\pi^2\Lambda_{np}} \rightarrow Z \lesssim \frac{3\pi}{8\Lambda_{np}L} \simeq 0.15 \quad \text{for } \Lambda_{np} \simeq 8/L. \quad (5.5)$$

On the other hand the introduction of these z -factors affects the radiative Higgs potential or the radiative squark masses m_Q^2 , m_U^2 only at quadratic order in the dimensionless Z 's (This is shown explicitly in Appendix C). On this basis we expect that the calculations of the Higgs and squark masses are correct within a few %. A more critical quantity is $\delta V'$, since the electroweak and the top contributions cancel quite accurately against each other and are renormalized by different factors ($1 + \mathcal{O}(Z^2)$). As already mentioned in Sect. 4.4.2, although making uncertain the relation between ML and $1/L$, this has little influence, however, on the relation between m_h and $1/L$.

5.3 Spectrum

The value of $1/L$ determines in a simple way the spectrum of the towers of gauginos, Higgsinos and gauge bosons: up to small effects due to EWSB the lightest gauginos and Higgsinos are at $1/R$, whereas the first KK states of the vector towers are at $2/R$. The heaviness of gauginos–higgsinos is a peculiar feature of these models, in the QLT being stronger than in the CSM. The lightest superpartner is therefore a squark or a slepton, most likely charged, which can be stable or practically stable if a small $U(1)_R$ -breaking coupling is present¹ or if right-handed neutrino superfields are introduced as in Sect. 5.7. This difference with respect to many MSSM-like theories is of great relevance for experimental searches. The first KK states corresponding to the SM particles are instead at $2/R$ with suppressed couplings to SM matter.

The masses of the sfermions of charge Q and hypercharge Y are given by

$$m^2 = m_{tree}^2 + m_{rad}^2 + Y m_Z^2 - Q m_W^2, \quad (5.6)$$

where m_{tree} is the tree level mass, including the Yukawa contribution, and m_{rad} is the one loop contribution, as in Eq. (4.13). As seen in Sect. 4.4.1, both m_{tree} and m_{rad} depend upon the corresponding localization parameter ML . For $ML = 0$, $m_{tree} = \pi/(2L)$ dominates and the sfermion becomes degenerate with the gauginos and the higgsinos. For $ML \gtrsim 1$, m_{rad} dominates and rapidly approaches the localized limit where

$$m_{rad}(\tilde{Q}) = (370 \text{ GeV}) \frac{1}{L \text{ TeV}}, \quad (5.7a)$$

$$m_{rad}(\tilde{U}) = (382 \text{ GeV}) \frac{1}{L \text{ TeV}}, \quad (5.7b)$$

$$m_{rad}(\tilde{D}) = (310 \text{ GeV}) \frac{1}{L \text{ TeV}}, \quad (5.7c)$$

$$m_{rad}(\tilde{L}) = (137 \text{ GeV}) \frac{1}{L \text{ TeV}}, \quad (5.7d)$$

$$m_{rad}(\tilde{E}) = (79 \text{ GeV}) \frac{1}{L \text{ TeV}}. \quad (5.7e)$$

Up to the D-term effects in Eq. (5.6), these are lower values for the sfermion masses.

The masses which are unequivocally determined are those belonging to the Q and U hypermultiplets that play a crucial role in EWSB, $\tilde{t}_L, \tilde{t}_R, \tilde{b}_L$, being correlated

¹Differences between stability and quasi-stability are of little importance for collider physics but may be crucial for cosmological issues.

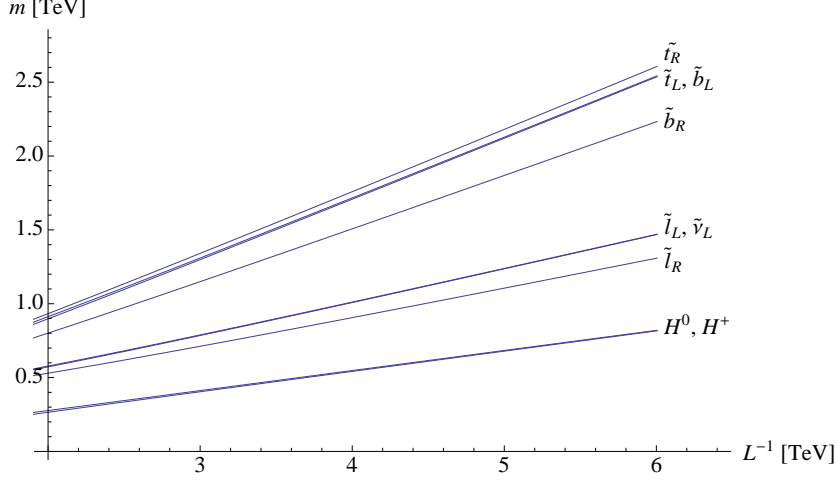


Figure 5.2: Physical masses for the squarks and sleptons from hypermultiplets with $M_Q = M_U = M_D = M_L = M_E = M$, and for the scalars of H_d with $M_{H_d} = 0$. As $1/L$ increases so does M , so that the squark and slepton masses become dominated by the radiative contributions of Eqs. (5.7a – 5.7e).

to the compactification scale. For $1/L \gtrsim 2$ TeV, eq. (5.7a) gives the mass of the left handed stop and sbottom, split by $m_{tree}(\tilde{t}) = m_t$, whereas $\left(m_{rad}(\tilde{U})^2 + m_t^2\right)^{1/2}$ is the mass of the right-handed stop.

For lower values of $1/L$, if a tree level mass of the Higgs hypermultiplets is present (see Sect. 4.6), the third generation squarks can be progressively delocalized. In this case Eqs. (5.7) give a lower bound, with the overall masses that can go up to 800 GeV even for $1/L$ below 1 TeV.

Eqs. (5.6,5.7d) apply also to the masses of the scalars in the second Higgs hypermultiplet H_d , without a VEV and with gauge couplings identical to those of a left-handed slepton multiplet. Not to undo EWSB, the Higgs hypermultiplets are always almost fully delocalized, $|M_H L| \leq 0.1$. Eq. (5.7d) is strictly valid for $1/L \gtrsim 2$ TeV and $m_{rad}(\tilde{H}) \gtrsim 270$ GeV. For smaller values of $1/L$ a tree level Higgs mass can play a role and can raise the total mass of the charged and neutral scalars in H_d , relative to Eq. (5.7d), by about 100 GeV at $1/L \simeq 1$ TeV. Note that, in this case, the mass of the neutral H_d is below 100 GeV for $1/L \lesssim 1.4$ TeV, but, since H_d has no VEV this is not presently excluded.

Finally Fig. 5.2 shows masses for the other squarks and sleptons of the third generation in the case where all the matter hypermultiplet masses are taken equal

to each other and $M_{H_d} = 0$. If $M_L = M_E = 0$ sleptons are much heavier and the spectrum differs from the one in Fig. 5.2 only by their presence.

5.4 Constraints from precision observables

The effects on EWPT arise from various sources. First of all there are calculable loop effects generated by non supersymmetric operators. In fact, as we have shown in Sect. 2.2, Supersymmetry is globally broken: the mass splitting between particles belonging to the same supersymmetric multiplet is $1/L$. However the residual SUSY of the theory restricts the form of the possible counterterms. Observables corresponding to operators which have no counterterm allowed by the residual SUSY are thus necessarily finite.

Beyond these calculable effects one should also consider the effect of supersymmetric operators, mainly those localized at the boundaries. Indeed one has to look for operators respecting the $N = 1$ supersymmetries present at the boundaries and which affect EWPT. The fact that they are allowed by Supersymmetry makes 1-loop calculations divergent. These operators, whose coefficients have negative dimension in mass, are generated by radiative corrections at the scale where perturbation theory breaks down and are weighted by powers of $1/\Lambda L$. In order to build a fully reliable and predictive theory that solves the Little Hierarchy Problem, one has to consider the impact of such operators on EWPT. We analyze the localized operators assuming that their coefficients saturate perturbation theory at the scale Λ , estimating them by 5D NDA [96].

5.4.1 Universal effects

We make an analysis in terms of the form factors \hat{S}, \hat{T}, W, Y introduced in [22]. Such an analysis is valid for a wide class of “universal theories” in which the only gauge interaction (except QCD) of all the light fermions of the SM are described by

$$\mathcal{L}_{\text{int}} = \bar{\Psi} \gamma^\mu (T^a \bar{W}_\mu^a + Y \bar{B}_\mu) \Psi, \quad (5.8)$$

where \bar{W}, \bar{B} are not necessary the physical W, B . In our case, if no localization parameter is present, it follows from momentum conservation in the 5th dimension that, at tree level, the “interpolating” fields \bar{W}, \bar{B} are exactly the zero modes of the 5D gauge bosons. We shall come back to the localization effects later on.

Upon use of the equations of motion and neglecting terms vanishing with the fermion masses, a complete set of dimension-6 operators which contribute to

\hat{S}, \hat{T}, W, Y are [119]:

$$\mathcal{O}_{WB} = \frac{1}{gg'} (H^\dagger \tau^a H) W_{\mu\nu}^a B_{\mu\nu}, \quad (5.9a)$$

$$\mathcal{O}_H = \left| H^\dagger D_\mu H \right|^2, \quad (5.9b)$$

$$\mathcal{O}_{BB} = \frac{1}{2g'^2} (\partial_\rho B_{\mu\nu})^2, \quad (5.9c)$$

$$\mathcal{O}_{WW} = \frac{1}{2g^2} (D_\rho W_{\mu\nu}^a)^2. \quad (5.9d)$$

If they appear in a 4D lagrangian as

$$\delta\mathcal{L} = \frac{1}{v^2} (c_{WB}\mathcal{O}_{WB} + c_H\mathcal{O}_H + c_{WW}\mathcal{O}_{WW} + c_{BB}\mathcal{O}_{BB}), \quad (5.10)$$

where $v = \langle H \rangle = 174 \text{ GeV}$ is the Higgs vev, they give the following contributions to the EW form factors²

$$\hat{S} = 2\frac{c_W}{s_W}c_{WB}, \quad \hat{T} = -c_H, \quad W = -g^2c_{WW}, \quad Y = -g^2c_{BB}. \quad (5.11)$$

Since at the boundaries there are $N = 1$ supersymmetries left unbroken, we have to find the supersymmetric completion of the operators Eq. (5.9).

This can be easily accomplished using supersymmetric gauge covariant derivatives (see for example [120]). A simple power counting shows that all the SUSY and gauge invariant operators up to dimension-6 only, involving Higgs and vector superfields are

$$\int d^4\theta (\hat{H}^\dagger e^{gV} \hat{H})^2, \quad (5.12a)$$

$$\int d^2\theta \text{Tr} \left(\nabla^\mu \hat{W}^\alpha \nabla_\mu \hat{W}_\alpha \right) + \text{h.c.}, \quad (5.12b)$$

$$\int d^2\theta \text{Tr} \left(C_{\dot{\alpha}\dot{\beta}} \nabla^{\alpha\dot{\alpha}} \hat{W}_\alpha \nabla^{\beta\dot{\beta}} \hat{W}_\beta \right) + \text{h.c.}, \quad (5.12c)$$

$$\int d^4\theta \hat{H}^\dagger e^{gV} \hat{W}^\alpha e^{-gV} \nabla_\alpha e^{gV} \hat{H} + \text{h.c.}, \quad (5.12d)$$

$$\int d^4\theta \hat{H}^\dagger e^{gV} \nabla^\mu \nabla_\mu \hat{H}, \quad (5.12e)$$

$$\int d^4\theta \hat{H}^\dagger e^{gV} \hat{H}, \quad (5.12f)$$

$$\int d^2\theta \text{Tr} \left(\hat{W}^\alpha \hat{W}_\alpha \right) + \text{h.c.}, \quad (5.12g)$$

²The normalization of the vector fields is such that $\mathcal{L}_{\text{kin}} = -\frac{1}{4g^2} W_{\mu\nu}^a W_{\mu\nu}^a - \frac{1}{4g'^2} B_{\mu\nu} B_{\mu\nu}$

where \hat{H} is the Higgs chiral superfield while V is a general vector superfield and \hat{W}^α its chiral supersymmetric field strength. They refer both to the W and to the B vector fields. The symbol C is the usual antisymmetric matrix used in raising and lowering spinorial indices. In our notation $C_{\dot{\alpha}\dot{\beta}} = \sigma_2$.

Using (anti)commutation rules, the other unlisted operators can be shown to be equivalent to suitable combinations of the previous ones. Expanding them in component fields, one can see that all the operators in (5.9) are originated, up to terms that vanish by the equations of motion and/or in the limit of massless fermions. Therefore the basis selected in [22] can be supersymmetrized to $N = 1$ in 4D. In particular the first operator originates \mathcal{O}_H , the second and the third originate \mathcal{O}_{WW} and \mathcal{O}_{BB} while the fourth contributes to \mathcal{O}_{WB} . On the contrary the localized kinetic terms (5.12f-g) only contribute through the mixing of the zero modes with the Kaluza-Klein states. The related effects, also of “universal” nature, are however subdominant in the parameter region of interest, with respect to the direct contributions from dimension-6 operators and we shall neglect them in the following.

To estimate the coefficients of the operators Eq. (5.9) we use 5D NDA. Notice that the existence of the supersymmetric operators Eq. (5.12) makes the 1-loop corrections to these coefficients divergent. For example, the Yukawa contributions to c_H , or \hat{T} , has a quadratic sensitivity to the UV, while the dependence of \hat{S} is logarithmic. This can be easily found by dimensional analysis. In fact the coefficient c_H of the operator \mathcal{O}_H localized at one of the boundaries and written in terms of the 5D fields has dimension of $(\text{mass})^{-4}$. 1-loop Yukawa corrections will be proportional to the fourth power of the 5D Yukawa coupling. Then the quadratic dependence on Λ comes out immediately, by remembering that the dimension of a 5D Yukawa coupling is $(\text{mass})^{-3/2}$. In the same way c_{WB} for a localized contribution has dimension of $(\text{mass})^{-3}$ and the Yukawa corrections to \mathcal{O}_{WB} are proportional to the square of the Yukawa coupling giving a logarithmic dependence on Λ .

Let us now suppose that the operators Eq. (5.12) contribute to a localized term $\delta\mathcal{L}_4$ in Eq. (2.12), where the fields H, W_μ^a and B_μ are 5D fields localized at a boundary. The dominant contribution to the EWPT from the operators of dimensions 6 in Eq. (5.12a-e) comes from the zero modes of the various fields, *i.e.* the standard gauge and Higgs bosons. The localized operators we are interested

in are then the following

$$\delta\mathcal{L}_4 = C_H \left| \bar{H}^\dagger D_\mu \bar{H} \right|^2 + \frac{C_{WB}}{gg'} \left(\bar{H}^\dagger \tau^a \bar{H} \right) W_{\mu\nu}^a B_{\mu\nu} + \frac{C_{BB}}{2g'^2} (\partial_\rho B_{\mu\nu})^2 + \frac{C_{WW}}{2g^2} (D_\rho W_{\mu\nu}^a)^2, \quad (5.13)$$

where \bar{H} is the zero mode of the Higgs boson with canonical 5D normalization, whereas the vector bosons are already normalized to 4D (and g, g' are the standard 4D gauge couplings). Using naive dimensional analysis one finds

$$C_H = \frac{(24\pi^3)^2}{16\pi^2} \frac{1}{\Lambda^4}, \quad C_{WB} = gg' \frac{24\pi^3}{16\pi^2} \frac{1}{\Lambda^3}, \quad C_{BB} = C_{WW} = \frac{1}{16\pi^2} \frac{1}{\Lambda^2}. \quad (5.14)$$

To connect the 5-dimensional coefficients of Eq. (5.14) to the 4-dimensional coefficients of Eq. (5.10) one has to rescale the 5D Higgs field in terms of the 4D zero mode: $\bar{H} = H/\sqrt{4L}$. Using Eqs. (5.10,5.11) one gets

$$\hat{S}(\mathcal{O}_{WB}) \sim \frac{3\pi}{4} g^2 \frac{(vL)^2}{(\Lambda L)^3} \simeq 0.6 \cdot 10^{-4} \frac{(L \cdot \text{TeV})^2}{(\Lambda L/8)^3}, \quad (5.15a)$$

$$\hat{T}(\mathcal{O}_H) \sim \frac{9\pi^4}{4} \frac{(vL)^2}{(\Lambda L)^4} \simeq 1.6 \cdot 10^{-3} \frac{(L \cdot \text{TeV})^2}{(\Lambda L/8)^4}, \quad (5.15b)$$

$$W(\mathcal{O}_{WW}) \sim Y(\mathcal{O}_{BB}) \sim \frac{g^2}{16\pi^2} \frac{(vL)^2}{(\Lambda L)^2} \simeq 1.3 \cdot 10^{-6} \frac{(L \cdot \text{TeV})^2}{(\Lambda L/8)^2}. \quad (5.15c)$$

One can notice that the dominant contributions come from C_H . C_{WW}, C_{BB}, C_{WB} become comparable to C_H only for values of the cut-off $\Lambda L \simeq 100$ which can never be attained (see Fig. 5.1). Comparing the contributions Eq. (5.15) to the experimental values [22]

$$\begin{aligned} \hat{S} &= (-0.7 \pm 1.3) \cdot 10^{-3}, & \hat{T} &= (-0.5 \pm 0.9) \cdot 10^{-3}, \\ W &= (0.2 \pm 0.6) \cdot 10^{-3}, & Y &= (0.0 \pm 0.6) \cdot 10^{-3}, \end{aligned} \quad (5.16)$$

we can obtain the bound shown in Fig. 5.3. The shaded region is excluded at 99 % of C.L. The sign of C_H is irrelevant. The black point represents the CSM described in Sec. 2, the red continuous line represents the QLT model described in Sec. 4 for $M_U = M_Q = M_D$ and $M_H = 0$, while the region inside the green lines corresponds to the QLT model varying M_H as described in Sec. 4. The red continuous line is stopped at $1/L \simeq 2 \text{ TeV}$ because the Higgs mass drops below the experimental limit (see Fig. 4.4) and at about 4.5 TeV when a fine-tuning of about 10 % in the potential occurs. The shape of the region delimited by the green

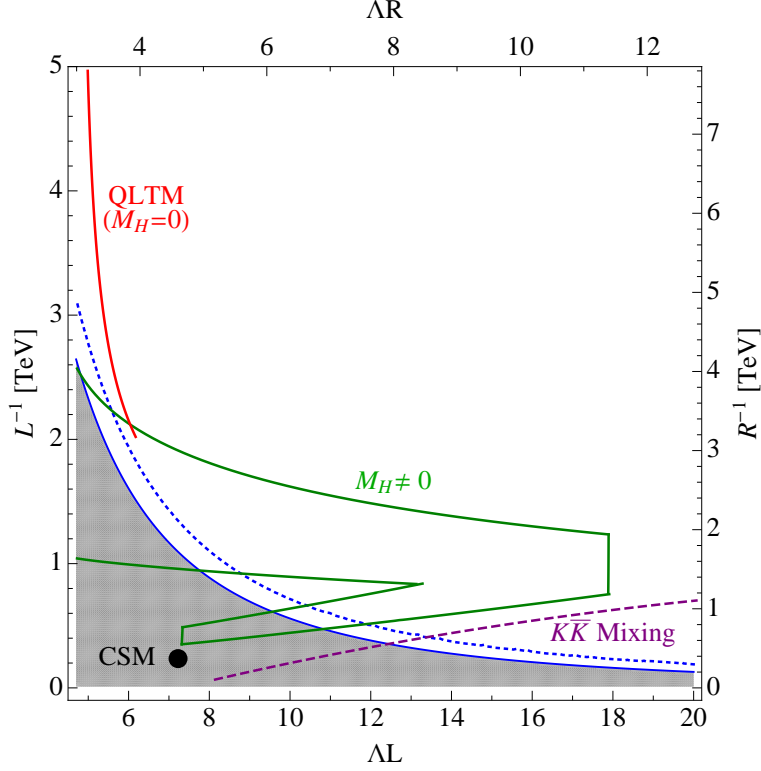


Figure 5.3: Bounds on the CSM and the QLT models from EWPT. The shaded region is excluded at 99 % of C.L.

lines depends on the fact that the cutoff is determined by both the top and the bottom Yukawa couplings (see Fig. 5.1). One has to remember that the connection between ML and $1/L$ is not as precise as the one between the Higgs mass and $1/L$. Thus the red continuous line can move horizontally of about $\Delta(\Lambda L) \simeq 4.5$ due to this uncertainty. From these universal effects it seems problematic to reconcile the CSM with the EWPT. One should not forget, on the other hand, that Eqs. (5.15) are a naive estimate, dependent on a high power of ΛL . Furthermore, an unknown contribution coming from the UV completion of the theory could provide a fine-tuned cancellation in order to make the size of the contribution to \hat{T} in Eq. (5.15b) sufficiently small. Conversely, in the QLT model both for $M_H = 0$ and for $M_H \neq 0$, the typical values of $1/L$ are large enough not to create conflicts with EWPT.

5.4.2 Non universal flavor-diagonal effects

If the hypermultiplet masses do not vanish, then the interpolating fields of Eq. (5.8) do not correspond to the zero modes anymore, but to a linear combination with all the KK states. This fact can induce effects that may be visible once EW observables corresponding to different energy scales are compared, *e.g.* low energy observables vs. LEP vs. LEP2. Moreover if the hypermultiplet masses differ among leptons and quarks and among different generations of leptons, there will be violations of lepton universality and of quark-lepton universality of the weak interactions (*i.e.* non-unitarity of the CKM matrix), besides possible Flavor and CP-Violation which will be analyzed in Sect. 5.5.

All these quantities are constrained at the order of 10^{-3} . On the other hand the typical size of the expected effect is $(vL)^2 \Delta ML$ where ΔM is the mass difference between two generations or between leptons and quarks in the case of quark-lepton universality. Since $(vL)^2$ is already $\mathcal{O}(10^{-3})$, these bounds are not able to significantly constrain the bulk masses beyond $\mathcal{O}(1)$ factors. Finally $M_L \neq 0$ for the first generation has an impact on the determination of the Fermi constant. This is effectively equivalent to a shift in the T (and U) parameter(s). However it is easy to realize, by using the fermionic wave-functions of App. A that this constrains $ML \lesssim 2$ only if $1/L \sim 2 \text{ TeV}$ (this bound loosens quickly once the compactification scale is increased). Hence non universal flavor-diagonal effects do not provide effective constraints on the hypermultiplet masses of the leptons and the first two generation quarks.

We now turn to the non-universal effects involving the bottom quark.

In the CSM a localized operator

$$\int d^4\theta \hat{H}^\dagger \hat{H} Q_3^\dagger e^{gV} Q_3 \quad (5.17)$$

is generated, with a similar coefficient to C_H in Eq. (5.14). It is a correction to the $Zb\bar{b}$ vertex and thus one obtains a similar bound to the one discussed in the previous Subsection.

In the QLTM and for $M_H = 0$ it is the bottom Yukawa coupling which becomes non perturbative first, hence one expects that the most important contribution comes from the operator (5.17) localized at the $y = L$ boundary. But since the left-handed bottom gets quasi-localized mostly at the $y = 0$ boundary, a wave function suppression is present, making this effect negligible. A similar argument can be made for the right-handed bottom quark. Now, however, M_{D_3} is not constrained to be similar to M_{Q_3} by EWSB. The contribution from such localized operator

would at most be of the order of

$$\begin{aligned}
|\epsilon_b| &\sim g' \frac{Y_b}{2} \frac{(24\pi^3)^2}{16\pi^2} \frac{(vL)^2}{(\Lambda L)^4} \frac{x}{\cosh(2x) + \sinh(2x) - 1} \\
&\sim 2 \cdot 10^{-3} \frac{(L \cdot \text{TeV})^2}{(\Lambda L/8)^4} \frac{x}{\cosh(2x) + \sinh(2x) - 1}
\end{aligned}$$

with $x = M_{D_3}L$ and $Y_b = 1/3$. Since ϵ_b is constrained at $\mathcal{O}(10^{-2})$ level, it does not pose a significant constraint on M_{D_3} .

If we turn M_H on, then successful EWSB occurs for lower values of ML where it is the top Yukawa coupling that determines the cut-off. Then one should consider the operator at $y = 0$. However one obtains a bound that does not differ significantly from the one obtained above from \widehat{T} , which is weaker than the one coming from flavor violation effects, analyzed in the following.

In addition to this kind of effect, if we turn on a mass term for the third generation of quarks, the interpolating field defined by Eq. (5.8) is no longer the same for all the light fermions since, for the bottom, it is a superposition of all the KK modes. Then for the third generation an additional interaction to Eq. (5.8) is present at the tree level which gives non universal effects mainly concerning the bottom quark. These effects produce 4-fermion interactions involving the bottom quark and modify the $Zb\bar{b}$ vertex only in presence of localized kinetic terms for the gauge or Higgs multiplets. The size of this effect is comparable to the one produced by the operator of Eq. (5.17).

5.5 Flavor and CP violation

The quasi-localization of some matter hypermultiplets gives rise to new interactions which limit $1/L$ from below in a definitely stronger way than in the case of matter homogeneously spread throughout the bulk, as in [88].

Depending on the size of the masses, different effects can possibly arise from tree level processes. Indeed non-flat profiles can couple matter zero modes to non-zero modes of gauge bosons and their tree level exchange can generate modifications to the Fermi constant already discussed in Sect 5.4.2 or lead to Flavor Changing Neutral Currents (FCNC) [121].

We now consider the bounds coming from those processes that violate Flavor and CP. For concreteness we will illustrate it in the quark sector, the case of the lepton sector being analogous. The presence of hypermultiplet masses that are not proportional to the identity in family space renders physical those mixing matrices

which are otherwise unphysical in the SM. In particular if one starts in the basis where the bulk mass matrices are diagonal, the subsequent diagonalization of the quark Yukawa couplings, produces other nontrivial structures in flavor space beside the Cabibbo-Kobayashi-Maskawa matrix, V_{CKM} . Structures like $D_L^\dagger M_Q^n D_L$, $D_R^\dagger M_D^n D_R$, $U_L^\dagger M_Q^n U_L$, where $U_{L,R}$, $D_{L,R}$ are those unitary matrices that diagonalize the quark Yukawa couplings, are now physical. Indeed, since in presence of a bulk mass the quark zero modes are not anymore orthogonal to the KK gauge bosons, these terms generically introduce new FCNCs and new sources of CP-Violation already at tree level via KK gauge boson exchange.

An analogous situation happens with the leptons. In particular the exchange of the KK photon and Z bosons would induce processes like $\mu \rightarrow 3e$ and $\tau \rightarrow 3e$, whose very strong experimental bounds impose $M_{L_i} \equiv M_L$ and $M_{E_i} \equiv M_E$.

On the other hand in the quark sector the strongest constraints will come from neutral meson mixings (of K, D, B_d , B_s) thru a tree level exchange of KK gluons because g_s is the strongest coupling. As in the leptonic case, possible differences between first and second generation masses are strongly constrained from $K^0 - \bar{K}^0$ and $D^0 - \bar{D}^0$ mixing. In fact parametrically the contribution to the mixing amplitude reads (for $ML \lesssim 1$)

$$\begin{aligned} M_{12}^{sd} &\sim B_K F_K^2 m_K (D_{12}^\dagger M_1 D_{11} + D_{12} M_2 D_{22}^\dagger)^2 g_s^2 / 90, \\ M_{12}^{cu} &\sim B_D F_D^2 m_D (U_{12}^\dagger M_1 U_{11} + U_{12} M_2 U_{22}^\dagger)^2 g_s^2 / 90, \end{aligned}$$

where M is the hypermultiplet mass matrix and D , U are the down quark mixing matrices that diagonalize the Yukawa couplings. Moreover in the formulas above we did not distinguish between left-handed and right-handed fields. Note that for the case of the left-handed doublet D_{12} and U_{12} cannot be simultaneously zero since their difference determines the Cabibbo angle in the CKM matrix and these bounds cannot be evaded purely by alignment [122, 123]. If one assumes $D_{11,22} \sim \mathcal{O}(1)$ and $D_{12} = -D_{21} \sim \mathcal{O}(\lambda_c) \sim 0.1$ as in the CKM matrix (and analogously for U_{ij}) one finds that $|M_2 L - M_1 L| \lesssim 10^{-3} \div 10^{-4}$ for $L^{-1} \sim \text{TeV}$. Barring any unexplained cancelation, in the following we will therefore assume that³ $M_{Q_1} = M_{Q_2} \equiv M_Q$, $M_{U_1} = M_{U_2} \equiv M_U$, $M_{D_1} = M_{D_2} \equiv M_D$. This amounts to impose a flavor $U(2)$ symmetry in the bulk, broken only by the Yukawa couplings localized on the branes. In this case the flavor transitions mediated by KK states proceed via mixing with the third generation. In other words, under these assumptions,

³This prevents any geometrical explanation of the structure of the Yukawa couplings in setups with flat backgrounds and compactification scales at the TeV.

the flavor structure of the QLT model is well described by the so-called Next-to-Minimal Flavor Violation (NMFV) [17]. In this case the above expressions now reads

$$\begin{aligned} M_{12}^{sd} &\sim B_K F_K^2 m_K (D_{32}^\dagger D_{31})^2 g_s^2/3 \cdot L^2 f_{4F}(M_{Q_3} L), \\ M_{12}^{cu} &\sim B_D F_D^2 m_D (U_{32}^\dagger U_{31})^2 g_s^2/3 \cdot L^2 f_{4F}(M_{Q_3} L), \end{aligned}$$

with

$$f_{4F}(x) = \begin{cases} \frac{x^2}{30} - 4\frac{x^4}{945} & x \lesssim 1.5 \\ \frac{2}{x^2} - \frac{3}{x} + \frac{4}{3} & x \gtrsim 1.5 \end{cases}$$

In the case of the third generation, the quark bulk masses are linked to $1/L$ by the requirement of a successful EWSB. Assuming that $D_{L,R}$ have the same structure of V_{CKM} , *i.e.* $D_{13} \sim \lambda_C^3$, $D_{23} \sim \lambda_C^2$ where λ_C is the sine of the Cabibbo angle, one can re-express the constraint as a bound on $1/L$

$$L^{-1} \gtrsim 5.6 f_{4F}^{1/2}(M_{Q_3} L) \text{ TeV}.$$

Here the strongest bound comes from the ϵ -parameter in K physics: one needs $1/L \gtrsim 2 \text{ TeV}$ [121]. This bound applies to the QLTM model. In the region where $1/L \lesssim 2 \text{ TeV}$ (and $M_H \neq 0$) there is a weaker bound due to the weaker localization, as shown in Fig. 5.3 together with the bounds obtained from the EWPT. This bound corresponds to the case of a purely left-handed 4-fermion operator ($LLLL$), where the mixing is mediated by D_L . It is tightly connected to EWSB since the hypermultiplet mass of the left-handed top and bottom are determined by it.

In principle one can have a $LLRR$ vector operator involving quarks of different chiralities if KK gluons can connect $SU(2)_L$ -doublet quarks with singlet ones. Upon a Fierz rotation, this operator correspond to a scalar LR -mixing operator. Including QCD running effects and the fact that scalar LR 4-fermions operators have matrix elements among physical meson states that are chirally enhanced, one finds that the bound gets about one order of magnitude stronger than the one for a $LLLL$ operator [124]. However this contribution depend on $M_{D_3} - M_{D_{1,2}}$ and can be easily made negligible if $M_{D_3} \sim M_{D_{1,2}}$ or if $M_{D_i} L \ll 1$. Even though it cannot constitute a lower bound on $1/L$ it has a clear impact on the superparticle spectrum: if the right-handed sbottom \tilde{b}_R is light as the other third generation squarks, then also the right-handed strange and down squarks \tilde{s}_R , \tilde{d}_R are light and quasi-degenerate with it. On the contrary, since the bounds on $M_{U_3} - M_{U_{1,2}}$ are very weak, potentially large FCNCs in top decays are still allowed and possibly detectable at the LHC [125].

Finally, a few comments are in order on other contributions to Flavor and CP-Violating processes. The contributions coming from loops of SUSY particles are very small, given the heaviness and the Dirac nature of the gauginos. Other effects can come from possible brane localized terms, in particular kinetic terms for the quarks and leptons.

However, it is conceivable that these terms are generated by non perturbative effects triggered by the 3rd generation Yukawa couplings becoming strong. Moreover the scale Λ in the above formula is controlled by the 3rd generation bulk masses. It is then natural to assume that the structure in flavor space of these kinetic terms will look like $\lambda_U^\dagger \text{diag}(0, 0, 1) \lambda_U$ in the basis where the bulk masses are diagonal. Under this assumption their effect is of the same order (or smaller) than the ones already considered.

Finally, in the case of the CSM the bulk masses vanish at tree level and the ones induced radiatively by the Fayet-Iliopoulos term will be naturally flavor universal. In this case all the information about flavor is only contained in the Yukawa matrices. This implies that the flavor structure of the CSM is the one of Minimal Flavor Violation (MFV) [126].

5.6 Phenomenology of Sparticle Production

5.6.1 General Features

The precise phenomenology of sparticle production will depend upon the choice of the hypermultiplet masses. There are, however, a few features of this phenomenology that have an universal character. Because the lightest superpartner (LSP) is a squark or a slepton, this scalar is pair produced in a hadron collider, either directly or by cascade decay, most of the times via a strong interaction cross section determined by $1/L$ (and ML).

If the LSP is colored, then it will hadronize picking up one or two quarks, and creating either a heavy meson or a baryon. While the meson is the lightest state, the energies involved make it easy to produce baryons as well. Even though the precise spectroscopy of the states containing a spin-0 colored triplet is unknown, the typical splittings will be $\lesssim 1 \text{ GeV}$. This newly formed bound state⁴ (R-hadron) will then traverse the detector, interacting with the detector material

⁴In the following we will call the meson $M_u^{+,0}$ and the baryon $B_u^{+,+,0}$ (together with their antiparticles), where the upper indices determine the electric charge and the lower one stand for an up-type (down-type) squark.

and losing energy. The amount of energy lost in an interaction is small, of the order of the GeV, much less than the total energy of the meson, since all the scattering processes proceed through the light quarks, the heavy squark being just a spectator. Besides the standard elastic and inelastic (meson production) processes, R-hadrons can also undergo charge exchange processes like $M^+n \rightarrow M^0p$ or baryon number changing processes like $Mp \rightarrow B\pi$. Note that the latter are possible for mesons, while the inverse is only possible for antibaryons, because of the environment having positive baryon number. The detection strategies for these particles depend on these effects. The neutral particles can be searched as missing transverse energy. When both particles, produced back-to-back, hadronize into neutral states the missing energy will tend to cancel, hence one needs to look for associated production of visible particles. The simplest case is given by QCD Initial State Radiation (ISR), looking for recoil against a jet. In this case the signal may be looked in mono-jet searches, $pp, p\bar{p} \rightarrow R^0\bar{R}^0 + \text{jet}$. On the other hand, a long lived charged massive particle is looked for as a muon-like track and it is discriminated from muons mainly by time-of-flight measurements and energy loss patterns. Moreover the charge exchange length is

$$\lambda_{ch.ex.} \sim 10m \left(\frac{mb}{\sigma_{ch.ex.}} \right) \left(\frac{10g}{\rho} \right)$$

which renders this effect negligible. Even though charge exchange does not drastically alter the detection strategies outlined above, baryonization can. In fact a sizable fraction of meson are converted into baryons after relatively short distances. Since baryonization can also change the charge of the particle, then it could convert neutral R-hadrons into charged ones [127, 128].

Besides the common features described above, the collider phenomenology is strongly dependent on the details of the superparticle spectrum. In the case of the CSM with small or intermediate-size masses, the spectrum has been described in Sect. 3.2, while for the QLTM in Sect. 5.3. In the QLT model, we found that the superparticle spectrum is completely determined by $M_L, M_E, M_Q, M_U, M_{Q_3}, M_{U_3}$ and M_D (and of course $1/L$), once the bounds coming from Flavor and CP violating observables described in the previous Section are taken into account. Moreover M_{Q_3} and M_{U_3} are constrained by EWSB and the consistency condition derived from Eq. (3.11), $\text{Tr}(M_i Y_i) = 0$, has to hold. Finally, since all the superparticles are pair produced, only those states that are lighter than $1 \div 2$ TeV are relevant for the LHC (and TeVatron) phenomenology.

Before continuing with the description of possible scenarios and their searches

at the LHC, we will review the present bounds coming from TeVatron direct searches.

5.6.2 Bounds from TeVatron searches

CDF performed a search [109] for stable Charged Massive Particles (CHAMPs) by looking for muon-like tracks with low velocity. Their limit on the production cross section is $\sigma \lesssim 50$ fb for a strongly interacting particle and $\sigma \lesssim 10$ fb for a weakly interacting one, in both cases after requiring $p_T > 40$ GeV and $0.4 \leq \beta \leq 0.9$. In the case of squark production (with 2 quasi-degenerate squarks) it corresponds to a lower bound of about 270 GeV on the squark mass, as it is illustrated in Fig. 3.2 for the CSM with small masses. Note that for low compactification radii, also the production of gluinos and heavier squarks ($\tilde{g}\tilde{g}$, $\tilde{g}\tilde{q}$, $\tilde{q}\tilde{q}$) contributes significantly. This is mostly relevant for the case of intermediate size stop mass. In this case the total production cross section for stop, both direct and through a cascade decay, is higher by a factor of ~ 5 . The bound is then $m_{\tilde{t}} \gtrsim 330$ GeV, as shown in Fig. 3.5. While the cascade is made out of off-shell multi-body decays (*e.g.* $\tilde{q} \rightarrow qWb\tilde{t}$) due to the squeezing of the spectrum, still the velocity of the final particle is generically of the same order of the one of the parent, which is always peaked for $\beta \gtrsim 0.3 \div 0.4$. The same searches do not pose any constraints on the QLT due to the heaviness of the spectrum.

Finally a few words on Higgs searches are worth mentioning. TeVatron recently excluded at 95% C.L. the mass window of $160 \div 170$ GeV for a SM-like Higgs. However in all these models, when the compactification scale is low, the coupling of the Higgs boson to top quarks is suppressed due to the mixing with KK modes, as explained in Sect. 3.1. This fact suppresses the Higgs coupling to two gluons [111] and reduces the production cross section at hadronic machines. The net suppression is of the order of $20 \div 40\%$ in the $160 \div 170$ GeV window with respect to the SM values, beyond but not far from the current TeVatron reach.

5.6.3 LHC searches scenarios in the QLT model

In the QLT model one can then single out a few qualitatively different superparticle spectra and briefly describe the corresponding LHC phenomenology. Since the high scale in the model is quite determined by the EWSB, the main criterion distinguishing these different scenarios is therefore the nature of the Lightest Supersymmetric Particle (LSP) at the bottom of the spectrum.

One can then consider the following cases:

- The lightest sparticles are \tilde{t}_L, \tilde{t}_R and \tilde{b}_L , as is the case where $M_{Q_3} = M_{U_3} = -M_{H_d}$ and all the other hypermultiplet masses are vanishingly small. In this case the bottom of the spectrum is given by hadrons made out of stop or sbottoms, with masses in the $1 \div 2$ TeV range, as can be read off from Fig. 5.2, as functions of $1/L$. (The other superparticles shown in the figure, such as \tilde{b}_R and the sleptons, are much heavier, at $\simeq \pi/(2L)$ in the present case.) The search is therefore for 2 heavy CHAMPS, 1 CHAMP and large missing transverse energy, \cancel{E}_T , or for a mono-jet and \cancel{E}_T , depending on the number of LSP hadronizing in charged states. Moreover, given the small mass splittings, the decay of the heavier stop/sbottom states will proceed via collinear di-jet, di-lepton (both charged and neutral) emission from off-shell W 's and Z 's⁵.
- The lightest sparticle is a down-type squark, most likely a \tilde{b}_R , as is the case for $M_{Q_3} = M_{U_3} = M_D = 2M_{H_d}$ with other hypermultiplet masses vanishingly small. The masses for the squarks in this case can be read off from Fig. 5.2. (The sleptons are much heavier, with masses $\simeq \pi/(2L)$). Also in this case the bottom of the spectrum is composed by almost degenerate superhadrons, containing \tilde{b}_R or light generation right-handed squarks. Differently from the previous cases now there is also a sufficient mass gap between the stops and LSPs to allow more complex cascade decays containing, *e.g.* real W -bosons and b -jets.
- The lightest sparticle is a charged slepton as in the case when all hypermultiplet masses are equal (see Fig. 5.2). Given the heaviness of the charged sleptons, $m_{\tilde{l}} \gtrsim 600$ GeV, the Drell-Yan direct production channel has a very low production cross section, requiring a lot of integrated luminosity at the LHC. On the other hand sleptons will be also copiously produced via cascade decays of the heavier colored states, always in association with at least a (charged) lepton and, in most cases, with a t - or a b -quark.
- Finally the lightest sparticle could be a neutral slepton as in the case $M_Q = M_U = -M_L$ and $M_E = 0$. A sneutrino would give rise to a missing energy signal, similar to the standard MSSM scenarios. However since the gauginos are much heavier than the sfermions, all the cascade steps will

⁵In case of hadronic decays of the W 's and Z 's this fact could reduce the sensitivity of the missing energy searches, since missing energy aligned with jets could be interpreted as a jet energy mismeasurement.

be 3-body decays. Then the kinematic features in the invariant masses of the cascades will correspond to endpoints, rendering slightly more difficult a precise determination of the superparticle spectrum.

5.7 Neutrino Masses and Dark Matter

As it has been shown in the previous Chapters, the models described here are effective theories with a UV cutoff of a few TeV. It is therefore very difficult in this theories to address those issues which are usually connected to much higher energy scales.

In particular one loses the prediction that the gauge couplings will unify at some scale M_* . The fact that the gauge couplings seem to converge towards a common value, one of the main motivations for the introduction of low scale SUSY, is now totally dependent on the unknown UV completion of the model.

The same is true for the origin of the neutrino masses, if thought as originating in the traditional see-saw mechanism: assuming that the neutrino Yukawa couplings are $\mathcal{O}(1)$, the see-saw scale is $10^{14} \text{ GeV} \gg \text{TeV}$. However, as it is well known, it is possible that the neutrino masses will be generated from physics inside the effective theory, as long as the Yukawa couplings are sufficiently small (which is still a technically natural choice). In this way one partly loses the rationale for the smallness of m_ν , but may obtain effects in an energy range which is experimentally accessible.

Moreover, in the 5D case, part of the smallness of the neutrino masses may be easily accounted for geometrically, by localizing the 5D bulk fields associated to the (RH) ν 's far from the brane where the neutrino Yukawa couplings reside. In this case one can allow 5D Yukawas not as small as in the traditional 4D case, up to a point of extreme localization in which they are of the same order of the electron Yukawa coupling. In particular, after introducing three hypermultiplets associated to right-handed neutrinos N_i , singlets under the SM gauge group, one can add a Yukawa coupling between N_i and L_i localized at $y = 0$ and a Majorana mass term M_ν at $y = L$. The latter may be introduced or not. Moreover one can assume that $M_\nu \sim 1/L \sim m_{SUSY}$ or $M_\nu \sim \Lambda \sim 5m_{SUSY}$.

The presence of the hypermultiplets associated to the RH neutrinos may also be beneficial for other issues. In particular it implies the presence of additional supersymmetric particles, the RH sneutrinos. The possibility of strong localization of the N_i , suggested by the smallness of m_ν , and the fact that they are singlets under the SM gauge group, render $\tilde{\nu}_R$ the lightest supersymmetric particle (LSP). Since

$\tilde{\nu}_R$ is neutral, stable and weakly interacting, it is a possible candidate for Dark Matter and may resolve the cosmological problems associated to charged/colored LSPs (stop, sbottom or charged sleptons) without requiring the introduction of any sources of R-parity breaking⁶.

It is therefore interesting to explore the possibility that $\tilde{\nu}_R$ is a viable DM candidate. The case of a RH sneutrino LSP has been extensively considered in the literature [129, 130, 131, 132]. In particular the smallness of the Yukawa couplings renders the next-to-lightest SUSY particle (NLSP) a long lived particle. The abundance of $\tilde{\nu}_R$ is then essentially set by the abundance of the NLSP and by the ratio of their masses

$$\Omega_{\tilde{\nu}} h^2 = \frac{m_{\tilde{\nu}}}{m_{NLSP}} \Omega_{NLSP} h^2.$$

Moreover, if the NLSP lifetime is very long, such that it decays around Big Bang Nucleosynthesis (BBN), there may be constraints from the observed primordial nuclei abundances [133]. Energy injection from late decays may also affect the CMB spectrum [134]. An analysis of these constraints is *e.g.* given in [135], while more detailed analyses that consider also constraints coming from sneutrino annihilations in stellar cores are given in [131]. If $\tilde{\nu}_R$ is light enough, the decay $Z \rightarrow \tilde{\nu}_R \tilde{\nu}_R$ could be kinematically accessible. However the smallness of the Yukawa couplings renders irrelevant the LEP constraints.

Differently from the case of the MSSM, in which the NLSP is either a neutralino or a charged slepton, in the QLT the NLSP is either a charged slepton or top or bottom squark. However in the case of a stop or sbottom quark their abundance at freeze-out is already smaller than the present DM abundance because the strong interactions keep them longer in equilibrium. Their abundance is further suppressed by subsequent annihilation after the QCD phase transition [136, 137]. Hence the stop relic abundance cannot provide the correct $\tilde{\nu}$ abundance for it to be a viable DM candidate.

On the contrary, the scenario of a slepton (in particular a stau) NLSP and a sneutrino LSP has been extensively analyzed in the literature [135, 131] and found to provide the correct DM abundance while being consistent with the various constraints⁷ over a wide range of parameter space of the standard MSSM.

⁶Indeed the gravitino and the fermionic superpartner associated to the radion field are expected to have masses $\mathcal{O}(1/L)$ and therefore cannot be used as DM candidates. However there might be other light states once issues like the stabilization of the radius of the extra dimension are properly addressed.

⁷The relevant constraints are those from late energy injection from NLSP decays during or

The quantities entering in the calculations are the stau and the $\tilde{\nu}$ masses determining the kinematics and the $\tilde{\nu}_L$ - $\tilde{\nu}_R$ mixing angle which fixes the NLSP lifetime. While the QLT model is quite different from the MSUGRA scenario studied in the literature, in the QLT all these quantities can be changed independently because they are controlled by 4 different parameters: M_L , M_N , Y_N and M_ν . These are basically unconstrained, except for the requirement of getting the right size for the neutrino masses. Even though the size of the neutrino masses is (only partially) correlated with the size of the sneutrino mixing angle, the same is also true in the MSSM scenarios studied in the literature. Hence, while we will not embark here in a detailed computation of the DM abundance and of the BBN constraints for the QLT model, it should be straightforward to arrange the values of the parameters listed above to render viable this slepton NLSP/sneutrino LSP DM scenario.

after Big Bang Nucleosynthesis and from high energy neutrinos coming from DM annihilations in the Sun.

Chapter 6

Conclusions

In this work we have presented a detailed study of EWSB on a compact extra dimension. The models studied here are based on SUSY, broken by boundary conditions, à la Scherk-Schwarz, along the flat extra dimension. As in the MSSM, SUSY breaking triggers Electroweak Symmetry Breaking via radiative corrections from the top Yukawa interactions. However, differently than in the MSSM, the SUSY breaking pattern is determined by the low-energy geometrical structure of the extra-dimension and it does not require the presence of any messenger sector.

The boundary conditions break the $SU(2)_R$ group of $N = 2$ SUSY (in 4D language) down to a local $U(1)_R$, the direction of the breaking being dependent on the position along the fifth dimension. This twisting of the $SU(2)_R \rightarrow U(1)_R$ breaking reduces $N = 2$ SUSY locally to $N = 1$ and globally to $N = 0$. Being essentially non-local, this extra dimensional SUSY breaking is softer than in standard 4D scenarios¹.

There are also other few key features arising in these models that are not found in the conventional MSSM. One of these is the possibility to maintain an intact R-symmetry at low energy, that forbids Majorana masses for the gauginos (being now Dirac particles), the A-terms and the $B\mu$ -term: all welcome ingredients in solving/alleviating common problems of the MSSM [139]. In this work we have shown that a successful EWSB still takes place, and that the soft SUSY breaking terms depend only on few parameters, namely the length of the extra dimension and the bulk mass parameters for the matter (and Higgs) multiplets.

As it was explained in Chapter 2, the presence of bulk masses distorts the wave

¹Indeed extra dimensional SUSY breaking has motivated the study of so-called *supersoft* SUSY breaking scenarios in 4D [138].

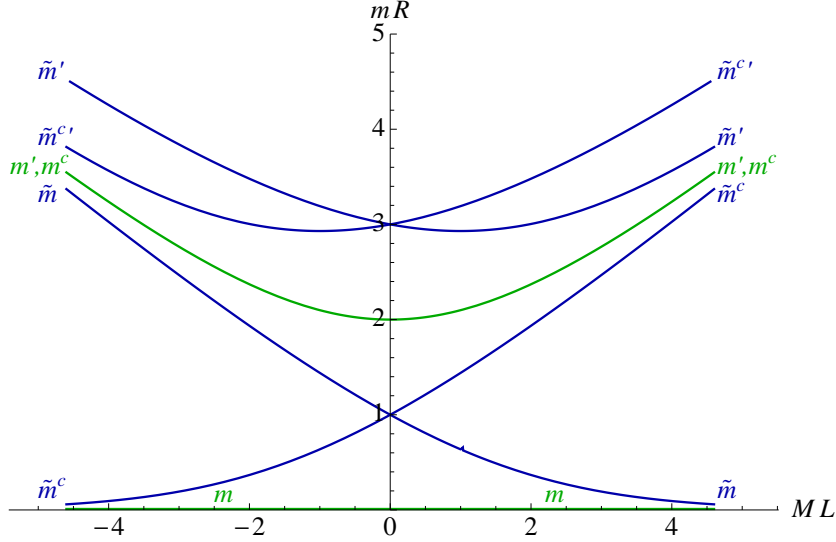


Figure 6.1: Spectrum of a matter hypermultiplet, presented in Chapter 2.

functions of the various fields. The effects are strongest for the lowest modes, which gets localized towards one of the boundaries. Moreover the mass spectrum is also affected, with all the KK modes getting progressively decoupled as shown *e.g.* in Fig. 6.1.

Thus the phenomenology strongly depends on the size of the bulk masses. Focusing on the EWSB one can identify different models by looking at the size of the 5D masses for the top and Higgs hypermultiplets. The scale of comparison is the compactification scale $L^{-1} \equiv (2\pi R)^{-1}$.

In Chapter 3 we have studied both the case of negligible bulk masses, $ML \ll 1$, and the one with small but sizable masses, $ML \lesssim 1$, while the study of large bulk masses, $ML \gtrsim 1$, has been carried out in Chapters 3 and 4. Here we will summarize again our main findings.

6.1 Models with negligibly small bulk masses

The limit of zero bulk masses is constituted by the Constrained Standard Model, introduced in [88]. The bulk masses are zero at tree level and all the fields are able to freely propagate in the bulk of the extra dimension. However these masses, even if not present, may be generated by 5D anomalies associated to the breaking of spatial parity along the extra dimension [104], and will be proportional to the

	A	B
$1/R$	360 ± 70	$420 \div 1000$
h	133 ± 10	Fig. 3.7
\tilde{t}_1, \tilde{u}_1	210 ± 20	$1/R(1 \pm 8\%) - m_t$
$\chi^\pm, \chi^0,$ $\tilde{g}, \tilde{q}, \tilde{l}$	360 ± 70	$1/R(1 \pm 20\%)$
\tilde{t}_2, \tilde{u}_2	540 ± 30	$1/R(1 \pm 8\%) + m_t$
A_1, q_1, l_1, h_1	720 ± 140	$2/R(1 \pm 20\%)$

Table 6.1: The particle spectrum and $1/R$ in absence of any mass term and in presence of a FI term, presented in Chapter 3.

hypercharge of the different fields.

The masses relevant for EWSB are the ones of the Higgs and of the top quark multiplets. Since the induced values for these masses are small, their addition constitutes only a small deformation of the original CSM. The main difference is that now the compactification radius is not fixed, but it is allowed to vary in a range and with it all the superparticle masses, the KK spectra and the Higgs boson mass. The results presented in Chapter 3 are briefly reported here in Table 6.1 and Fig. 6.2.

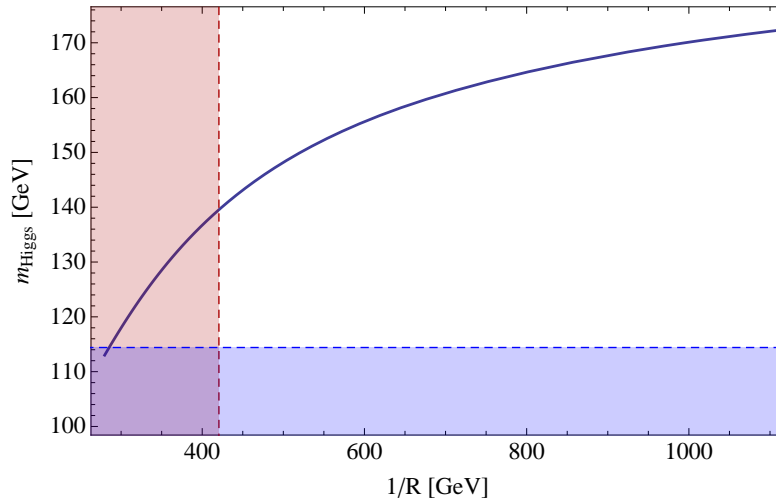


Figure 6.2: Higgs mass versus $1/R$ in presence of a Fayet-Iliopoulos term, as shown in Chapter 3.

Given the quite low value of the compactification scale, in the few hundreds GeV range, the model exposes problems concerning the EWPTs, in particular the ρ parameter [88, 4]. Hence it does not solve the LEP Paradox. Moreover, because of the peculiar character of the collider signatures (a light, squeezed supersymmetric spectrum with a long-lived colored massive particle as the LSP), the model has already been easily searched for in the TeVatron data, which excluded part of its parameter space. The exclusion regions are summarized in Fig. 6.2. Presently there is still an open window characterized by a fairly large Higgs boson mass, $m_H = 140 \div 180$ GeV, that will be explored in the near future by both Higgs and CHAMPs searches at the TeVatron (and the LHC).

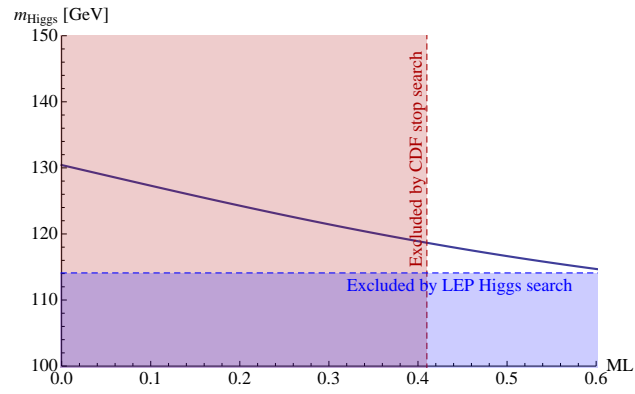
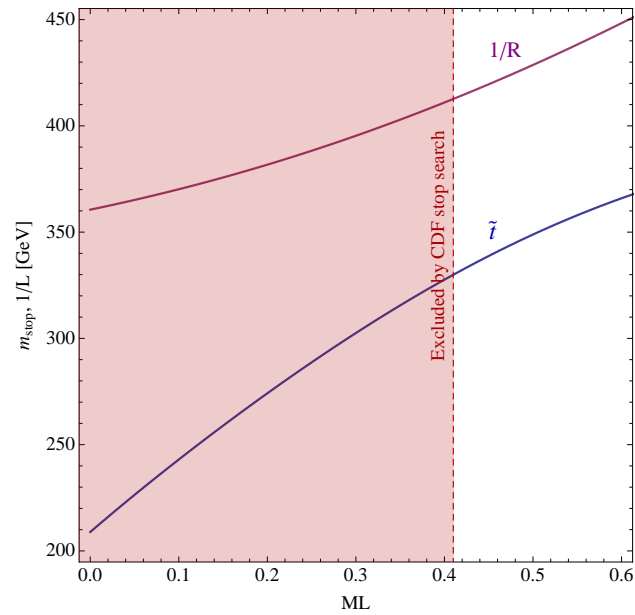
6.2 Models with sizable bulk masses for the top multiplets

We then studied the case where some of the bulk masses are sizable, but in the range $|ML| \lesssim 1$. We focused on the top quark multiplet ones, being the most relevant for the EWSB². The bulk mass affects the relation between the top mass and the Yukawa coupling and changes the values of the physical stop masses. Successful EWSB happens with larger values for the compactification scale and smaller values for the Higgs boson mass, as described in Chapter 3 and shown again in Figs. 6.3-6.4.

Even in this case, the presence of a colored LSP puts stringent bounds from TeVatron data, excluding most of the parameter space of this model. A window characterized by a very light Higgs $m_h \lesssim 120$ GeV is still open. The search for the Higgs boson in this window is rather difficult, given the suppressed Higgs production cross section at hadron colliders and its suppressed coupling to $\gamma\gamma$. However, the superparticles are still light, below 1 TeV, allowing the experimental search in the near future.

Since this model is also characterized by the presence of large and uncalculable contributions to the EWPT, in the second part of this work we explored a different class of models, with large bulk masses and higher values of the compactification scale.

²A non-zero bulk mass distorts the wave-function for the zero modes, allowing a coupling to a single KK excitation. Given the lightness of the spectrum, flavor and EWPT bounds forbid sizable masses for the first two generations in this model.

Figure 6.3: Higgs mass as function of ML . From Chapter 3.Figure 6.4: Stop mass and $1/R$ as functions of ML . From Chapter 3.

6.3 Models with large bulk masses

An interesting phenomenology arises when the bulk masses of the top hypermultiplets are large. In this case the top/stop lightest states get quasi-localized close to a boundary, chosen to be the one where the Yukawa coupling resides. In this Quasi-Localized Top (QLT) model, presented in Chapter 4, the lightest stop becomes much lighter than the compactification scale. The stop mass is dominated by the leading radiative corrections, implying a stronger cancellation between the top–stop loops. This is an interesting step towards the resolution of the LEP Paradox: it parametrically increases the separation between the compactification scale and the electroweak scale without too large finetuning. Indeed, given this cancellation, there is no EWSB at 1-loop and also at 2-loop order in the exact localization limit. However, at the same time the light stop is not able to raise much the Higgs mass above the experimental limit, yielding to a model with a quite light Higgs. If the hypermultiplet mass for the Higgs boson is not turned on, the EWSB is totally determined by $1/L$ and the third generation quark bulk masses. Fixing one of these parameters by the measured value of the Fermi constant G_F one can establish relation between the compactification scale and the Higgs mass, that was computed in Chapter 4 at a few-% accuracy by including the leading logarithmic two-loop contributions and it is shown again in Fig. 6.5.

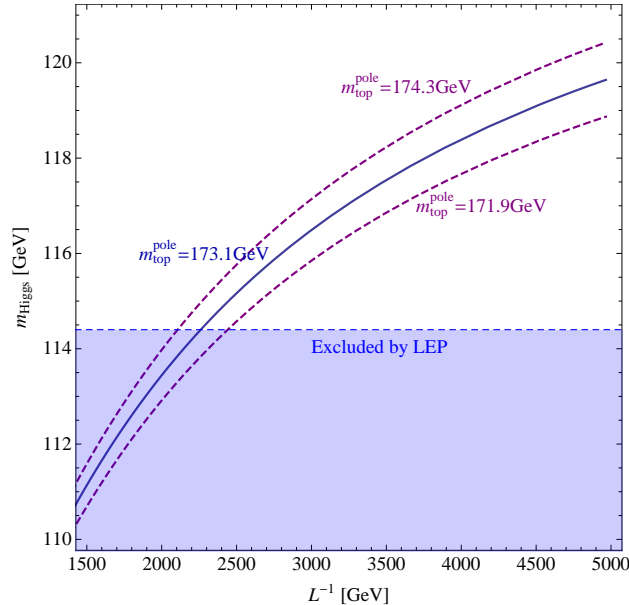


Figure 6.5: Higgs mass as function of $1/L$ in the QLT model.

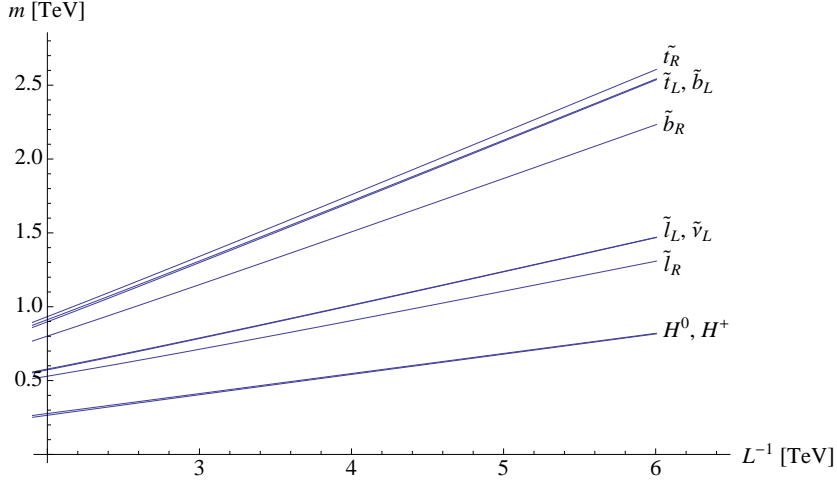


Figure 6.6: Physical masses for the squarks and sleptons from hypermultiplets with $M_Q = M_U = M_D = M_L = M_E = M$, and for the scalars of H_d with $M_{H_d} = 0$. Taken from Chapter 5.

While in the CSM the spectrum of the superparticles and of the KK excitations of the SM particles is essentially determined by the compactification scale L alone, in the QLT the phenomenology is more dependent on the specific values of the bulk mass parameters.

A possible spectrum of the light superparticles is shown here in Fig. 6.6, while a detailed analysis has been presented in Chapter 5.

Thus one has the required picture of somewhat split scales, necessary to solve the Little Hierarchy Problem: $1/R \gtrsim 3$ TeV together with the gauginos and part of the sfermions, the KK excitations in the 5–20 TeV range, a light SM-like Higgs, and only the stop and sbottoms bounded to be below $1 \div 2$ TeV (with possibly other scalar superpartners).

Moreover the cutoff of the effective theory is higher than ~ 10 TeV, automatically rendering the model safe from higher dimensional operators contributing to EWPT and flavor processes. In Chapter 5 we have also shown how the model is safe from the bounds coming from Flavor and CP-Violation and from those imposed by the EWPT.

While the KK states are out of reach of the present and near future colliders, the supersymmetric spectrum may in principle be studied at the LHC. It is quite different from the standard MSSM scenarios. The gauginos are much heavier than

the sfermions, a condition difficult to realize in the MSSM due to the renormalization group running effects. Moreover, the existence of a charged long lived particle at the bottom of the spectrum is a quite generic feature in this model. Its precise nature and whether it is colored or not are however model dependent. The possible collider searches for the QLT model have been described in Chapter 5.

Since a colored/charged stable particle constitutes a cosmological problem (often considered as one of the major drawbacks of this type of models), we also have briefly explored the possibility of having a good Dark Matter candidate. It is straightforward to extend the QLT model to get both a DM candidate and neutrino masses within the effective theory, by adding right-handed neutrino hypermultiplets. In this case the true LSP is a sneutrino, but since the couplings are suppressed by the neutrino masses, the NLSP is stable on collider timescales, leaving the LHC phenomenology intact.

Finally we have also analyzed the case where a sizable Higgs bulk mass is added to the QLT model. Its effect is to progressively lower the compactification scale and increase the Higgs boson mass, as explained in Chapter 4 and shown here in Fig. 6.7, smoothly interpolating between the QLT model and the model summarized in Sect. 6.1.

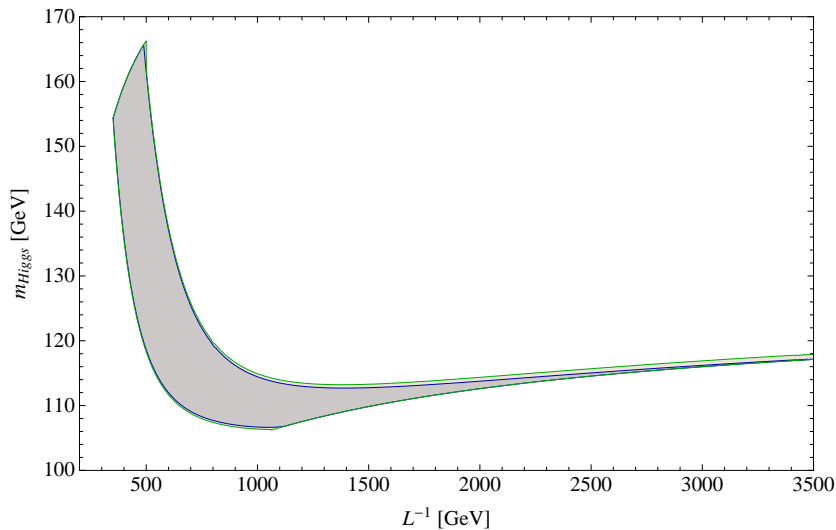


Figure 6.7: Expected range of Higgs masses with the inclusion of a hypermultiplet Higgs mass and a maximum fine tuning in the slope of the potential at 10% level. Taken from Chapter 4.

6.4 Other directions

To conclude, a few comments on issues not addressed in this Thesis are in order. Given the bottom-up approach undertaken and the focus on the Little Hierarchy Problem, a few model-building aspects have not been directly explored here. In particular a viable mechanism for the stabilization of the radius of the extra dimensions has been assumed throughout this work. A few possibilities for radius stabilization are known [140, 141, 142, 143] and may require the introduction of new fields. However the new degrees of freedom may easily be heavier than a TeV or, if much lighter, may have very suppressed couplings with the SM particles (as it is the case *e.g.* for the radion itself). Hence the approach of studying the phenomenology of these models without including the radius stabilization mechanism is still justified.

Appendix A

The spectrum

In this Appendix we calculate the KK spectrum of Higgs and matter hypermultiplets in presence of a mass term M as in Eq. (2.13).

Let (φ, ψ, F) , (φ^c, ψ^c, F^c) be either a Higgs or a matter hypermultiplet. In presence of a mass term as in Eq. (2.13) and upon eliminating the F-terms the Lagrangian is:

$$\begin{aligned} \mathcal{L} = & |\partial_M \varphi|^2 + |\partial_M \varphi^c|^2 + i\psi \sigma^\mu \partial_\mu \bar{\psi} + i\psi^c \sigma^\mu \partial_\mu \bar{\psi}^c + \psi^c \partial_y \psi + \bar{\psi}^c \partial_y \bar{\psi} \\ & - M^2 \left(|\varphi|^2 + |\varphi^c|^2 \right) + 2M (\delta(y) + \delta(y-L)) \left(|\varphi|^2 - |\varphi^c|^2 \right) \\ & + M\eta(y) \left(\psi\psi^c + \bar{\psi}\bar{\psi}^c \right), \end{aligned} \quad (\text{A.1})$$

where $M = 0, 1, 2, 3, 5$ while $\mu = 0, 1, 2, 3$.

Thus the equations of motion are

$$\left[\partial_M \partial^M + M^2 - 2M (\delta(y) + \delta(y-L)) \right] \varphi = 0, \quad (\text{A.2a})$$

$$\left[\partial_M \partial^M + M^2 + 2M (\delta(y) + \delta(y-L)) \right] \varphi^c = 0, \quad (\text{A.2b})$$

$$\left[\partial_M \partial^M + M^2 - 2M (\delta(y) - \delta(y-L)) \right] \psi = 0, \quad (\text{A.2c})$$

$$\left[\partial_M \partial^M + M^2 + 2M (\delta(y) - \delta(y-L)) \right] \psi^c = 0. \quad (\text{A.2d})$$

Eqs. (A.2) must be solved imposing the proper boundary conditions to the fields $\varphi, \varphi^c, \psi, \psi^c$. Note that the delta functions in the left-hand side of Eqs. (A.2) are both present only if the field under consideration has $(+, +)$ parity under $Z_2 \times Z'_2$ symmetry. In all other cases the wave function vanishes at $y = 0$ and/or $y = L$ and the delta functions in the corresponding points are irrelevant.

A.1 Matter hypermultiplets

If we consider a matter hypermultiplet, then Eq. (A.2) become

$$[\partial_M \partial^M + M^2 - 2M(\delta(y) - \delta(y-L))] \psi = 0, \quad (\text{A.3a})$$

$$[\partial_M \partial^M + M^2] \psi^c = 0, \quad (\text{A.3b})$$

$$[\partial_M \partial^M + M^2 - 2M\delta(y)] \varphi = 0, \quad (\text{A.3c})$$

$$[\partial_M \partial^M + M^2 + 2M\delta(y-L)] \varphi^c = 0. \quad (\text{A.3d})$$

Taking for the wave functions the following form

$$\psi(x, y) = \begin{cases} \tilde{\psi}(x) [A_\psi \sin k(y-L) + B_\psi \cos k(y-L)] & y \in (0, L) \\ \tilde{\psi}(x) [-A_\psi \sin k(y-L) + B_\psi \cos k(y-L)] & y \in (L, 2L) \end{cases} \quad (\text{A.4a})$$

$$\psi^c(x, y) = \tilde{\psi}^c(x) A_{\psi^c} \sin ky \quad y \in (0, 2L) \quad (\text{A.4b})$$

$$\varphi(x, y) = \tilde{\varphi}(x) A_\varphi \sin k(y-L) \quad y \in (0, 2L) \quad (\text{A.4c})$$

$$\varphi^c(x, y) = \tilde{\varphi}^c(x) \begin{cases} A_{\varphi^c} \sin ky & y \in (0, L) \\ B_{\varphi^c} \sin k(2L-y) & y \in (L, 2L) \end{cases} \quad (\text{A.4d})$$

the mass of every field is given by $m^2 = M^2 + k^2$ where k is constrained by Eqs. (A.3). Imposing the proper conditions on the wave functions and their first derivatives on the boundary we get the following equations for k :

$$\psi(+, +) \implies (k^2 + M^2) \sin(kL) = 0, \quad (\text{A.5a})$$

$$\psi^c(-, -) \implies \sin(kL) = 0, \quad (\text{A.5b})$$

$$\varphi(+, -) \implies \tan(kL) = \frac{k}{M}, \quad (\text{A.5c})$$

$$\varphi^c(-, +) \implies \tan(kL) = -\frac{k}{M}. \quad (\text{A.5d})$$

A few things are worth noticing:

1. One can get the equations for the bound states by analytical continuation, setting $k = i\rho$ in Eq. (A.5)
2. The bound state $\psi(+, +)$ is massless for every value of M , while the excited states have masses $(m_\psi^2)_n = M^2 + \left(\frac{\pi n}{L}\right)^2$, $n = 1, 2, \dots$

3. The equation for $\psi^c(-, -)$ is unaffected by the presence of M because of the vanishing of the wave function at $y = 0, L$

Finally it is convenient to give the approximate expressions for the mass eigenvalues of the scalar states, in the limit of small ML :

$$m_n^2 L^2 \sim \frac{\pi^2}{4} (2n+1)^2 \mp 2ML + (ML)^2 \left(1 - \frac{4}{(2n+1)^2 \pi^2}\right), \quad (\text{A.6})$$

where the \mp corresponds to the $(+, -)$ and $(-, +)$ cases respectively.

A.2 Higgs hypermultiplet

If we consider a Higgs hypermultiplet, then Eq. (A.2) become

$$[\partial_M \partial^M + M^2 - 2M(\delta(y) + \delta(y-L))] h = 0, \quad (\text{A.7a})$$

$$[\partial_M \partial^M + M^2] h^c = 0, \quad (\text{A.7b})$$

$$[\partial_M \partial^M + M^2 - 2M\delta(y)] \lambda = 0, \quad (\text{A.7c})$$

$$[\partial_M \partial^M + M^2 + 2M\delta(y-L)] \lambda^c = 0. \quad (\text{A.7d})$$

With the same procedure of the matter case one gets the equations

$$h(+, +) \implies \tan(kL) = -\frac{2kM}{k^2 - M^2}, \quad (\text{A.8a})$$

$$h^c(-, -) \implies \sin(kL) = 0, \quad (\text{A.8b})$$

$$\lambda(+, -) \implies \tan(kL) = \frac{k}{M}, \quad (\text{A.8c})$$

$$\lambda^c(-, +) \implies \tan(kL) = \frac{k}{M}. \quad (\text{A.8d})$$

Note that Eq. (A.8a) for the bound state of the h field leads to a negative squared mass if $M > 0$.

Solving Eq. (A.7a) for the zero mode of the Higgs scalar we find for the wave function, normalized to $\int_0^{4L} dy |h^{(0)}(y)|^2 = 1$,

$$h^{(0)}(y) = \frac{-k \cos k(y-L) - M \sin k(y-L)}{\sqrt{-2M + 2(k^2 + M^2)L + 2M \cos 2kL + \left(k - \frac{M^2}{k}\right) \sin 2kL}}, \quad (\text{A.9})$$

with k the solution of Eq. (A.8a). Expression (A.9) is valid for $y \in [0, L]$. Note that if $M \rightarrow 0$, then $h^{(0)}(y) \rightarrow (4L)^{-1/2}$.

A.3 Spectrum in presence of a VEV for the Higgs field

If we have a top quark hypermultiplet, then the top Yukawa coupling¹

$$\mathcal{L}_Y = \frac{\lambda_t}{2} [\delta(y) + \delta(y - 2L)] \int d^2\theta \hat{h} \hat{Q} \hat{U} + \text{h.c.} \quad (\text{A.10})$$

leads to a mass term when we replace the Higgs zero mode $h^{(0)}$ with its VEV v . To calculate the spectrum in presence of such a term it is convenient to rewrite the Lagrangian Eq. (A.1) without eliminating the F auxiliary fields and use the following vectors

$$X = \begin{pmatrix} \varphi \\ F^{c\dagger} \end{pmatrix}, \quad Y = \begin{pmatrix} \varphi^c \\ F^\dagger \end{pmatrix}, \quad Z = \begin{pmatrix} \psi \\ \bar{\psi}^c \end{pmatrix}. \quad (\text{A.11})$$

Then Eq. (A.1) becomes

$$\begin{aligned} \mathcal{L} = & \begin{pmatrix} X_{U,Q}^\dagger & Y_{Q,U}^\dagger \end{pmatrix} M_B \begin{pmatrix} X_{U,Q} \\ Y_{Q,U} \end{pmatrix} \\ & + \begin{pmatrix} \bar{Z}_{U,Q} & Z_{Q,U}^t \end{pmatrix} M_F \begin{pmatrix} Z_{U,Q} \\ \bar{Z}_{Q,U}^t \end{pmatrix}, \end{aligned} \quad (\text{A.12})$$

where

$$M_B = \begin{pmatrix} -\square + 4M_{U,Q}\delta_L & \partial_y - \eta(y) M_{U,Q} & 0 & \lambda_t \alpha^* \\ -\partial_y - \eta(y) M_{U,Q} & 1 & 0 & 0 \\ 0 & 0 & -\square - 4M_{Q,U}\delta_L & -\partial_y - \eta(y) M_{Q,U} \\ \lambda_t \alpha & 0 & \partial_y - \eta(y) M_{Q,U} & 1 \end{pmatrix}, \quad (\text{A.13a})$$

$$M_F = \begin{pmatrix} \partial_y + \eta(y) M_{U,Q} & i\sigma^\mu \partial_\mu & 0 & 0 \\ i\bar{\sigma}^\mu \partial_\mu & -\partial_y + \eta(y) M_{U,Q} & 0 & \lambda_t \alpha^* \\ \lambda_t \alpha & 0 & -\partial_y + \eta(y) M_{Q,U} & i\sigma^\mu \partial_\mu \\ 0 & 0 & i\bar{\sigma}^\mu \partial_\mu & \partial_y + \eta(y) M_{Q,U} \end{pmatrix}, \quad (\text{A.13b})$$

$$\alpha = \frac{1}{2} [\delta(y) + \delta(y - 2L)] v h^{(0)}(y=0), \quad \delta_L = \delta(y - L),$$

with $h^{(0)}(y=0)$ the Higgs zero mode wave function, Eq. (A.9) at $y=0$.

¹Here we are working on the interval $(0, 4L)$.

Taking for the wave functions the form of Eq. (A.4) (in this case one must consider also the wave functions of $F_{U,Q}, F_{Q,U}^c$) and imposing the proper boundary conditions, one can get the equations for the masses of the fields $\varphi_{U,Q}, \psi_{U,Q}, \varphi_{U,Q}^c, \psi_{U,Q}^c$.

For the top quark $\psi_{U,Q}$ and the top squark $\varphi_{U,Q}$ (the lowest modes) one gets

$$m_t^2 = \frac{\lambda_t^2 v^2 |h^{(0)}(0)|^2}{16} (k_U^t \coth(k_U^t L) + M_U) (k_Q^t \coth(k_Q^t L) + M_Q), \quad (\text{A.14})$$

$$\begin{aligned} (k_U^{\tilde{t}} \coth(k_U^{\tilde{t}} L) - M_U) (k_Q^{\tilde{t}} \coth(k_Q^{\tilde{t}} L) + M_Q) = \frac{\lambda_t^2 v^2 |h^{(0)}(0)|^2}{16} \\ \left(m_t^2 - 2M_Q (k_Q^{\tilde{t}} \coth(k_Q^{\tilde{t}} L) + M_Q) \right), \end{aligned} \quad (\text{A.15})$$

where $k_{U,Q}^{t,\tilde{t}} = \sqrt{M_{U,Q}^2 - m_{t,i}^2}$. The wave function of the top quark zero mode, normalized to $\int_0^{4L} dy |\psi_0^{U,Q}(y)|^2 = 1$, is obtained by solving Eq. (A.3a). For $y \in [0, L)$ we have

$$\psi_0^{U,Q}(y) = \frac{k_{U,Q} \cosh k_{U,Q}(L-y) + M_{U,Q} \sinh k_{U,Q}(L-y)}{\sqrt{-2m_t^2 L + 2M_{U,Q} (\cosh 2k_{U,Q} L - 1) + \left(k_{U,Q} + \frac{M^2}{k_{U,Q}}\right) \sinh 2k_{U,Q} L}}. \quad (\text{A.16})$$

The usual 4D top Yukawa coupling, defined as the coupling among the zero modes of the fields h, ψ_U, ψ_Q , is given by

$$y_t = \hat{y}_t \eta_0^h \eta_0^U \eta_0^Q, \quad (\text{A.17})$$

where $\hat{y}_t = \lambda_t (4L)^{-3/2}$ and η_0^i ($i = h, U, Q$) are the wave functions, Eqs. (A.9–A.16) at $y = 0$ normalized in such a way that

$$\int_0^{4L} dy |\eta_0^i(y)|^2 = 4L. \quad (\text{A.18})$$

Inserting Eq. (A.17) into Eq. (A.14) we obtain the relation between the top quark mass m_t and the 4D Yukawa coupling y_t .

Appendix B

5D Propagators

In order to obtain the mixed momentum–coordinate space propagators for the components φ , ψ , F of a hypermultiplet, we start from the 5D Lagrangian without eliminating the auxiliary fields. If $M \neq 0$ the relevant part of this Lagrangian is:

$$\begin{aligned}
\mathcal{L} = & |\partial_\mu \varphi|^2 + |\partial_\mu \varphi^c|^2 + |F|^2 + |F^c|^2 + i\bar{\psi}\sigma^\mu \partial_\mu \psi + i\psi^c \sigma^\mu \partial_\mu \bar{\psi}^c + \\
& + [F\partial_y \varphi^c - F^c \partial_y \varphi + \text{h. c.}] - M\eta(y) [F\varphi^c + F^c \varphi + \text{h. c.}] \\
& + [\psi^c \partial_y \psi + \text{h. c.}] + M\eta(y) [\psi^c \psi + \text{h. c.}] \\
& + 4M\delta(y-L) \left[|h|^2 - |h^c|^2 \right], \tag{B.1}
\end{aligned}$$

for the generic hypermultiplet of components φ , ψ , F and their conjugates. The boundary term at L in the last line is necessary to maintain 5D SUSY invariance under ξ^{-+} transformations¹. Let us focus first on the propagators for the top–stop sector, assuming from now on that the parities are those of the matter multiplets. Using the vectors defined in Eq. (A.11), \mathcal{L} can be recast in a more compact form as in Appendix A:

$$\mathcal{L} = X^\dagger A X + Y^\dagger B Y + \bar{Z} C Z \tag{B.2}$$

where

$$A = \begin{pmatrix} -\square + 4M\delta(y-L) & \partial_y - M\eta(y) \\ -\partial_y - M\eta(y) & 1 \end{pmatrix}$$

¹Using the formulation in terms of 4D N=1 superfields [93] one privileges only one of the two local supersymmetries, here ξ^{+-} . This explains the apparent asymmetry between $y=0$ and $y=L$.

$$\begin{aligned}
B &= \begin{pmatrix} -\square - 4M\delta(y-L) & -\partial_y - M\eta(y) \\ \partial_y - M\eta(y) & 1 \end{pmatrix} \\
C &= \begin{pmatrix} \partial_y + M\eta(y) & i\sigma^\mu \partial_\mu \\ i\bar{\sigma}^\mu \partial_\mu & -\partial_y + M\eta(y) \end{pmatrix}
\end{aligned} \tag{B.3}$$

Note that the components of X (or Y , Z) have the same quantum numbers but different boundary conditions.

Let us focus, for example, on the propagator

$$G[(x-x')_\mu; y, y'] = \langle \varphi(x'_\mu, y') \varphi^\dagger(x_\mu, y) \rangle, \tag{B.4}$$

the others being analogous. In general all the correlation functions will depend on both² y and y' because of the non conservation of the 5th component of momentum in the segment $[0, L]$. However, being interested in calculating only loops formed using Yukawa interactions which are localized at $y = 0$, we can impose without any problem $y' = 0$ from the very beginning of the calculation, reducing the dependence of the Eq. (B.4) only to $(x-x')_\mu$ and y .

One can arrange propagators in matrices using the vectors previously defined. In particular, defining

$$\begin{aligned}
\mathcal{G}(x-x'; y) &= \langle X(x, y) X^\dagger(x', 0) \rangle \\
&= \begin{pmatrix} \langle \varphi(x, y) \varphi^\dagger(x', 0) \rangle & \langle \varphi(x, y) F^c(x', 0) \rangle \\ \langle F^{c\dagger}(x, y) \varphi^\dagger(x', 0) \rangle & \langle F^{c\dagger}(x, y) F^c(x', 0) \rangle \end{pmatrix},
\end{aligned} \tag{B.5}$$

the equations of motion for the scalar Green functions are:

$$A\mathcal{G}(x-x'; y) = i\sigma_3 \delta^{(4)}(x-x') \frac{1}{2} (\delta(y) + \delta(y-2L)), \tag{B.6}$$

where σ_3 is the usual Pauli matrix. Multiplying the 1st row of A by the 1st column of \mathcal{G} we get a system of 2 differential equations, which after passing to Euclidean 4-momentum, assumes the form:

$$\begin{cases} -k_4^2 g(y) + 4M\delta(y-L)g(y) + (\partial_y - M\eta(y)) f(y) = i\delta(y)/2 \\ (-\partial_y - M\eta(y))g(y) + f(y) = 0 \end{cases}$$

where $g(y) = \langle \varphi(y) \varphi^\dagger(0) \rangle$ and $f(y) = \langle F^{c\dagger}(y) \varphi^\dagger(0) \rangle$. These coupled equations must be solved imposing the $(+, -)$ and the $(-, +)$ boundary conditions in y on

²Or on $\bar{y} = (y+y')/2$ and $\Delta y = (y-y')$.

g and f respectively, using the same techniques of Appendix A. One finally gets the $\langle\varphi\varphi^\dagger\rangle$ propagator $G_\varphi(k_4, y; M)$:

$$G_\varphi(k_4, y; M) = \langle\varphi\varphi^\dagger\rangle(y) = \frac{-i \sinh[k(L-y)]}{4[k \cosh(kL) - M \sinh(kL)]}, \quad (\text{B.7})$$

where $k = \sqrt{k_4^2 + M^2}$. Analogously the $\langle FF^\dagger\rangle$ (+, -) and $\langle\psi\psi^\dagger\rangle$ (+, +) propagators are:

$$\begin{aligned} G_F(k_4, y; M) &= \frac{i k_4^2}{4} \frac{\sinh[k(L-y)]}{[k \cosh(kL) + M \sinh(kL)]} \left(1 + \frac{2M}{k_4^2} (k \coth(kL) + M) \right), \\ G_\psi(k_4, y; M) &= \frac{-i \not{k}_4 k \cosh[k(L-y)] + M \sinh[k(L-y)]}{4k_4^2 \sinh(kL)}, \end{aligned} \quad (\text{B.8})$$

where $\not{k}_4 = \sigma \cdot k_4$.

In the limit $M \rightarrow 0$ these propagators become:

$$\begin{aligned} G_\varphi(k_4, y; M=0) &= \frac{-i \sinh[k_4(L-y)]}{4k_4 \cosh(k_4L)}, \\ G_F(k_4, y; M=0) &= \frac{i k_4 \sinh[k_4(L-y)]}{4 \cosh(k_4L)}, \\ G_\psi(k_4, y; M=0) &= \frac{-i \not{k}_4 \cosh[k_4(L-y)]}{4k_4 \sinh(k_4L)}. \end{aligned} \quad (\text{B.9})$$

For the sake of completeness we give also the propagator of those fields in the gauge multiplet and in the Higgs multiplet (at $M_H = 0$) that can propagate from $y_1 = 0$ to $y_2 = y$. These propagators are given in Feynman gauge.

$$\begin{aligned} G_{A_\mu}(k_4, y) &= \frac{i g_{\mu\nu} \cosh[k_4(L-y)]}{4k_4 \sinh(k_4L)}, \\ G_\lambda(k_4, y) &= \frac{-i \not{k}_4 \sinh[k_4(L-y)]}{4k_4 \cosh(k_4L)}, \\ G_D(k_4, y) &= \frac{i}{4} \delta(y), \end{aligned} \quad (\text{B.10})$$

$$\begin{aligned} G_h(k_4, y) &= \frac{-i \cosh[k_4(L-y)]}{4k_4 \sinh(k_4L)}, \\ G_{\tilde{h}}(k_4, y) &= \frac{-i \not{k}_4 \sinh[k_4(L-y)]}{4k_4 \cosh(k_4L)}, \\ G_{F_h}(k_4, y) &= \frac{ik_4 \cosh[k_4(L-y)]}{4 \sinh(k_4L)}. \end{aligned} \quad (\text{B.11})$$

The propagators from $y_1 = L$ to $y_2 = y$ can be recovered from the previous ones through using elementary symmetry principles on boundary conditions and on the sign of ML .

Finally, for the calculation of loops involving gauge interactions, bulk-bulk propagators may be needed. These depend on two 5D coordinates, y and y' . They can be easily derived with the formalism described above, the only differences being in the fact that the right hand side of Eq. (B.6) now depends on $[\delta(y - y') + \delta(y - y' - 2L)]$. Here we just quote the results for the matter hypermultiplet:

$$\begin{aligned}
G_{\psi\bar{\psi}} &= \frac{-i \mathcal{K}_4}{2k_4^2} \frac{k}{\sinh(kL)} [\omega_0^-(y)\omega_L^+(y')\theta(y' - y) + \omega_0^-(y')\omega_L^+(y)\theta(y - y')], \\
G_{\bar{\psi}^c\psi^c} &= \frac{i \mathcal{K}_4}{2k \sinh(kL)} [sh_0(y)sh_L(y')\theta(y' - y) + sh_0(y')sh_L(y)\theta(y - y')], \\
G_{\psi\psi^c} &= \frac{i}{2 \sinh(kL)} [\omega_0^-(y)sh_L(y')\theta(y' - y) - sh_0(y')\omega_L^+(y)\theta(y - y')], \\
G_{\bar{\psi}^c\bar{\psi}} &= \frac{-i}{2 \sinh(kL)} [\omega_L^+(y')sh_0(y)\theta(y' - y) - sh_L(y)\omega_0^-(y')\theta(y - y')], \\
G_{\phi\phi^\dagger} &= \frac{i}{2k\omega_0^-(L)} [sh_L(y')\omega_0^-(y)\theta(y' - y) - sh_L(y)\omega_0^-(y')\theta(y - y')], \\
G_{\phi F^c} &= \frac{-i}{2\omega_0^-(L)} \left[\omega_0^-(y)\omega_L^-(y')\theta(y' - y) + \frac{k_4^2}{k^2} sh_0(y')sh_L(y)\theta(y - y') \right], \\
G_{F^{c\dagger}\phi^\dagger} &= \frac{ik_4^2}{2k^2\omega_0^-(L)} \left[sh_0(y)sh_L(y')\theta(y' - y) + \frac{k^2}{k_4^2} \omega_0^-(y')\omega_L^-(y)\theta(y - y') \right], \\
G_{F^{c\dagger}F^c} &= \frac{ik_4^2}{2k\omega_0^-(L)} [sh_0(y)\omega_L^-(y')\theta(y' - y) - sh_0(y')\omega_L^-(y)\theta(y - y')], \\
G_{\phi^c\phi^{c\dagger}} &= \frac{i}{2k\omega_0^-(L)} [\omega_L^-(y')sh_0(y)\theta(y' - y) - \omega_L^-(y)sh_0(y')\theta(y - y')], \\
G_{\phi^c F} &= \frac{ik_4^2}{2k^2\omega_0^-(L)} \left[sh_0^-(y)sh_L^-(y')\theta(y' - y) + \frac{k^2}{k_4^2} \omega_0^-(y')\omega_L^-(y)\theta(y - y') \right], \\
G_{F^\dagger\phi^{c\dagger}} &= \frac{i}{2\omega_0^-(L)} \left[\omega_0^-(y)\omega_L^-(y')\theta(y' - y) + \frac{k_4^2}{k^2} sh_0(y')sh_L(y)\theta(y - y') \right], \\
G_{F^\dagger F} &= \frac{-ik_4^2}{2k\omega_0^-(L)} [\omega_0^-(y)\tilde{\omega}_L^+(y')\theta(y' - y) - \omega_0^-(y')\tilde{\omega}_L^+(y)\theta(y - y')], \quad (\text{B.12})
\end{aligned}$$

where

$$\omega_0^\pm(x) = \cosh(kx) \pm \frac{M}{k} \eta(x) \sinh(kx),$$

$$\omega_L^\pm(x) = \cosh[k(L-x)] \pm \frac{M}{k} \eta(x) \sinh[k(L-x)],$$
$$\tilde{\omega}_L^\pm(x) = \frac{k^2 + M^2}{k_4^2} \sinh[k(L-x)] \pm \frac{2Mk}{k_4^2} \eta(x) \cosh[k(L-x)]$$

and $sh_0(x) = \sinh(kx)$, $sh_L(x) = \sinh[k(L-x)]$.

Appendix C

Effects of localized terms

In this Appendix, we discuss the possible effects of the presence of $N = 1$ supersymmetric terms localized at the boundaries. Among these terms there are the kinetic terms for Vector multiplets, Higgs and matter hypermultiplets, and supersymmetric higher order operators. As an example we present and quantify the effects that can arise from these operators for the Higgs hypermultiplet. This case is of relevance for the discussion of Chapter 5 and easily shows what happens in the case of zero bulk masses.

C.1 Boundary kinetic terms

The presence of kinetic terms localized at the boundaries are in a sense worrisome because their effect is to mix the low lying modes with the higher KK ones and, by gauge invariance, to couple SM particles to heavy gauge vector bosons. The physical states become admixtures of zero modes and excited KK states, and in the case of matter, flavor transitions via the exchange of a heavy gauge boson become possible. In principle these effects can manifest themselves by altering some electroweak or flavor physics observable.

C.1.1 Higgs hypermultiplets

Let us keep $M_H = 0$. Then the effect of a term like

$$\delta\mathcal{L} = \delta(y)z_H^0 \int d^4\theta H^\dagger e^V H + \delta(y-L)z_H^L \int d^4\theta H'^\dagger e^{V'} H' \quad (\text{C.1})$$

does not affect the masslessness of the Higgs zero mode. In fact, after rescaling all the fields in the Higgs hypermultiplets by the constant quantity

$1/\sqrt{1 + (z_H^0 + z_H^L)/(4L)}$ The equation for the scalar (+, +) spectrum becomes

$$\partial_5^2 h = - (1 + \delta(y)z_H^0 - \delta(y-L)z_H^L) m^2 h, \quad (\text{C.2})$$

that can be rewritten as

$$\tan m_n L = 2m_n \frac{(z_H^L - z_H^0)}{4 + m_n^2 z_H^L z_H^0}, \quad (\text{C.3})$$

where m_n is the mass of the n th eigenmode. This equation has $m_n = 0$ as a solution, showing the presence of a massless zero mode. Furthermore, the wave-function of the zero mode is not altered, remaining just a constant¹. So there is no mixing with higher modes when $M_H = 0$. There is, however, in the covariant derivative the term that couples the Higgs zero mode with the KK excitations of the vector bosons. When h_0 acquires a VEV, this term generates a mass mixing term for the gauge bosons, that upon integrating in the 5th coordinate is

$$-\sqrt{2}m_V^2 V_\mu^{(0)} \sum_{n>0} \left[\frac{Z_H^0 + (-1)^n Z_H^L}{1 + Z_H^0 + Z_H^L} V^{\mu,(n)} \right], \quad (\text{C.4})$$

where we have set $z/(4L) = Z$ to render the kinetic terms adimensional. The zero mode vector boson mass is thus shifted by the exchange of heavy vector bosons by the amount:

$$\delta m_V^2 = \frac{m_V^4 L^2}{3} [(Z_H^0)^2 + (Z_H^L)^2 - Z_H^0 Z_H^L], \quad (\text{C.5})$$

where we used the fact that the mass of the gauge boson is $\simeq \pi n/L$ and that the Z 's are small. This shows that the Higgs potential and the spectrum are affected only at the order Z^2 . Being more precise, this is not true for the Yukawa couplings where a factor $1/\sqrt{1 + Z_H^0 + Z_H^L}$ has appeared. However this rescaling is universal and affects only the relation between the 5D Yukawa couplings and the quark and lepton masses. In particular it renders less precise the determination of the cutoff Λ , by the same factor. If M_H is different from zero, then the same effects can be generated also from the mass M_H because the Higgs now has a nontrivial profile along the 5th dimension and can couple with all the vector bosons. This effect can be calculated and included straightforwardly using the Higgs wave-function given in Appendix A. However, for small bulk masses, this effect is negligible.

¹Remember that we have already done the rescaling

Appendix D

Independence of EWSB from

$M_{D_3}L$

In this Appendix, we discuss how many bulk mass parameters the theory possesses and how many of them enter the EWSB calculation. Without loss of generality the bulk mass matrix for each charge sector can be taken diagonal, so that there is a separate mass parameter for each matter and Higgs hypermultiplet. The masses for the scalar and fermion components take the form

$$\begin{aligned} \mathcal{L}_m = & \dots + \psi^c \partial_y \psi + M \eta(y) (\psi^c \psi + \text{h.c.}) - M^2 (|\phi|^2 + |\phi^c|^2) \\ & - 2M (\delta(y) + \delta(y - L)) (|\phi|^2 - |\phi^c|^2), \end{aligned} \quad (\text{D.1})$$

where $\eta(y) = +1$ (-1) for $y > 0$ (< 0), and the ∂_y piece is included because what matters is a relative sign between ∂_y and M . These mass terms have a brane contribution to maintain the form of the unbroken local Supersymmetry [1]. Despite the presence of so many parameters, the physics of EWSB is sensitive to only three of them: M_{Q_3} , M_{U_3} and M_{H_u} . It is perhaps obvious that the masses for the lighter generation quarks are irrelevant — they have small Yukawa couplings which give only small radiative contributions to the scalar potential — but it is not obvious that M_{D_3} is irrelevant. A large value for M_{Q_3} localizes b_L largely on the brane distant from the bottom Yukawa coupling, so that the 5D bottom Yukawa coupling must be large to overcome the wave-function suppression. Nevertheless, we find that the radiative contribution to the Higgs potential through the bottom Yukawa coupling is always suppressed by $(m_b/m_t)^2$.

We consider here only the case of a single Higgs hypermultiplet. Everything that follows may be directly generalized to the two Higgs case analyzed in the text.

The relevant part of the Lagrangian for studying the contribution of the radiative correction from the bottom quark Yukawa coupling to the scalar potential is:

$$\mathcal{L} = \lambda_t \delta(y) (\tilde{q} F_U h + F_Q \tilde{t} h - q t h) - \lambda_b \delta(y - L) (\tilde{q}^{c*} F'_D h^* + F'_Q \tilde{b}^{c*} h^* - q b h^*). \quad (\text{D.2})$$

Here, the chiral supermultiplets under the $N = 1$ Supersymmetry acting at $y = 0$ are given by

$$H = (h, \tilde{h}, F_H), \quad (\text{D.3})$$

$$Q_3 = (\tilde{q}, q, F_Q), \quad (\text{D.4})$$

$$U_3 = (\tilde{t}, t, F_U). \quad (\text{D.5})$$

and the chiral supermultiplets under the $N = 1$ Supersymmetry acting at $y = L$ are given by

$$H'^c = (-h^*, \tilde{h}^c, F'_H), \quad (\text{D.6})$$

$$Q'_3 = (\tilde{q}^{c*}, q, F'_Q), \quad (\text{D.7})$$

$$D'_3 = (\tilde{b}^{c*}, b, F'_D). \quad (\text{D.8})$$

The Lagrangian in Eq. (D.2) can be derived from the superpotential term $W = \lambda_t \delta(y) (Q_3 U_3 H) + \lambda_b \delta(y - L) (Q'_3 D'_3 H'^c)$.

In terms of mixed momentum-position propagators, the ratio of bottom to top Yukawa contributions in the Higgs mass squared clearly depends on the ratios $G_q(k_4; 0, 0)/G_q(k_4; L, L)$, $G_{\tilde{q}}(k_4; 0, 0)/G_{\tilde{q}^{c*}}(k_4; L, L)$ and $G_{F_Q}(k_4; 0, 0)/G_{F'_Q}(k_4; L, L)$. These ratios of propagators are all equal in the infrared, which dominates the loop integral, and given by $\exp(-2M_Q L)$. This exactly cancels the enhancement of the 5D bottom Yukawa coupling due to the small wavefunction overlap. Therefore, the contribution to the Higgs mass squared due to the bottom Yukawa interaction is down by a factor of $(m_b/m_t)^2$ and can be safely neglected. We can similarly neglect all the other Yukawa contributions relative to the top one. The most general such theory of EWSB is therefore parameterized by a three dimensional space spanned by $(M_{Q_3}, M_{U_3}, M_{H_u})$.

Appendix E

The 2 loop contribution to the Higgs potential

In this Appendix we give some details of the 2 loop contribution to the Higgs potential $\delta V_{\text{top}}^{2\text{ loop}}$.

At the 2-loop level there are two contributions. The first one comes from the expansion, in Eq. (4.9), of the one loop corrections in Eqs. (4.12) after expressing $m_{0,t}$, $m_{0,Q}$ and $m_{0,U}$ in terms of the renormalized masses m_t , m_Q and m_U respectively. The second contribution is a pure 2-loop correction and corresponds to the diagrams of Fig. 4.1 in terms of the top superfields U, Q , the Higgs superfield H and the $SU(3)$ vector superfield V . In localized approximation for U and Q , only V and H are 5-dimensional superfields.

Defining

$$C(x) = x \coth(x), \quad T(x) = x \tanh(x), \quad (\text{E.1})$$

the pure 2-loop gauge correction (arising from the diagrams Fig. 4.1-b) is given by the following expression

$$V_{2\text{loop,gauge}} = 4 g_s^2 \int \frac{d^4 p}{(2\pi)^4} \frac{d^4 q}{(2\pi)^4} \frac{T(qL)}{q^2} \times \\ \times \left[\frac{-2q^2}{\left((p-q)^2 + m_Q^2\right) (p^2 + m_t^2)} - \frac{2p^2}{\left((p-q)^2 + m_Q^2\right) (p^2 + m_t^2)} \right]$$

$$\begin{aligned}
& + \frac{2(p-q)^2}{\left((p-q)^2 + m_Q^2\right)(p^2 + m_t^2)} - \frac{2q^2}{(p^2 + m_t^2)\left((p-q)^2 + m_U^2\right)} \\
& - \frac{2p^2}{(p^2 + m_t^2)\left((p-q)^2 + m_U^2\right)} + \frac{2(p-q)^2}{(p^2 + m_t^2)\left((p-q)^2 + m_U^2\right)} \Big] \\
& + 4g_s^2 \int \frac{d^4p}{(2\pi)^4} \frac{d^4q}{(2\pi)^4} \frac{C(qL)}{q^2} \times \\
& \times \left[\frac{4}{\left((p-q)^2 + m_Q^2\right)} + \frac{q^2}{(p^2 + m_Q^2)\left((p-q)^2 + m_Q^2\right)} \right. \\
& - \frac{p^2}{(p^2 + m_Q^2)\left((p-q)^2 + m_Q^2\right)} - \frac{(p-q)^2}{(p^2 + m_Q^2)\left((p-q)^2 + m_Q^2\right)} \\
& + \frac{2q^2}{(p^2 + m_t^2)\left((p-q)^2 + m_t^2\right)} - \frac{2p^2}{(p^2 + m_t^2)\left((p-q)^2 + m_t^2\right)} \\
& - \frac{2(p-q)^2}{(p^2 + m_t^2)\left((p-q)^2 + m_t^2\right)} - \frac{8m_t^2}{(p^2 + m_t^2)\left((p-q)^2 + m_t^2\right)} \\
& + \frac{4}{(p^2 + m_U^2)} + \frac{q^2}{(p^2 + m_U^2)\left((p-q)^2 + m_U^2\right)} \\
& \left. - \frac{p^2}{(p^2 + m_U^2)\left((p-q)^2 + m_U^2\right)} - \frac{(p-q)^2}{(p^2 + m_U^2)\left((p-q)^2 + m_U^2\right)} \right].
\end{aligned}$$

Analogously the pure 2-loop Yukawa correction (arising from the diagrams Fig. 4.1-a) is given by the following expression

$$\begin{aligned}
V_{2\text{loop,Yuk.}} & = 3y_t^2 \int \frac{d^4p}{(2\pi)^4} \frac{d^4q}{(2\pi)^4} \frac{T(qL)}{q^2} \times \\
& \times \left[\frac{(p-q)^2}{\left((p-q)^2 + m_Q^2\right)(p^2 + m_t^2)} - \frac{p^2}{\left((p-q)^2 + m_Q^2\right)(p^2 + m_t^2)} \right. \\
& \left. - \frac{q^2}{\left((p-q)^2 + m_Q^2\right)(p^2 + m_t^2)} - \frac{p^2}{\left((p-q)^2 + m_Q^2 - m_t^2\right)(p^2 + m_t^2)} \right]
\end{aligned}$$

$$\begin{aligned}
& + \frac{(p-q)^2}{\left((p-q)^2 + m_Q^2 - m_t^2\right) (p^2 + m_t^2)} - \frac{q^2}{\left((p-q)^2 + m_Q^2 - m_t^2\right) (p^2 + m_t^2)} \\
& - \frac{1}{p^2 + m_U^2} + \frac{p^2}{(p-q)^2 (p^2 + m_U^2)} - \frac{q^2}{(p-q)^2 (p^2 + m_U^2)} \\
& + \frac{p^2}{\left((p-q)^2 + m_t^2\right) (p^2 + m_U^2)} - \frac{(p-q)^2}{\left((p-q)^2 + m_t^2\right) (p^2 + m_U^2)} \\
& - \left. \frac{q^2}{\left((p-q)^2 + m_t^2\right) (p^2 + m_U^2)} \right] \\
& + 3y_t^2 \int \frac{d^4 p}{(2\pi)^4} \frac{d^4 q}{(2\pi)^4} \frac{C(qL)}{q^2} \times \\
& \times \left[\frac{p^2}{(p^2 + m_Q^2) \left((p-q)^2 + m_Q^2\right)} + \frac{m_Q^2 - m_t^2}{(p^2 + m_Q^2) \left((p-q)^2 + m_Q^2\right)} \right. \\
& + \frac{p^2}{(p^2 + m_Q^2) \left((p-q)^2 + m_Q^2 - m_t^2\right)} + \frac{m_Q^2 - m_t^2}{(p^2 + m_Q^2) \left((p-q)^2 + m_Q^2 - m_t^2\right)} \\
& - \frac{1}{p^2 + m_t^2} - \frac{p^2}{(p-q)^2 (p^2 + m_t^2)} + \frac{q^2}{(p-q)^2 (p^2 + m_t^2)} \\
& - \frac{p^2}{(p^2 + m_t^2) \left((p-q)^2 + m_t^2\right)} - \frac{(p-q)^2}{(p^2 + m_t^2) \left((p-q)^2 + m_t^2\right)} \\
& + \frac{q^2}{(p^2 + m_t^2) \left((p-q)^2 + m_t^2\right)} + \frac{1}{p^2 + m_U^2} \\
& + \frac{q^2}{\left((p-q)^2 + m_Q^2\right) (p^2 + m_U^2)} + \frac{q^2}{\left((p-q)^2 + m_Q^2 - m_t^2\right) (p^2 + m_U^2)} \\
& \left. + \frac{(p-q)^2}{(p^2 + m_U^2) \left((p-q)^2 + m_U^2\right)} + \frac{-m_t^2 + m_U^2}{(p^2 + m_U^2) \left((p-q)^2 + m_U^2\right)} \right].
\end{aligned}$$

In the 2-loop potential, we have used the physical (renormalized) quantities m_t^2 , m_U^2 , m_Q^2 because the corrections are of higher order. When one takes the derivatives of the potential one has to remember that

$$v^2 \frac{d}{dv^2} = m_t^2 \left(\frac{\partial}{\partial m_t^2} + \frac{\partial}{\partial m_U^2} + \frac{\partial}{\partial m_Q^2} \right), \quad (\text{E.2})$$

because all the 3 masses depend on the VEV v .

The integrals in p can be performed analytically. Then, to get the leading logarithmic contributions as $L \rightarrow 0$, one can use the asymptotic behavior of the q -integrand functions. In this way one gets the results given in Eqs. (4.14)-(4.15).

Appendix F

1-loop Renormalization functions at order α_t, α_s

In order to compute the physical masses in Eqs. (4.12a)-(4.12c), the one loop corrections $\mathcal{O}(\alpha_t, \alpha_s)$ to the propagators of the U, Q -multiplets and to the Yukawa vertex are needed.

At order α_t the propagators of the top, stop and auxiliary field get corrected from the exchange of the Higgs supermultiplet H and a U (or Q) quark multiplet.

These corrections can be parameterized as usual

$$\begin{array}{c} H \\ \text{---} \bigcirc \text{---} \\ \varphi_{U,Q} \qquad \varphi_{U,Q} \\ Q, U \end{array} = i (p^2 B_\varphi^{U,Q}(p^2) - \delta m_{U,Q}^2)$$

$$\begin{array}{c} H \\ \text{---} \bigcirc \text{---} \\ \psi_{U,Q} \qquad \psi_{U,Q} \\ Q, U \end{array} = i \not{p} B_\psi^{U,Q}(p^2)$$

$$\text{Diagram} = -iB_F^{U,Q}(p^2)$$

where we have used a superfield notation in the loop and an Euclidean external momentum p . The Yukawa vertex receives no direct correction at order α_t because of the non-renormalization properties of the superpotential.

All the quantities defined above, to the order y_t^2 , are given by

$$B_F^U(0) = -y_t^2 \int \frac{d^4q}{(2\pi)^4} C(qL) \left[\frac{1}{q^2 + m_Q^2 + m_t^2} + \frac{1}{q^2 + m_Q^2} \right], \quad (\text{F.1a})$$

$$B_F^Q(0) = -y_t^2 \int \frac{d^4q}{(2\pi)^4} C(qL) \left[\frac{1}{q^2 + m_Q^2 + m_t^2} \right], \quad (\text{F.1b})$$

$$B_\varphi^Q(0) = y_t^2 \int \frac{d^4q}{(2\pi)^4} \frac{1}{q^2} \left\{ C(qL) \left[\frac{q^2(m_t^2 + m_U^2)}{(q^2 + m_t^2 + m_U^2)^3} - \frac{m_t^2(m_t^2 + m_U^2)}{(q^2 + m_t^2 + m_Q^2)^3} \right] - T(qL) \left[\frac{q^4 + 3m_t^2 q^2}{(q^2 + m_t^2)^3} \right] \right\}, \quad (\text{F.1c})$$

$$B_\varphi^U(0) = y_t^2 \int \frac{d^4q}{(2\pi)^4} \frac{1}{q^2} \left\{ C(qL) \left[\frac{q^2(m_t^2 + m_Q^2)}{(q^2 + m_t^2 + m_Q^2)^3} - \frac{m_t^2(m_t^2 + m_U^2)}{(q^2 + m_t^2 + m_U^2)^3} + \frac{q^2 m_Q^2}{(q^2 + m_Q^2)^3} \right] - T(qL) \left[\frac{q^4 + 3m_t^2 q^2}{(q^2 + m_t^2)^3} + \frac{1}{q^2} \right] \right\}, \quad (\text{F.1d})$$

$$B_\psi^Q(0) = -\frac{y_t^2}{2} \int \frac{d^4q}{(2\pi)^4} \frac{1}{q^2} \left\{ C(qL) \frac{q^2 + 2m_t^2}{(q^2 + m_t^2)^2} + T(qL) \frac{q^2}{(q^2 + m_U^2 + m_t^2)^2} \right\}, \quad (\text{F.1e})$$

$$B_\psi^U(0) = -\frac{y_t^2}{2} \int \frac{d^4q}{(2\pi)^4} \frac{1}{q^2} \left\{ C(qL) \left[\frac{q^2 + 2m_t^2}{(q^2 + m_t^2)^2} + \frac{1}{q^2} \right] - T(qL) \left[\frac{q^2}{(q^2 + m_Q^2 + m_t^2)^2} + \frac{q^2}{(q^2 + m_Q^2)^2} \right] \right\}, \quad (\text{F.1f})$$

$$\delta m_Q^2 = y_t^2 \int \frac{d^4q}{(2\pi)^4} \frac{1}{q^2} \left\{ C(qL) \left[\frac{q^2 + m_Q^2}{q^2 + m_Q^2 + m_t^2} + \frac{q^2}{q^2 + m_{0,u}^2 + m_t^2} \right] - T(qL) \frac{2q^2}{q^2 + m_t^2} \right\}, \quad (\text{F.1g})$$

$$\delta m_U^2 = y_t^2 \int \frac{d^4 q}{(2\pi)^4} \frac{1}{q^2} \left\{ C(qL) \left[\frac{q^2 + m_U^2}{q^2 + m_U^2 + m_t^2} + 1 + \frac{q^2}{q^2 + m_q^2 + m_t^2} + \frac{q^2}{q^2 + m_Q^2} \right] - T(qL) \left[\frac{2q^2}{q^2 + m_t^2} + 2 \right] \right\}, \quad (\text{F.1h})$$

where the functions $C(x)$ and $T(x)$ are given in Eq. (E.1). The integration over the momentum q has to be performed on Euclidean space.

At order α_s only the propagators of the top and the stops, but not of their auxiliary fields, get corrected from the exchange of the $SU(3)$ gauge supermultiplet V and of a quark multiplet. Performing the calculation in the Wess-Zumino gauge there is also a direct correction to the Yukawa interaction, so that

$$\begin{aligned} & \text{Diagram 1: } \varphi_{U,Q} \text{ --- } \text{Circle (V, U, Q)} \text{ --- } \varphi_{U,Q} = i(p^2 B_\varphi^{U,Q}(p^2) - \delta m_{U,Q}^2) \\ & \text{Diagram 2: } \psi_{U,Q} \text{ --- } \text{Circle (V, U, Q)} \text{ --- } \psi_{U,Q} = i\not{p} B_\psi^{U,Q}(p^2) \\ & \text{Diagram 3: } h \text{ --- } \text{Triangle (V, U, Q)} \text{ --- } \psi_U, \psi_Q = -iy_t Z_{y_t}(p^2) \end{aligned}$$

Parameterizing these g_s^2 -corrections as in the y_t^2 case, one has

$$B_\varphi^i(0) = \frac{8}{3} g_s^2 \int \frac{d^4 q}{(2\pi)^4} \frac{1}{q^2} \left\{ C(qL) \frac{q^2 + 2(m_i^2 + m_t^2)}{(q^2 + m_i^2 + m_t^2)^2} - T(qL) \frac{q^4 + 3q^2 m_t^2}{(q^2 + m_t^2)^3} \right\}, \quad (\text{F.2a})$$

$$B_\psi^i(0) = -\frac{4}{3}g_s^2 \int \frac{d^4q}{(2\pi)^4} \frac{1}{q^2} \left\{ C(qL) \frac{q^2 + 2m_t^2}{(q^2 + m_t^2)^2} + T(qL) \frac{q^2}{(q^2 + m_t^2 + m_t^2)^2} \right\}, \quad (\text{F.2b})$$

$$\delta m_i^2 = \frac{16}{3}g_s^2 \int \frac{d^4q}{(2\pi)^4} \frac{1}{q^2} \left\{ C(qL) - T(qL) \frac{q^2}{q^2 + m_t^2} \right\}, \quad (\text{F.2c})$$

$$Z_{y_t}(0) = \frac{16}{3}g_s^2 \int \frac{d^4q}{(2\pi)^4} \frac{1}{q^2} C(qL) \frac{q^2}{(q^2 + m_t^2)^2}, \quad (\text{F.2d})$$

where $i = U, Q$.

All the quantities defined above are regular in the IR except B_ψ^U . Because we are interested only in the logarithmic contributions to $\delta V''(v^2)$, we can evaluate the B_φ and B_F functions at vanishing external momentum. Instead, the functions B_ψ and Z_{y_t} , involved in Eq. (4.12a), have to be evaluated at $p^2 = m_t^2$. Given their expressions at $p^2 = 0$ one has to add

$$B_\psi^Q(m_t^2) - B_\psi^Q(0) = \frac{\alpha_s}{6\pi} + \frac{\alpha_t}{16\pi}, \quad (\text{F.3})$$

$$B_\psi^U(m_t^2) - B_\psi^U(0) = \frac{\alpha_s}{6\pi} + \frac{\alpha_t}{16\pi} + 4\pi\alpha_t \int \frac{d^4q}{(2\pi)^4} \left[\frac{1}{2q^4} + \frac{4 \log\left(\frac{2q}{m_t + \sqrt{4q^2 + m_t^2}}\right)}{m_t(4q^2 + m_t^2)^{\frac{3}{2}}} - \frac{1}{q^2(4q^2 + m_t^2)} \right], \quad (\text{F.4})$$

$$Z_{y_t}(m_t^2) - Z_{y_t}(0) = \frac{4\alpha_s}{3\pi} (2 - 3 \log 2). \quad (\text{F.5})$$

Note that the IR divergence in Eq. (F.4) cancels the one in $B_\psi^U(0)$.

Bibliography

- [1] R. Barbieri, G. Marandella, and M. Papucci, “Breaking the electroweak symmetry and supersymmetry by a compact extra dimension,” *Phys. Rev.* **D66** (2002) 095003, [arXiv:hep-ph/0205280](#).
- [2] R. Barbieri *et al.*, “Radiative electroweak symmetry breaking from a quasi-localized top quark,” *Nucl. Phys.* **B663** (2003) 141–162, [arXiv:hep-ph/0208153](#).
- [3] R. Barbieri, G. Marandella, and M. Papucci, “The Higgs mass as a function of the compactification scale,” *Nucl. Phys.* **B668** (2003) 273–292, [arXiv:hep-ph/0305044](#).
- [4] G. Marandella and M. Papucci, “Relating the electroweak scale to an extra dimension: Constraints from electroweak precision tests,” *Phys. Rev.* **D71** (2005) 055010, [arXiv:hep-ph/0407030](#).
- [5] T. Hambye, Y. Lin, A. Notari, M. Papucci, and A. Strumia, “Constraints on neutrino masses from leptogenesis models,” *Nucl. Phys.* **B695** (2004) 169–191, [arXiv:hep-ph/0312203](#).
- [6] M. Papucci, “NDA and perturbativity in Higgsless models,” [arXiv:hep-ph/0408058](#).
- [7] S. Foffa, A. Gasparini, M. Papucci, and R. Sturani, “Sensitivity of a small matter-wave interferometer to gravitational waves,” *Phys. Rev.* **D73** (2006) 022001, [arXiv:gr-qc/0407039](#).
- [8] **ALEPH** Collaboration, “Precision electroweak measurements on the Z resonance,” *Phys. Rept.* **427** (2006) 257, [arXiv:hep-ex/0509008](#).
- [9] **ALEPH** Collaboration, “Precision Electroweak Measurements and Constraints on the Standard Model,” [arXiv:0811.4682 \[hep-ex\]](#).

-
- [10] S. Davidson, S. Forte, P. Gambino, N. Rius, and A. Strumia, “Old and new physics interpretations of the NuTeV anomaly,” *JHEP* **02** (2002) 037, [arXiv:hep-ph/0112302](#).
- [11] M. S. Chanowitz, “The $Z \rightarrow i$ anti- b b decay asymmetry: Lose-lose for the standard model,” *Phys. Rev. Lett.* **87** (2001) 231802, [arXiv:hep-ph/0104024](#).
- [12] M. S. Chanowitz, “Electroweak Data and the Higgs Boson Mass: A Case for New Physics,” *Phys. Rev.* **D66** (2002) 073002, [arXiv:hep-ph/0207123](#).
- [13] G. Altarelli, “Introduction to the Terascale,” [arXiv:hep-ph/0611025](#).
- [14] P. Gambino, “The top priority: Precision electroweak physics from low to high energy,” *Int. J. Mod. Phys.* **A19** (2004) 808–820, [arXiv:hep-ph/0311257](#).
- [15] Z. Zhang, “Muon $g-2$: a mini review,” [arXiv:0801.4905 \[hep-ph\]](#).
- [16] Z. Ligeti, “The CKM matrix and CP violation,” *Int. J. Mod. Phys.* **A20** (2005) 5105–5118, [arXiv:hep-ph/0408267](#).
- [17] K. Agashe, M. Papucci, G. Perez, and D. Pirjol, “Next to minimal flavor violation,” [arXiv:hep-ph/0509117](#).
- [18] **Heavy Flavor Averaging Group** Collaboration, E. Barberio *et al.*, “Averages of b -hadron and c -hadron Properties at the End of 2007,” [arXiv:0808.1297 \[hep-ex\]](#).
- [19] B. W. Lee, C. Quigg, and H. B. Thacker, “Weak Interactions at Very High-Energies: The Role of the Higgs Boson Mass,” *Phys. Rev.* **D16** (1977) 1519.
- [20] M. S. Chanowitz and M. K. Gaillard, “The TeV Physics of Strongly Interacting W 's and Z 's,” *Nucl. Phys.* **B261** (1985) 379.
- [21] R. Barbieri and A. Strumia, “What is the limit on the Higgs mass?,” *Phys. Lett.* **B462** (1999) 144–149, [arXiv:hep-ph/9905281](#).
- [22] R. Barbieri, A. Pomarol, R. Rattazzi, and A. Strumia, “Electroweak symmetry breaking after LEP-1 and LEP-2,” *Nucl. Phys.* **B703** (2004) 127–146, [arXiv:hep-ph/0405040](#).

-
- [23] G. Cacciapaglia, C. Csaki, G. Marandella, and A. Strumia, “The minimal set of electroweak precision parameters,” *Phys. Rev.* **D74** (2006) 033011, [arXiv:hep-ph/0604111](#).
- [24] M. J. G. Veltman, “The Infrared - Ultraviolet Connection,” *Acta Phys. Polon.* **B12** (1981) 437.
- [25] N. Arkani-Hamed and S. Dimopoulos, “Supersymmetric unification without low energy supersymmetry and signatures for fine-tuning at the LHC,” *JHEP* **06** (2005) 073, [arXiv:hep-th/0405159](#).
- [26] N. Arkani-Hamed, S. Dimopoulos, and S. Kachru, “Predictive landscapes and new physics at a TeV,” [arXiv:hep-th/0501082](#).
- [27] B. Feldstein, L. J. Hall, and T. Watari, “Landscape Predictions for the Higgs Boson and Top Quark Masses,” *Phys. Rev.* **D74** (2006) 095011, [arXiv:hep-ph/0608121](#).
- [28] G. F. Giudice and R. Rattazzi, “Living dangerously with low-energy supersymmetry,” *Nucl. Phys.* **B757** (2006) 19–46, [arXiv:hep-ph/0606105](#).
- [29] L. J. Hall and Y. Nomura, “Evidence for the Multiverse in the Standard Model and Beyond,” *Phys. Rev.* **D78** (2008) 035001, [arXiv:0712.2454 \[hep-ph\]](#).
- [30] H. Georgi and S. L. Glashow, “Unity of All Elementary Particle Forces,” *Phys. Rev. Lett.* **32** (1974) 438–441.
- [31] S. Dimopoulos and H. Georgi, “Softly Broken Supersymmetry and SU(5),” *Nucl. Phys.* **B193** (1981) 150.
- [32] A. J. Buras, J. R. Ellis, M. K. Gaillard, and D. V. Nanopoulos, “Aspects of the Grand Unification of Strong, Weak and Electromagnetic Interactions,” *Nucl. Phys.* **B135** (1978) 66–92.
- [33] H. Georgi and C. Jarlskog, “A New Lepton - Quark Mass Relation in a Unified Theory,” *Phys. Lett.* **B86** (1979) 297–300.
- [34] e. ’t Hooft, Gerard *et al.*, “Recent Developments in Gauge Theories. Proceedings, Nato Advanced Study Institute, Cargese, France, August 26 - September 8, 1979,” New York, Usa: Plenum (1980) 438 P. (Nato Advanced Study Institutes Series: Series B, Physics, 59).

-
- [35] Y. A. Golfand and E. P. Likhtman, “Extension of the Algebra of Poincare Group Generators and Violation of p Invariance,” *JETP Lett.* **13** (1971) 323–326.
- [36] D. V. Volkov and V. P. Akulov, “Is the Neutrino a Goldstone Particle?,” *Phys. Lett.* **B46** (1973) 109–110.
- [37] J. Wess and B. Zumino, “A Lagrangian Model Invariant Under Supergauge Transformations,” *Phys. Lett.* **B49** (1974) 52.
- [38] S. Ferrara and O. Piguet, “Perturbation Theory and Renormalization of Supersymmetric Yang-Mills Theories,” *Nucl. Phys.* **B93** (1975) 261.
- [39] J. Wess and B. Zumino, “Supergauge Transformations in Four-Dimensions,” *Nucl. Phys.* **B70** (1974) 39–50.
- [40] S. Ferrara, L. Girardello, and F. Palumbo, “A General Mass Formula in Broken Supersymmetry,” *Phys. Rev.* **D20** (1979) 403.
- [41] R. Barbieri, S. Ferrara, D. V. Nanopoulos, and K. S. Stelle, “SUPERGRAVITY, R INVARIANCE AND SPONTANEOUS SUPERSYMMETRY BREAKING,” *Phys. Lett.* **B113** (1982) 219.
- [42] R. Barbieri, S. Ferrara, and C. A. Savoy, “Gauge Models with Spontaneously Broken Local Supersymmetry,” *Phys. Lett.* **B119** (1982) 343.
- [43] M. Dine and A. E. Nelson, “Dynamical supersymmetry breaking at low-energies,” *Phys. Rev.* **D48** (1993) 1277–1287, [arXiv:hep-ph/9303230](#).
- [44] M. Dine, A. E. Nelson, and Y. Shirman, “Low-energy dynamical supersymmetry breaking simplified,” *Phys. Rev.* **D51** (1995) 1362–1370, [arXiv:hep-ph/9408384](#).
- [45] Y. Nir and N. Seiberg, “Should squarks be degenerate?,” *Phys. Lett.* **B309** (1993) 337–343, [arXiv:hep-ph/9304307](#).
- [46] M. Dine, R. G. Leigh, and A. Kagan, “Flavor symmetries and the problem of squark degeneracy,” *Phys. Rev.* **D48** (1993) 4269–4274, [arXiv:hep-ph/9304299](#).

-
- [47] R. Barbieri, L. J. Hall, S. Raby, and A. Romanino, “Unified theories with $U(2)$ flavor symmetry,” *Nucl. Phys.* **B493** (1997) 3–26, [arXiv:hep-ph/9610449](#).
- [48] T. Appelquist, G. T. Fleming, and E. T. Neil, “Lattice Study of Conformal Behavior in $SU(3)$ Yang-Mills Theories,” [arXiv:0901.3766](#) [hep-ph].
- [49] L. Del Debbio, A. Patella, and C. Pica, “Fermions in higher representations. Some results about $SU(2)$ with adjoint fermions,” [arXiv:0812.0570](#) [hep-lat].
- [50] A. Hietanen, J. Rantaharju, K. Rummukainen, and K. Tuominen, “Minimal technicolor on the lattice,” *Nucl. Phys.* **A820** (2009) 191c–194c.
- [51] B. Holdom and J. Terning, “Large corrections to electroweak parameters in technicolor theories,” *Phys. Lett.* **B247** (1990) 88–92.
- [52] G. ’t Hooft, “A PLANAR DIAGRAM THEORY FOR STRONG INTERACTIONS,” *Nucl. Phys.* **B72** (1974) 461.
- [53] J. M. Maldacena, “The large N limit of superconformal field theories and supergravity,” *Adv. Theor. Math. Phys.* **2** (1998) 231–252, [arXiv:hep-th/9711200](#).
- [54] L. Randall and R. Sundrum, “A large mass hierarchy from a small extra dimension,” *Phys. Rev. Lett.* **83** (1999) 3370–3373, [arXiv:hep-ph/9905221](#).
- [55] C. Csaki, C. Grojean, L. Pilo, and J. Terning, “Towards a realistic model of Higgsless electroweak symmetry breaking,” *Phys. Rev. Lett.* **92** (2004) 101802, [arXiv:hep-ph/0308038](#).
- [56] R. Contino, Y. Nomura, and A. Pomarol, “Higgs as a holographic pseudo-Goldstone boson,” *Nucl. Phys.* **B671** (2003) 148–174, [arXiv:hep-ph/0306259](#).
- [57] I. R. Klebanov and M. J. Strassler, “Supergravity and a confining gauge theory: Duality cascades and chiSB-resolution of naked singularities,” *JHEP* **08** (2000) 052, [arXiv:hep-th/0007191](#).
- [58] N. Arkani-Hamed, M. Porrati, and L. Randall, “Holography and phenomenology,” *JHEP* **08** (2001) 017, [arXiv:hep-th/0012148](#).

-
- [59] R. Contino and A. Pomarol, “Holography for fermions,” *JHEP* **11** (2004) 058, [arXiv:hep-th/0406257](#).
- [60] M. A. Luty and T. Okui, “Conformal technicolor,” *JHEP* **09** (2006) 070, [arXiv:hep-ph/0409274](#).
- [61] F. Sannino and K. Tuominen, “Techniorientifold,” *Phys. Rev.* **D71** (2005) 051901, [arXiv:hep-ph/0405209](#).
- [62] I. Antoniadis, N. Arkani-Hamed, S. Dimopoulos, and G. R. Dvali, “New dimensions at a millimeter to a Fermi and superstrings at a TeV,” *Phys. Lett.* **B436** (1998) 257–263, [arXiv:hep-ph/9804398](#).
- [63] N. Arkani-Hamed, S. Dimopoulos, and G. R. Dvali, “The hierarchy problem and new dimensions at a millimeter,” *Phys. Lett.* **B429** (1998) 263–272, [arXiv:hep-ph/9803315](#).
- [64] R. Barbieri and A. Strumia, “The ‘LEP paradox’,” [arXiv:hep-ph/0007265](#).
- [65] R. Barbieri and G. F. Giudice, “Upper Bounds on Supersymmetric Particle Masses,” *Nucl. Phys.* **B306** (1988) 63.
- [66] K. Choi, A. Falkowski, H. P. Nilles, and M. Olechowski, “Soft supersymmetry breaking in KKL T flux compactification,” *Nucl. Phys.* **B718** (2005) 113–133, [arXiv:hep-th/0503216](#).
- [67] C. Csaki, G. Marandella, Y. Shirman, and A. Strumia, “The super-little Higgs,” *Phys. Rev.* **D73** (2006) 035006, [arXiv:hep-ph/0510294](#).
- [68] R. Barbieri, L. J. Hall, Y. Nomura, and V. S. Rychkov, “Supersymmetry without a Light Higgs Boson,” *Phys. Rev.* **D75** (2007) 035007, [arXiv:hep-ph/0607332](#).
- [69] R. Dermisek and J. F. Gunion, “Escaping the large fine tuning and little hierarchy problems in the next to minimal supersymmetric model and $h \rightarrow a a$ decays,” *Phys. Rev. Lett.* **95** (2005) 041801, [arXiv:hep-ph/0502105](#).
- [70] L. Susskind, “Dynamics of Spontaneous Symmetry Breaking in the Weinberg- Salam Theory,” *Phys. Rev.* **D20** (1979) 2619–2625.
- [71] S. Weinberg, “Implications of Dynamical Symmetry Breaking: An Addendum,” *Phys. Rev.* **D19** (1979) 1277–1280.

-
- [72] K. Agashe, R. Contino, L. Da Rold, and A. Pomarol, “A custodial symmetry for $Z b \text{ anti-}b$,” *Phys. Lett.* **B641** (2006) 62–66, [arXiv:hep-ph/0605341](#).
- [73] M. E. Peskin and T. Takeuchi, “Estimation of oblique electroweak corrections,” *Phys. Rev.* **D46** (1992) 381–409.
- [74] R. Barbieri, A. Pomarol, and R. Rattazzi, “Weakly coupled Higgsless theories and precision electroweak tests,” *Phys. Lett.* **B591** (2004) 141–149, [arXiv:hep-ph/0310285](#).
- [75] G. Cacciapaglia, C. Csaki, C. Grojean, and J. Terning, “Curing the Ills of Higgsless models: The S parameter and unitarity,” *Phys. Rev.* **D71** (2005) 035015, [arXiv:hep-ph/0409126](#).
- [76] K. Agashe, C. Csaki, C. Grojean, and M. Reece, “The S-parameter in holographic technicolor models,” *JHEP* **12** (2007) 003, [arXiv:0704.1821](#) [hep-ph].
- [77] C. Csaki, A. Falkowski, and A. Weiler, “The Flavor of the Composite Pseudo-Goldstone Higgs,” *JHEP* **09** (2008) 008, [arXiv:0804.1954](#) [hep-ph].
- [78] D. B. Kaplan and H. Georgi, “ $SU(2) \times U(1)$ Breaking by Vacuum Misalignment,” *Phys. Lett.* **B136** (1984) 183.
- [79] N. Arkani-Hamed, A. G. Cohen, and H. Georgi, “Electroweak symmetry breaking from dimensional deconstruction,” *Phys. Lett.* **B513** (2001) 232–240, [arXiv:hep-ph/0105239](#).
- [80] Z. Chacko, H.-S. Goh, and R. Harnik, “The twin Higgs: Natural electroweak breaking from mirror symmetry,” *Phys. Rev. Lett.* **96** (2006) 231802, [arXiv:hep-ph/0506256](#).
- [81] H.-C. Cheng and I. Low, “TeV symmetry and the little hierarchy problem,” *JHEP* **09** (2003) 051, [arXiv:hep-ph/0308199](#).
- [82] A. Delgado, A. Pomarol, and M. Quiros, “Supersymmetry and electroweak breaking from extra dimensions at the TeV-scale,” *Phys. Rev.* **D60** (1999) 095008, [arXiv:hep-ph/9812489](#).

-
- [83] J. F. Gunion and B. Grzadkowski, “Extra dimension Kaluza-Klein excitations and electroweak symmetry breaking,” [arXiv:hep-ph/0004058](#).
- [84] A. Delgado and M. Quiros, “Supersymmetry and finite radiative electroweak breaking from an extra dimension,” *Nucl. Phys.* **B607** (2001) 99–116, [arXiv:hep-ph/0103058](#).
- [85] N. Arkani-Hamed, L. J. Hall, D. Tucker-Smith, and N. Weiner, “Exponentially small supersymmetry breaking from extra dimensions,” *Phys. Rev.* **D63** (2001) 056003, [arXiv:hep-ph/9911421](#).
- [86] J. Scherk and J. H. Schwarz, “Spontaneous Breaking of Supersymmetry Through Dimensional Reduction,” *Phys. Lett.* **B82** (1979) 60.
- [87] J. Scherk and J. H. Schwarz, “How to Get Masses from Extra Dimensions,” *Nucl. Phys.* **B153** (1979) 61–88.
- [88] R. Barbieri, L. J. Hall, and Y. Nomura, “A constrained standard model from a compact extra dimension,” *Phys. Rev.* **D63** (2001) 105007, [arXiv:hep-ph/0011311](#).
- [89] I. Antoniadis, S. Dimopoulos, A. Pomarol, and M. Quiros, “Soft masses in theories with supersymmetry breaking by TeV-compactification,” *Nucl. Phys.* **B544** (1999) 503–519, [arXiv:hep-ph/9810410](#).
- [90] K. R. Dienes, E. Dudas, and T. Gherghetta, “Extra spacetime dimensions and unification,” *Phys. Lett.* **B436** (1998) 55–65, [arXiv:hep-ph/9803466](#).
- [91] R. Barbieri, L. J. Hall, and Y. Nomura, “Models of Scherk-Schwarz symmetry breaking in 5D: Classification and calculability,” *Nucl. Phys.* **B624** (2002) 63–80, [arXiv:hep-th/0107004](#).
- [92] L. J. Hall, H. Murayama, and Y. Nomura, “Wilson lines and symmetry breaking on orbifolds,” *Nucl. Phys.* **B645** (2002) 85–104, [arXiv:hep-th/0107245](#).
- [93] N. Arkani-Hamed, T. Gregoire, and J. G. Wacker, “Higher dimensional supersymmetry in 4D superspace,” *JHEP* **03** (2002) 055, [arXiv:hep-th/0101233](#).
- [94] A. Hebecker, “5D super Yang-Mills theory in 4-D superspace, superfield brane operators, and applications to orbifold GUTs,” *Nucl. Phys.* **B632** (2002) 101–113, [arXiv:hep-ph/0112230](#).

-
- [95] N. Arkani-Hamed, L. J. Hall, Y. Nomura, D. Tucker-Smith, and N. Weiner, “Finite radiative electroweak symmetry breaking from the bulk,” *Nucl. Phys.* **B605** (2001) 81–115, [arXiv:hep-ph/0102090](#).
- [96] Z. Chacko, M. A. Luty, and E. Ponton, “Massive higher-dimensional gauge fields as messengers of supersymmetry breaking,” *JHEP* **07** (2000) 036, [arXiv:hep-ph/9909248](#).
- [97] M. Zucker, “Minimal off-shell supergravity in five dimensions,” *Nucl. Phys.* **B570** (2000) 267–283, [arXiv:hep-th/9907082](#).
- [98] Z. Chacko and M. A. Luty, “Radion mediated supersymmetry breaking,” *JHEP* **05** (2001) 067, [arXiv:hep-ph/0008103](#).
- [99] D. E. Kaplan and N. Weiner, “Radion mediated supersymmetry breaking as a Scherk-Schwarz theory,” [arXiv:hep-ph/0108001](#).
- [100] M. Papucci, “Rottura di supersimmetria à la Scherk-Schwarz: esempi e proprietà di rinormalizzazione.” Diploma Thesis (in Italian), 2001.
- [101] N. Arkani-Hamed, A. G. Cohen, and H. Georgi, “Anomalies on orbifolds,” *Phys. Lett.* **B516** (2001) 395–402, [arXiv:hep-th/0103135](#).
- [102] C. A. Scrucca, M. Serone, L. Silvestrini, and F. Zwirner, “Anomalies in orbifold field theories,” *Phys. Lett.* **B525** (2002) 169–174, [arXiv:hep-th/0110073](#).
- [103] L. Pilo and A. Riotto, “On anomalies in orbifold theories,” *Phys. Lett.* **B546** (2002) 135–142, [arXiv:hep-th/0202144](#).
- [104] R. Barbieri, R. Contino, P. Creminelli, R. Rattazzi, and C. A. Scrucca, “Anomalies, Fayet-Iliopoulos terms and the consistency of orbifold field theories,” *Phys. Rev.* **D66** (2002) 024025, [arXiv:hep-th/0203039](#).
- [105] D. M. Ghilencea, S. Groot Nibbelink, and H. P. Nilles, “Gauge corrections and FI-term in 5D KK theories,” *Nucl. Phys.* **B619** (2001) 385–395, [arXiv:hep-th/0108184](#).
- [106] R. Barbieri, L. J. Hall, and Y. Nomura, “A constrained standard model: Effects of Fayet-Iliopoulos terms,” [arXiv:hep-ph/0110102](#).

-
- [107] S. Ferrara, L. Girardello, T. Kugo, and A. Van Proeyen, “RELATION BETWEEN DIFFERENT AUXILIARY FIELD FORMULATIONS OF N=1 SUPERGRAVITY COUPLED TO MATTER,” *Nucl. Phys.* **B223** (1983) 191.
- [108] E. A. Mirabelli and M. E. Peskin, “Transmission of supersymmetry breaking from a 4- dimensional boundary,” *Phys. Rev.* **D58** (1998) 065002, [arXiv:hep-th/9712214](#).
- [109] **CDF** Collaboration, T. Aaltonen *et al.*, “Search for Long-Lived Massive Charged Particles in 1.96 TeV $\bar{p}p$ Collisions,” [arXiv:0902.1266](#) [[hep-ex](#)].
- [110] D. Marti and A. Pomarol, “Fayet-Iliopoulos terms in 5d theories and their phenomenological implications,” *Phys. Rev.* **D66** (2002) 125005, [arXiv:hep-ph/0205034](#).
- [111] G. Cacciapaglia, M. Cirelli, and G. Cristadoro, “Gluon fusion production of the Higgs boson in a calculable model with one extra dimension,” *Phys. Lett.* **B531** (2002) 105–111, [arXiv:hep-ph/0111287](#).
- [112] “ATLAS detector and physics performance. Technical design report. Vol. 2,”. CERN-LHCC-99-15.
- [113] **CMS** Collaboration, G. L. Bayatian *et al.*, “CMS technical design report, volume II: Physics performance,” *J. Phys.* **G34** (2007) 995–1579.
- [114] J. M. Butterworth, A. R. Davison, M. Rubin, and G. P. Salam, “Jet substructure as a new Higgs search channel at the LHC,” *Phys. Rev. Lett.* **100** (2008) 242001, [arXiv:0802.2470](#) [[hep-ph](#)].
- [115] A. Pomarol and M. Quiros, “The standard model from extra dimensions,” *Phys. Lett.* **B438** (1998) 255–260, [arXiv:hep-ph/9806263](#).
- [116] A. Brignole, “Radiative corrections to the supersymmetric neutral Higgs boson masses,” *Phys. Lett.* **B281** (1992) 284–294.
- [117] R. Hempfling and A. H. Hoang, “Two loop radiative corrections to the upper limit of the lightest Higgs boson mass in the minimal supersymmetric model,” *Phys. Lett.* **B331** (1994) 99–106, [arXiv:hep-ph/9401219](#).

- [118] A. Manohar and H. Georgi, “Chiral Quarks and the Nonrelativistic Quark Model,” *Nucl. Phys.* **B234** (1984) 189.
- [119] B. Grinstein and M. B. Wise, “Operator analysis for precision electroweak physics,” *Phys. Lett.* **B265** (1991) 326–334.
- [120] S. J. Gates, M. T. Grisaru, M. Rocek, and W. Siegel, “Superspace, or one thousand and one lessons in supersymmetry,” *Front. Phys.* **58** (1983) 1–548, [arXiv:hep-th/0108200](#).
- [121] A. Delgado, A. Pomarol, and M. Quiros, “Electroweak and flavor physics in extensions of the standard model with large extra dimensions,” *JHEP* **01** (2000) 030, [arXiv:hep-ph/9911252](#).
- [122] Y. Nir, “Probing new physics with flavor physics (and probing flavor physics with new physics),” [arXiv:0708.1872 \[hep-ph\]](#).
- [123] K. Blum, Y. Grossman, Y. Nir, and G. Perez, “Combining $K - \bar{K}$ mixing and $D - \bar{D}$ mixing to constrain the flavor structure of new physics,” *Phys. Rev. Lett.* **102** (2009) 211802, [arXiv:0903.2118 \[hep-ph\]](#).
- [124] **UTfit** Collaboration, M. Bona *et al.*, “Model-independent constraints on $\Delta F=2$ operators and the scale of new physics,” *JHEP* **03** (2008) 049, [arXiv:0707.0636 \[hep-ph\]](#).
- [125] P. J. Fox, Z. Ligeti, M. Papucci, G. Perez, and M. D. Schwartz, “Deciphering top flavor violation at the LHC with B factories,” *Phys. Rev.* **D78** (2008) 054008, [arXiv:0704.1482 \[hep-ph\]](#).
- [126] G. D’Ambrosio, G. F. Giudice, G. Isidori, and A. Strumia, “Minimal flavour violation: An effective field theory approach,” *Nucl. Phys.* **B645** (2002) 155–187, [arXiv:hep-ph/0207036](#).
- [127] A. C. Kraan, “Interactions of heavy stable hadronizing particles,” *Eur. Phys. J.* **C37** (2004) 91–104, [arXiv:hep-ex/0404001](#).
- [128] R. Mackeprang and A. Rizzi, “Interactions of coloured heavy stable particles in matter,” *Eur. Phys. J.* **C50** (2007) 353–362, [arXiv:hep-ph/0612161](#).
- [129] T. Asaka, K. Ishiwata, and T. Moroi, “Right-handed sneutrino as cold dark matter,” *Phys. Rev.* **D73** (2006) 051301, [arXiv:hep-ph/0512118](#).

-
- [130] L. Covi and S. Kraml, “Collider signatures of gravitino dark matter with a sneutrino NLSP,” *JHEP* **08** (2007) 015, [arXiv:hep-ph/0703130](#).
- [131] C. Arina and N. Fornengo, “Sneutrino cold dark matter, a new analysis: relic abundance and detection rates,” *JHEP* **11** (2007) 029, [arXiv:0709.4477 \[hep-ph\]](#).
- [132] D. A. Demir, L. L. Everett, M. Frank, L. Selbuz, and I. Turan, “Sneutrino Dark Matter: Symmetry Protection and Cosmic Ray Anomalies,” [arXiv:0906.3540 \[hep-ph\]](#).
- [133] M. Kawasaki, K. Kohri, and T. Moroi, “Big-bang nucleosynthesis and hadronic decay of long-lived massive particles,” *Phys. Rev.* **D71** (2005) 083502, [arXiv:astro-ph/0408426](#).
- [134] T. Kanzaki, M. Kawasaki, K. Kohri, and T. Moroi, “Cosmological Constraints on Gravitino LSP Scenario with Sneutrino NLSP,” *Phys. Rev.* **D75** (2007) 025011, [arXiv:hep-ph/0609246](#).
- [135] T. Asaka, K. Ishiwata, and T. Moroi, “Right-handed sneutrino as cold dark matter of the universe,” *Phys. Rev.* **D75** (2007) 065001, [arXiv:hep-ph/0612211](#).
- [136] J. Kang, M. A. Luty, and S. Nasri, “The Relic Abundance of Long-lived Heavy Colored Particles,” *JHEP* **09** (2008) 086, [arXiv:hep-ph/0611322](#).
- [137] C. Jacoby and S. Nussinov, “The Relic Abundance of Massive Colored Particles after a Late Hadronic Annihilation Stage,” [arXiv:0712.2681 \[hep-ph\]](#).
- [138] P. J. Fox, A. E. Nelson, and N. Weiner, “Dirac gaugino masses and supersoft supersymmetry breaking,” *JHEP* **08** (2002) 035, [arXiv:hep-ph/0206096](#).
- [139] G. D. Kribs, E. Poppitz, and N. Weiner, “Flavor in supersymmetry with an extended R-symmetry,” *Phys. Rev.* **D78** (2008) 055010, [arXiv:0712.2039 \[hep-ph\]](#).
- [140] E. Ponton and E. Poppitz, “Casimir energy and radius stabilization in five and six dimensional orbifolds,” *JHEP* **06** (2001) 019, [arXiv:hep-ph/0105021](#).

-
- [141] G. von Gersdorff, M. Quiros, and A. Riotto, “Scherk-Schwarz supersymmetry breaking with radion stabilization,” *Nucl. Phys.* **B689** (2004) 76–90, [arXiv:hep-th/0310190](#).
- [142] E. Dudas and M. Quiros, “Five-dimensional massive vector fields and radion stabilization,” *Nucl. Phys.* **B721** (2005) 309–324, [arXiv:hep-th/0503157](#).
- [143] F. Paccetti Correia, M. G. Schmidt, and Z. Tavartkiladze, “Radion stabilization in 5D SUGRA,” *Nucl. Phys.* **B763** (2007) 247–267, [arXiv:hep-th/0608058](#).